ANL/APS/TB-1

# APS Undulator and Wiggler Sources: Monte-Carlo Simulation

by S. L. Xu, B. Lai, and P. J. Viccaro

Advanced Photon Source

Argonne National Laboratory, Argonne, Illinois 60439
operated by The University of Chicago
for the United States Department of Energy under Contract W-31-109-Eng-38

ANL/APS/TB-1

ANL/APS/TB-1

Argonne National Laboratory, with facilities in the states of Illinois and Idaho, is owned by the United States government, and operated by The University of Chicago under the provisions of a contract with the Department of Energy.

**DISCLAIMER**

This report was prepared as an account of work sponsored by an agency of the United States Government. Neither the United States Government nor any agency thereof, nor any of their employees, makes any warranty, express or implied, or assumes any legal liability or responsibility for the accuracy, completeness, or usefulness of any information, apparatus, product, or process disclosed, or represents that its use would not infringe privately owned rights. Reference herein to any specific commercial product, process, or service by trade name, trademark, manufacturer, or otherwise, does not necessarily constitute or imply its endorsement, recommendation, or favoring by the United States Government or any agency thereof. The views and opinions of authors expressed herein do not necessarily state or reflect those of the United States Government or any agency thereof.

Reproduced from the best available copy.

Available to DOE and DOE contractors from the
Office of Scientific and Technical Information
P.O. Box 62
Oak Ridge, TN 37831
Prices available from (615) 576-8401, FTS 626-8401

Available to the public from the
National Technical Information Service
U.S. Department of Commerce
5285 Port Royal Road
Springfield, VA 22161

Distribution Category: Atomic,
Molecular, and Chemical Physics
(UC-411)

ARGONNE NATIONAL LABORATORY
9700 South Cass Avenue
Argonne, Illinois 60439

ANL/APS/TB-1

# APS Undulator and Wiggler Sources: Monte-Carlo Simulation

by S. L. Xu, B. Lai, and P. J. Viccaro
Experimental Facilities Division
Advanced Photon Source

February 1992

work sponsored by
U.S. DEPARTMENT OF ENERGY
Office of Energy Research

# INTRODUCTION

Standard insertion devices will be provided to each sector by the Advanced Photon Source. It is important to define the radiation characteristics of these general purpose devices. In this document, results of Monte-Carlo simulation are presented. These results, based on the SHADOW program,[1] include the APS Undulator A (UA), Wiggler A (WA), and Wiggler B (WB).

In an undulator, the energy tuning is accomplished by changing the magnetic gap opening. Fig. 1 shows the first harmonic energy and the deflection parameter K, as a function of the magnetic gap size for Undulator A. Note that by varying the magnetic gap, the first harmonic energy may be tuned from 4.5 keV to 13.5 keV, which corresponds to a change in K from 2.1 to 0.3. The brilliance of the first and the third harmonic were calculated for this range of K values, and the spectra are displayed in Fig. 2. Very high brilliance on the order of $10^{18}$ is generally obtained from the first harmonic, while the third harmonic extends the spectral range up to 40 keV. The parameters of Undulator A used for this calculation are listed in Table 1, and the energies of the first 3 harmonics computed using:

$$E = \frac{nhc\ 2\gamma^2}{\lambda_u\,(1 + K^2/2)} \qquad n = 1, 2, 3$$

are listed in Table 2.

To adequately handle and make efficient use of this unprecedented brilliance in the hard x-rays, detailed information about its spatial distribution is needed. For this purpose, the angular

---

1 B. Lai and F. Cerrina, *Nucl. Instr. and Meth.* **A246**, 337 (1986); B. Lai, K. Chapman and F. Cerrina, *Nucl. Instr. and Meth.* **A266**, 544 (1988).

distribution of x-rays produced by Undulator A has been simulated here (see Figs. UA1 - UA57) for K ranging from 2.1 to 0.3 in steps of 0.1. For each K, the radiation pattern in angular space $(x',y')$ was modeled at the first 3 harmonic energies using an undulator modeling method described previously.[2] In each figure, the APS beam emittance case is shown together with the limiting case of zero emittance, so that contribution from higher harmonics and effects of emittance broadening may be easily identified. Note that in most cases, the central cone is dominated by the beam divergence. These angular plots, when multiplied by the distance from the source, represent the spatial flux pattern obtained in the far-field regime. For the near-field region, the spatial distribution is further broadened by the finite source size in $x$ and $y$ (besides the zero-emittance pattern is more complex).[3] A program to take into account the near-field effects is being developed at APS. Each diagram is generated with 1000 rays and is displayed over an angular limit of 1 mrad by 1 mrad in $x'$ and $y'$. Because a fixed number of rays (1000) is always used in creating the angular plots, they do not show the relative intensity variation between the harmonics. That information is contained in Fig. 2.

In the second part, similar angular plots for the two wigglers are presented (Figs. WA1 - WA8 and WB1 - WB8). Wiggler A (WA), with critical energy of 32.6 keV, is optimized for the high-energy region and will extend the spectral range to 200 keV and above (Fig. 3). Wiggler B (WB), on the other hand, is designed for the low-energy region with $E_c$ = 9.8 keV (Fig. 4). Because the radiation from a wiggler is more spread out in the horizontal direction $x'$, all the

---

2 K. Chapman, B. Lai, F. Cerrina and P. J. Viccaro, *Nucl. Instr. and Meth.* **A283**, 88 (1989).

3 See for instance R. P. Walker, *Nucl. Instr. and Meth.* **A267**, 537 (1988).

angular diagrams are plotted over a wider limit of 2.5 mrad by 2.5 mrad. The actual extent of the ray distribution is determined by $K/\gamma$. Thus, since WA has larger K than WB, the photons are distributed over 2 mrad for WA versus 1 mrad for WB. As for the spread in the vertical direction $y'$, note that the photons are confined within smaller and smaller angles as the photon energy increases, which is similar to bending magnet radiation. The parameters used in the wiggler calculation are listed in Table 3.

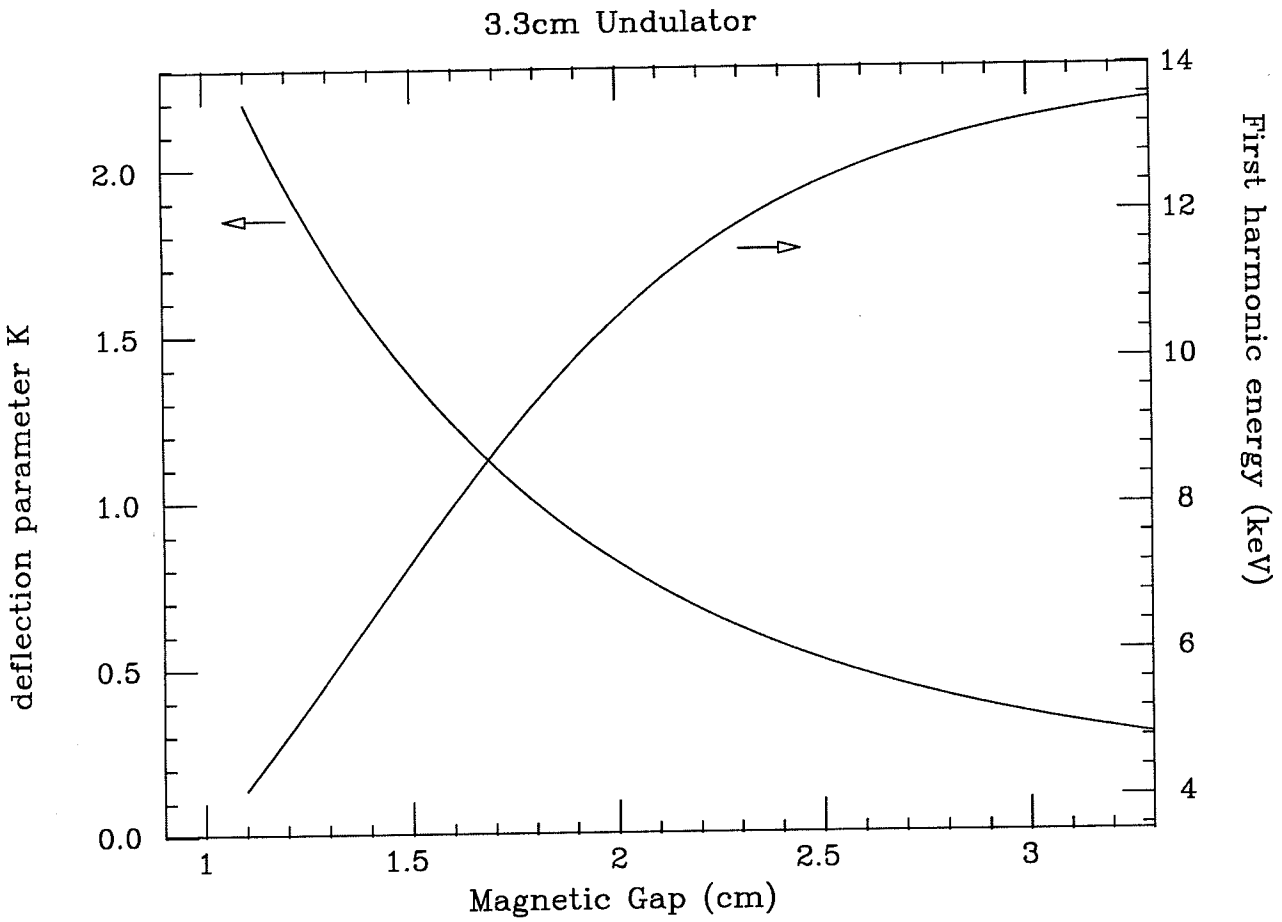


Fig. 1 First harmonic energy and deflection parameter K as a function of the magnetic gap for Undulator A.

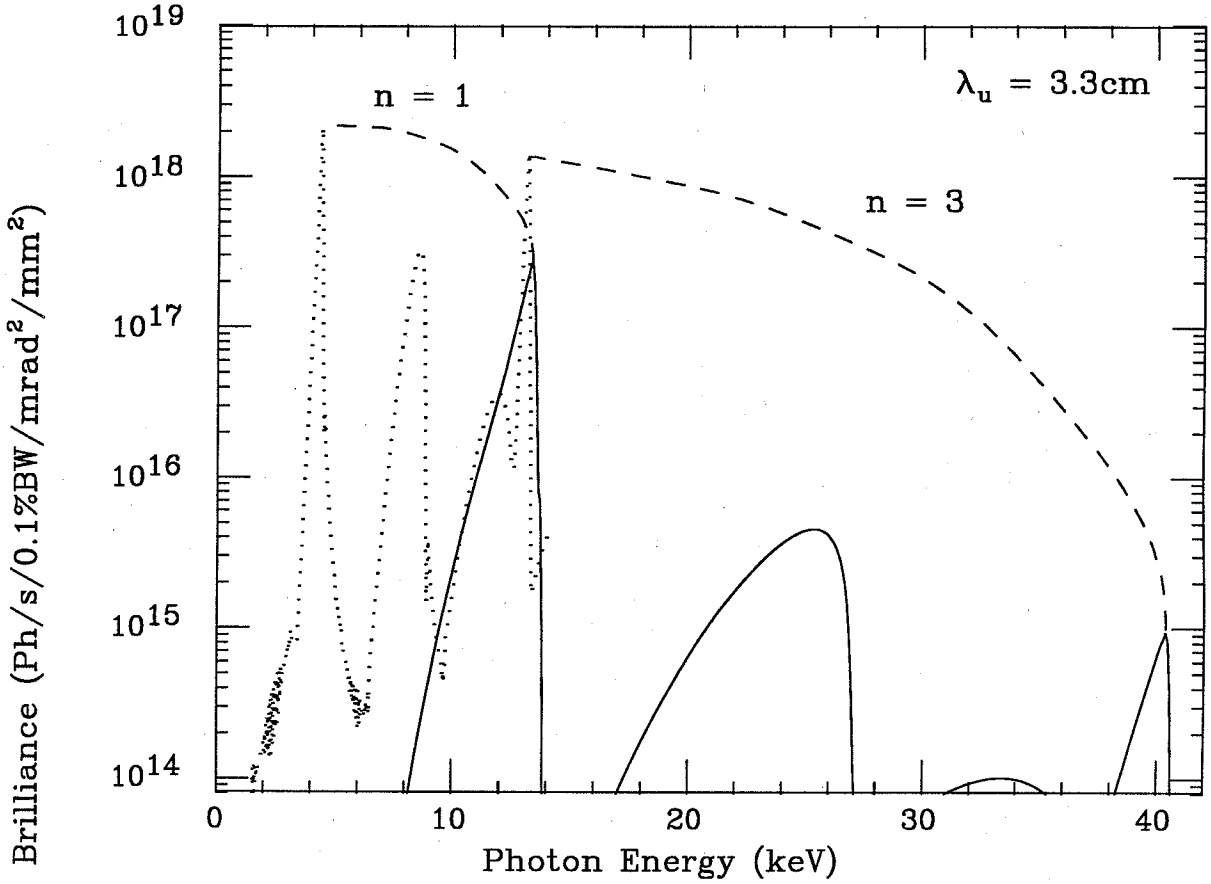


Fig. 2 On-axis brilliance of Undulator A. The spectral distribution of the first 3 harmonics are shown for the case of K = 0.3 (solid line) and K = 2.1 (dotted line). The overall envelope of the first and the third harmonic for the K-values in between are showed in dashed lines.

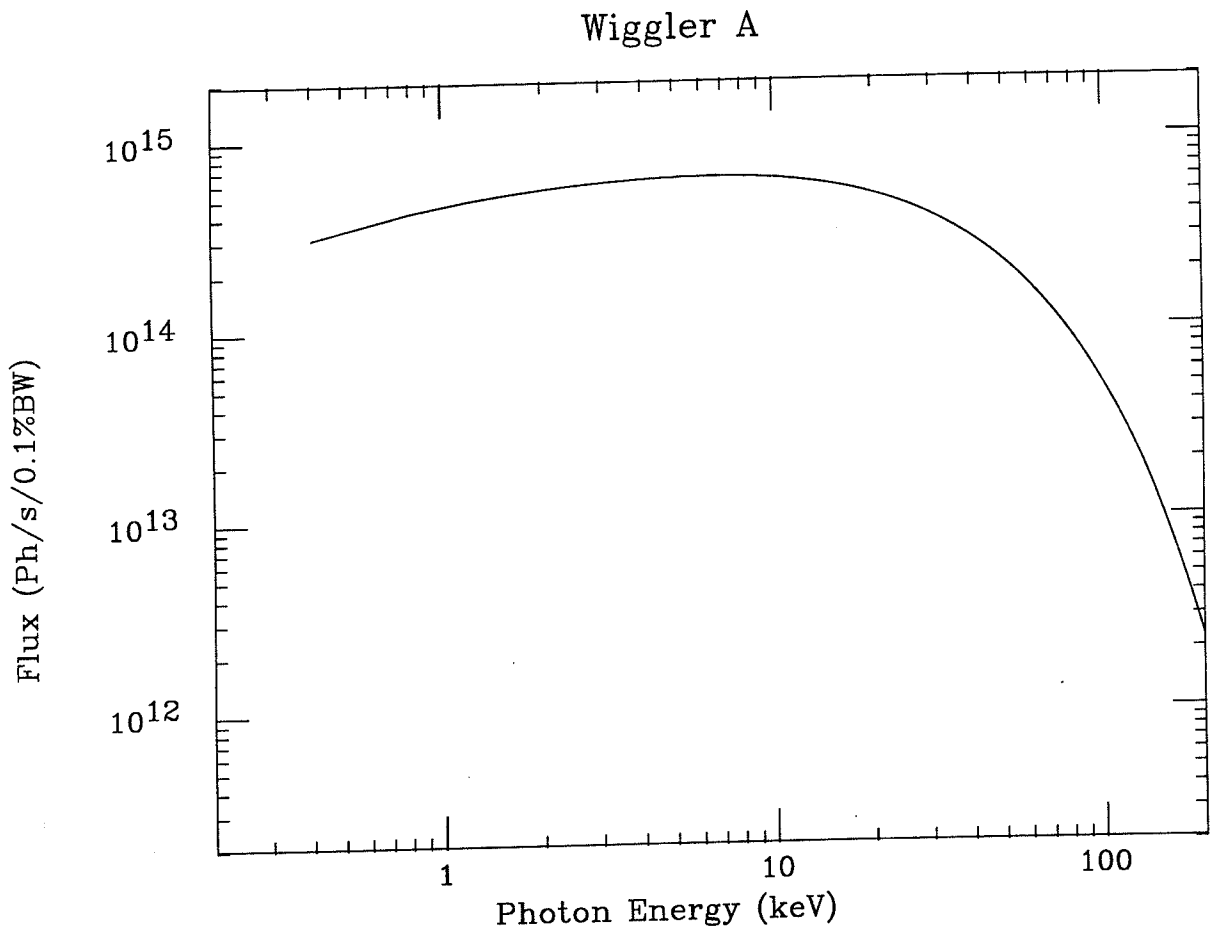


Fig. 3 Angle integrated flux for Wiggler A.

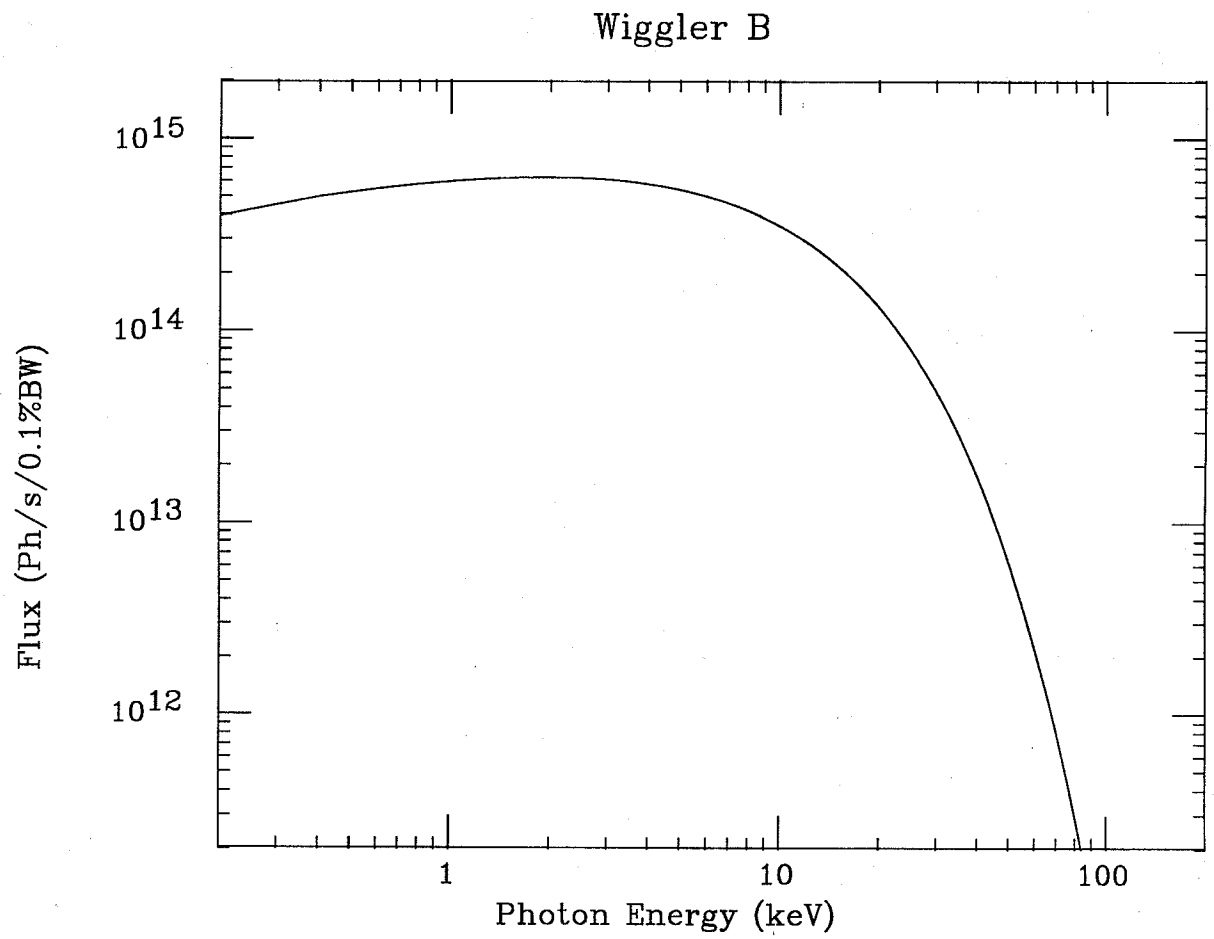


Fig. 4 Angle integrated flux for Wiggler B.

Table 1. Parameters of Undulator A used in calculation

| | |
|---|---|
| $\lambda_o$ | 3.3 cm |
| K | 0.3 - 2.1 |
| N | 70 periods |
| $E_b$ | 7.0 GeV |
| $I_b$ | 100 mA |
| $\sigma_x$ | 0.308 mm |
| $\sigma_y$ | 0.085 mm |
| $\sigma_{x'}$ | 24 μrad |
| $\sigma_{y'}$ | 9 μrad |
| $\Delta E/E$ | 0.1% Bandwidth |
| Maximum angle | 0.3 mrad |

| | | |
|---|---|---|
| Beam Emittance | UAS-0 | zero |
| | UAS-1 | $\varepsilon_x = 7.3$, $\varepsilon_y = 0.73$ nm-rad |

Table 2. Energy of the first 3 harmonics for Undulator A

| K = | 1st harmonic | 2nd harmonic | 3rd harmonic |
|---|---|---|---|
| 2.1 | 4.40 | 8.80 | 13.20 |
| 2.0 | 4.70 | 9.40 | 14.10 |
| 1.9 | 5.03 | 10.06 | 15.08 |
| 1.8 | 5.38 | 10.77 | 16.15 |
| 1.7 | 5.77 | 11.54 | 17.30 |
| 1.6 | 6.19 | 12.37 | 18.56 |
| 1.5 | 6.64 | 13.27 | 19.91 |
| 1.4 | 7.12 | 14.24 | 21.37 |
| 1.3 | 7.64 | 15.29 | 22.93 |
| 1.2 | 8.20 | 16.40 | 24.60 |
| 1.1 | 8.79 | 17.57 | 26.36 |
| 1.0 | 9.40 | 18.80 | 28.20 |
| 0.9 | 10.04 | 20.07 | 30.11 |
| 0.8 | 10.68 | 21.37 | 32.05 |
| 0.7 | 11.33 | 22.65 | 33.98 |
| 0.6 | 11.95 | 23.90 | 35.85 |
| 0.5 | 12.54 | 25.07 | 37.61 |
| 0.4 | 13.06 | 26.12 | 39.17 |
| 0.3 | 13.50 | 26.99 | 40.49 |

Table 3. Parameters of Wiggler A and Wiggler B used in calculation

| | WA | WB |
|---|---|---|
| $\lambda_o$ | 15 cm | 25 cm |
| K | 14 | 7 |
| N (periods) | 10 | 20 |
| $E_c$ | 32.57 keV | 9.77 keV |
| $2\theta$ | 2 mrad | 1 mrad |
| $E_b$ | 7 GeV | |
| $I_b$ | 100 mA | |
| $\Delta E/E$ | 0.1% Bandwidth | |
| $\sigma_x$ | 0.308 mm | |
| $\sigma_y$ | 0.085 mm | |
| $\sigma_{x'}$ | 24 μrad | |
| $\sigma_{y'}$ | 9 μrad | |
| $\varepsilon_x$ | 7.3 nm-rad | |
| $\varepsilon_y$ | 0.73 nm-rad | |

# APS UNDULATOR A

# RAY-TRACING RESULTS

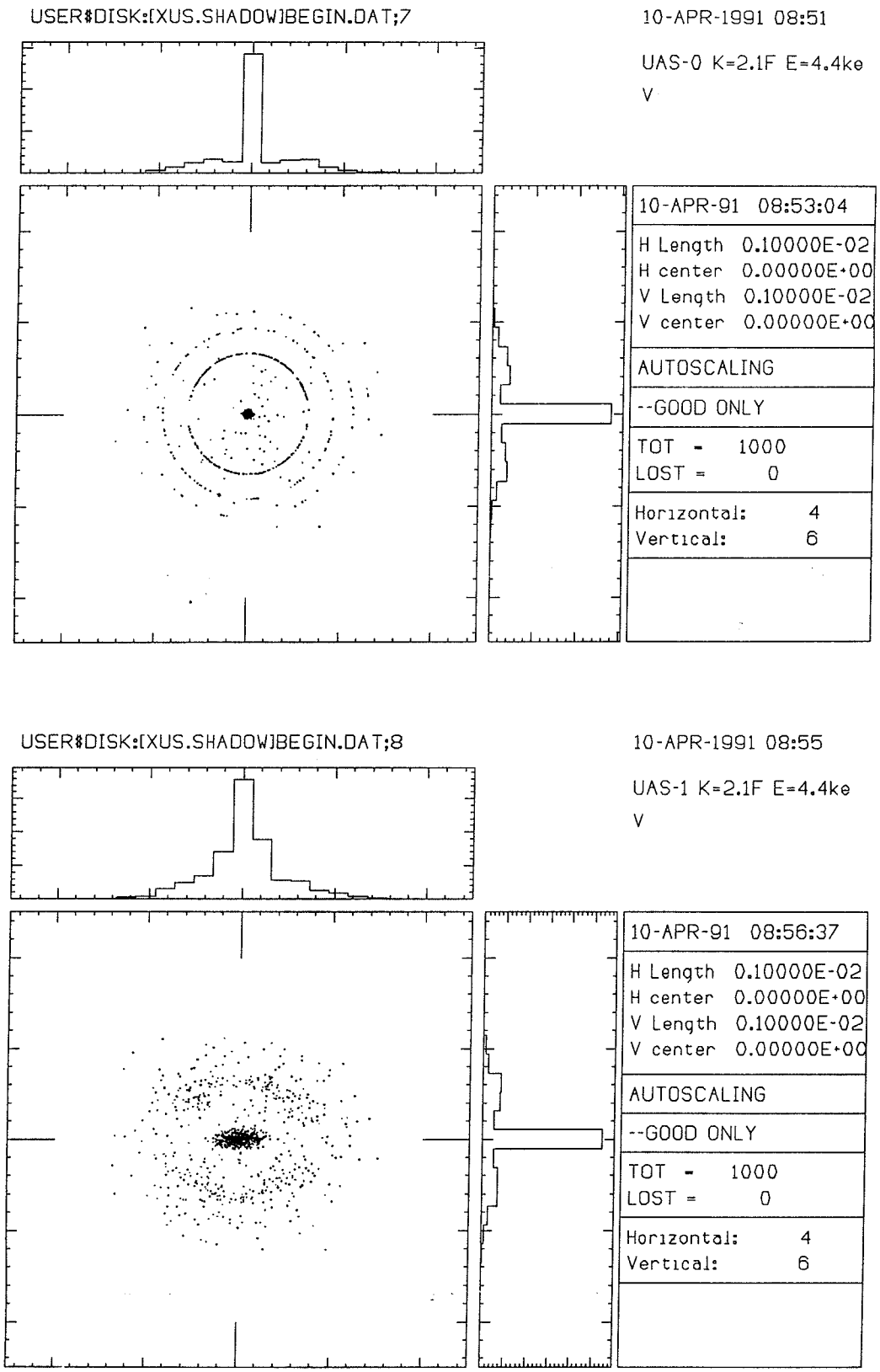


Fig. UA-1. The angular pattern at the first harmonic (hν = 4.40 keV) for K = 2.1. The zero-emittance case is shown on the top (UAS-0), while the bottom part shows the case for APS emittance (UAS-1). The limits for each plot are 1 mrad x 1 mrad.

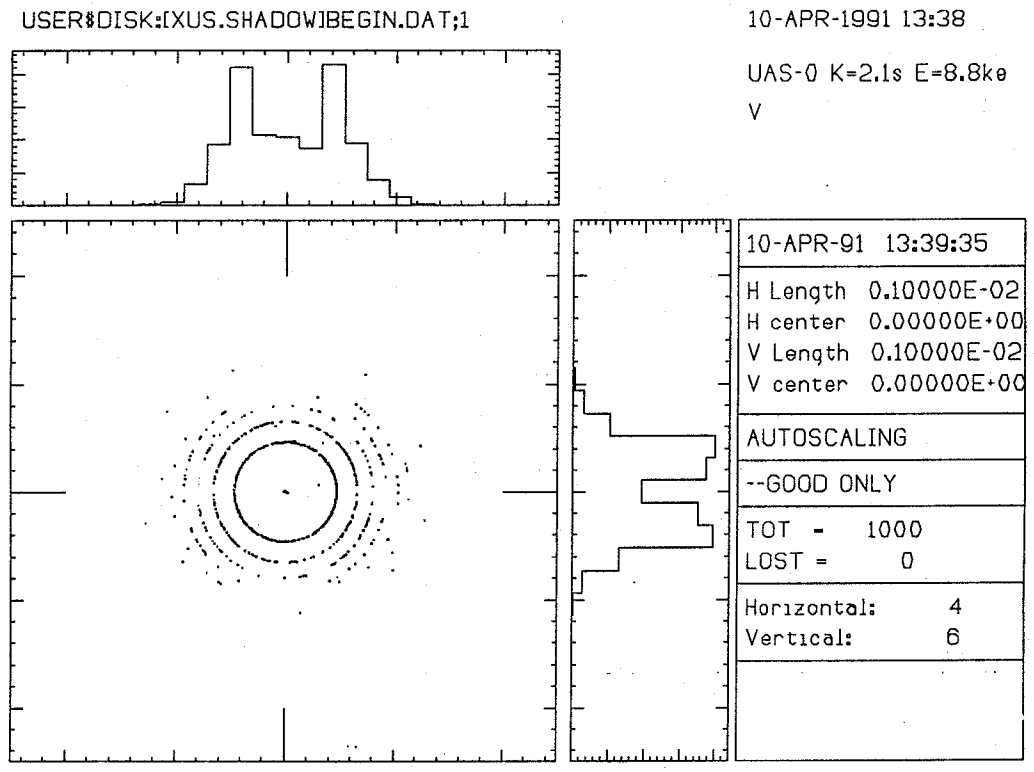


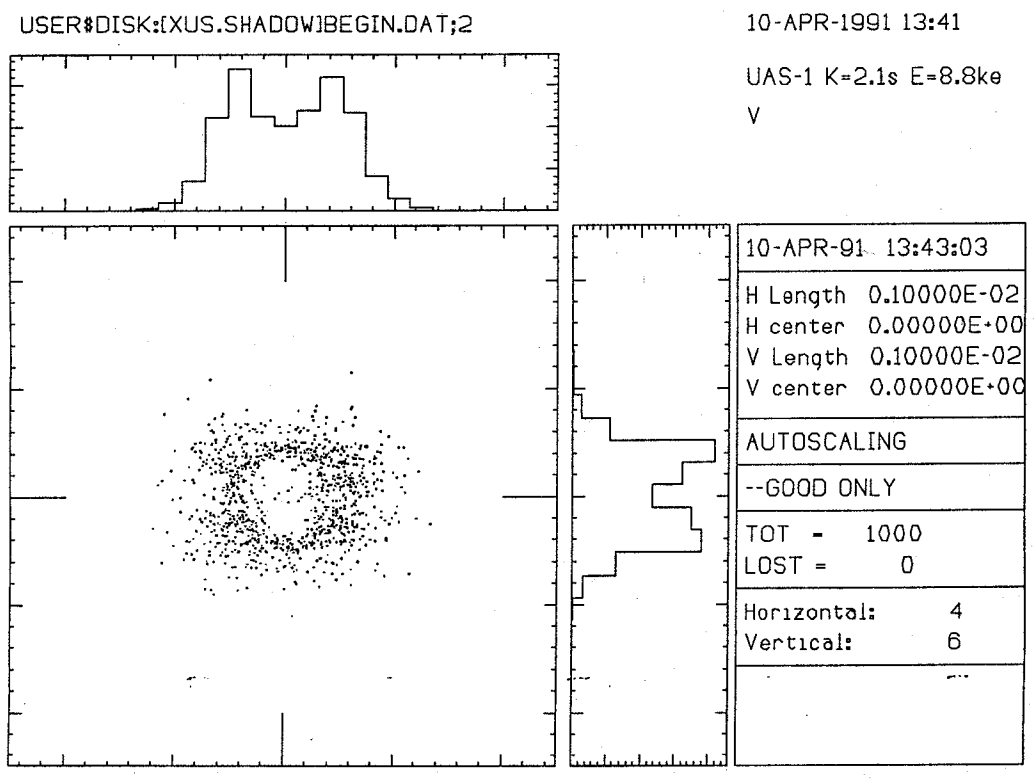


Fig. UA-2. K = 2.1, second harmonic.

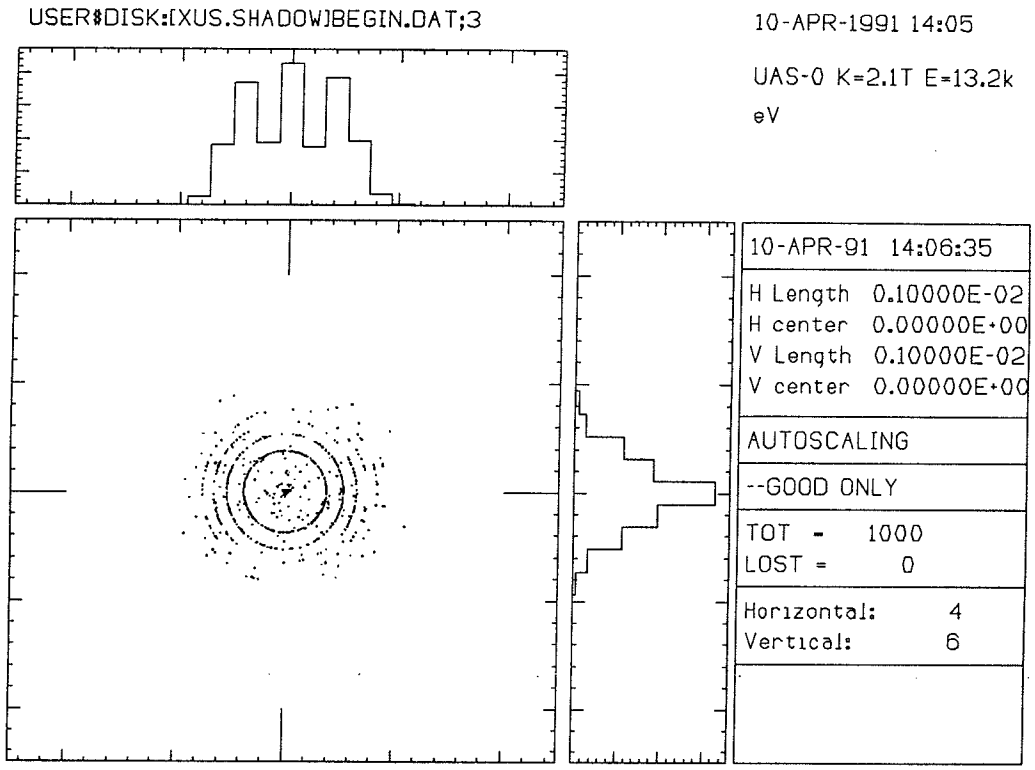


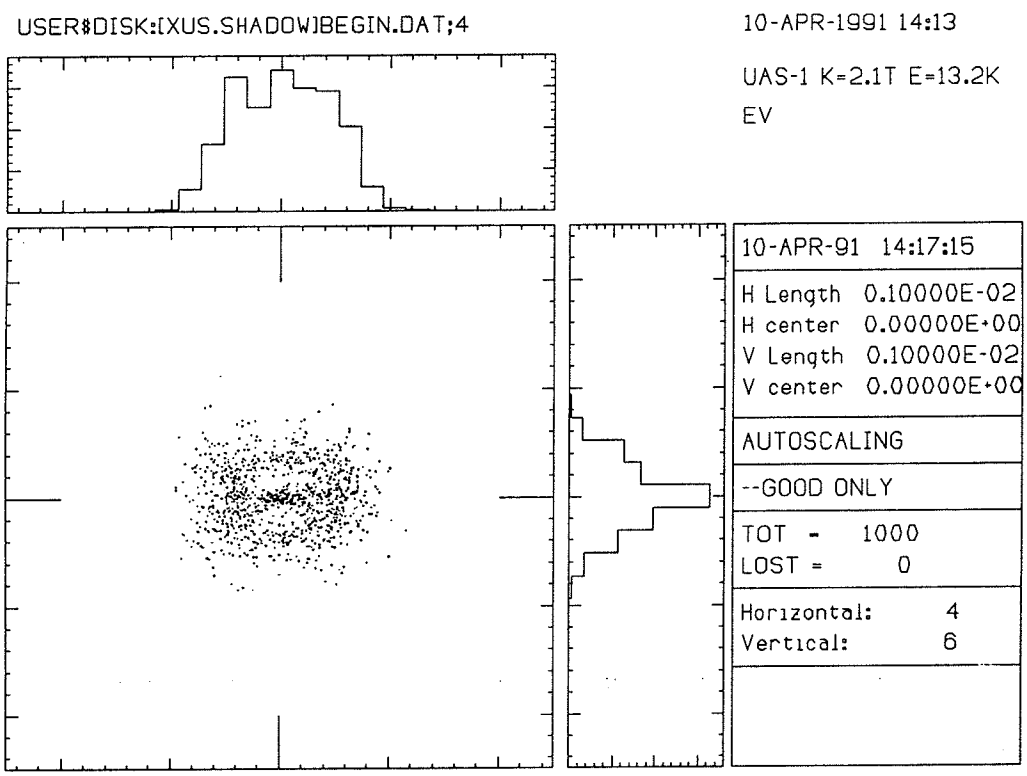


Fig. UA-3. K = 2.1, third harmonic.

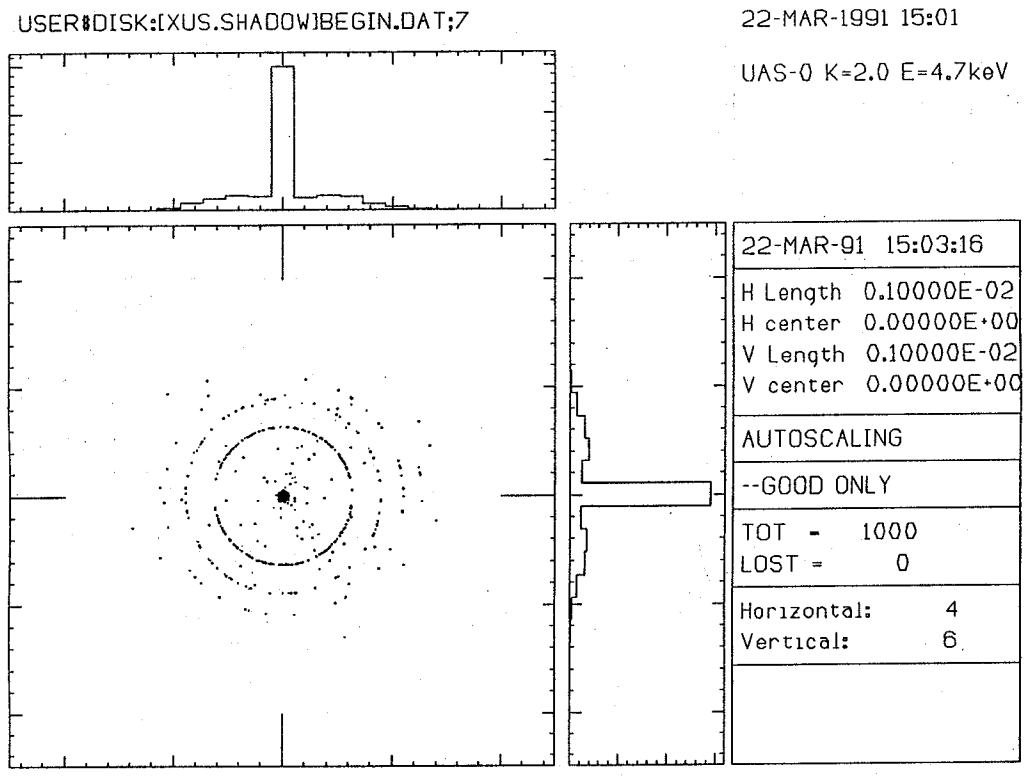


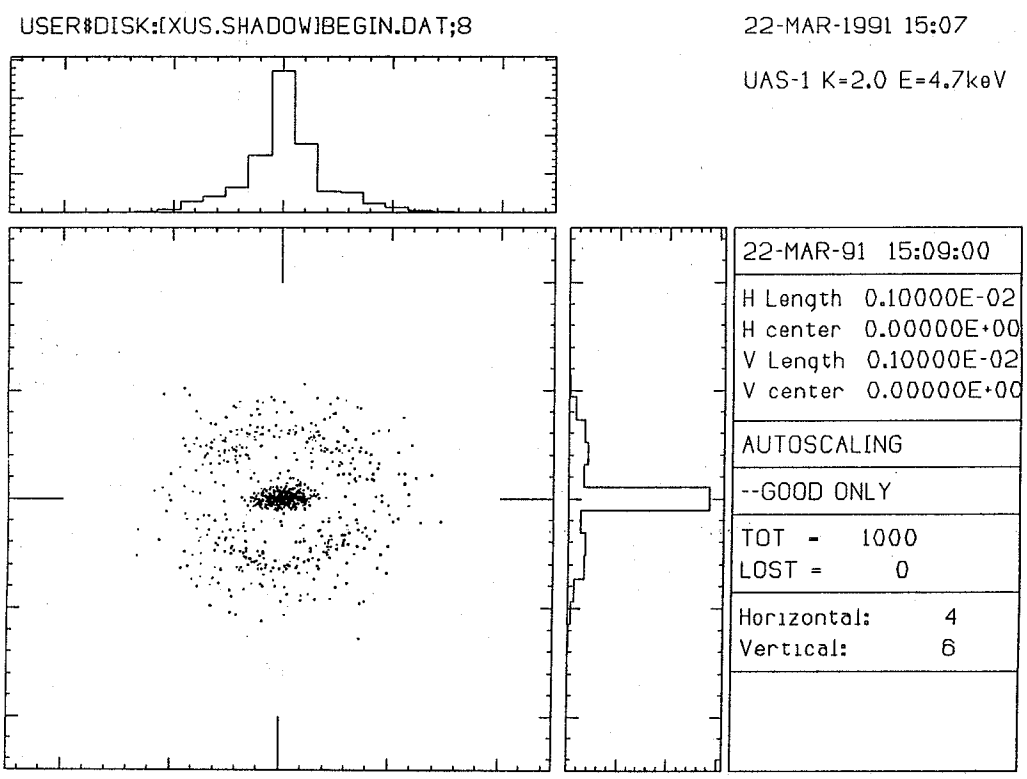


**Fig. UA-4. K = 2.0, first harmonic.**

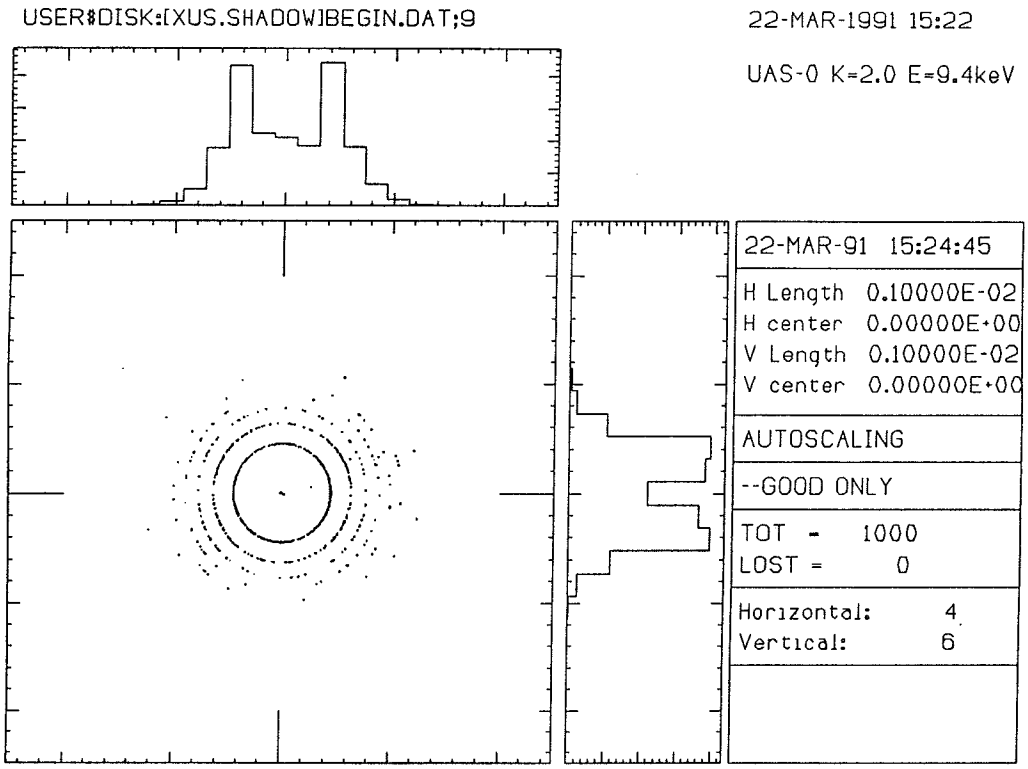


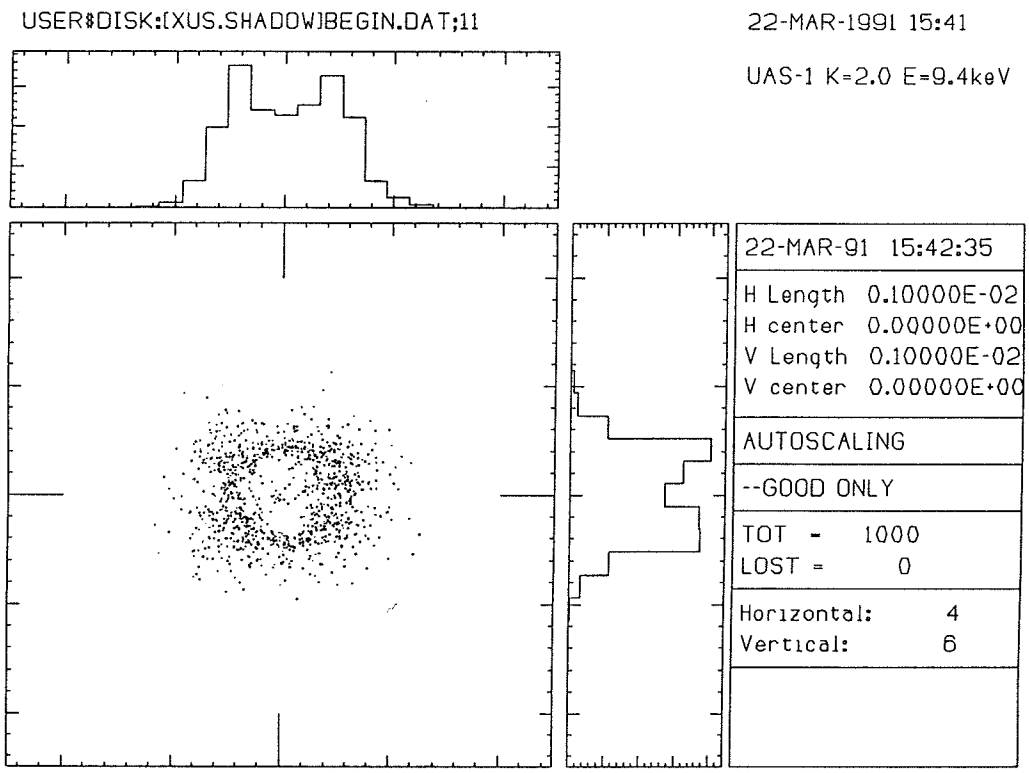


Fig. UA-5. K = 2.0, second harmonic.

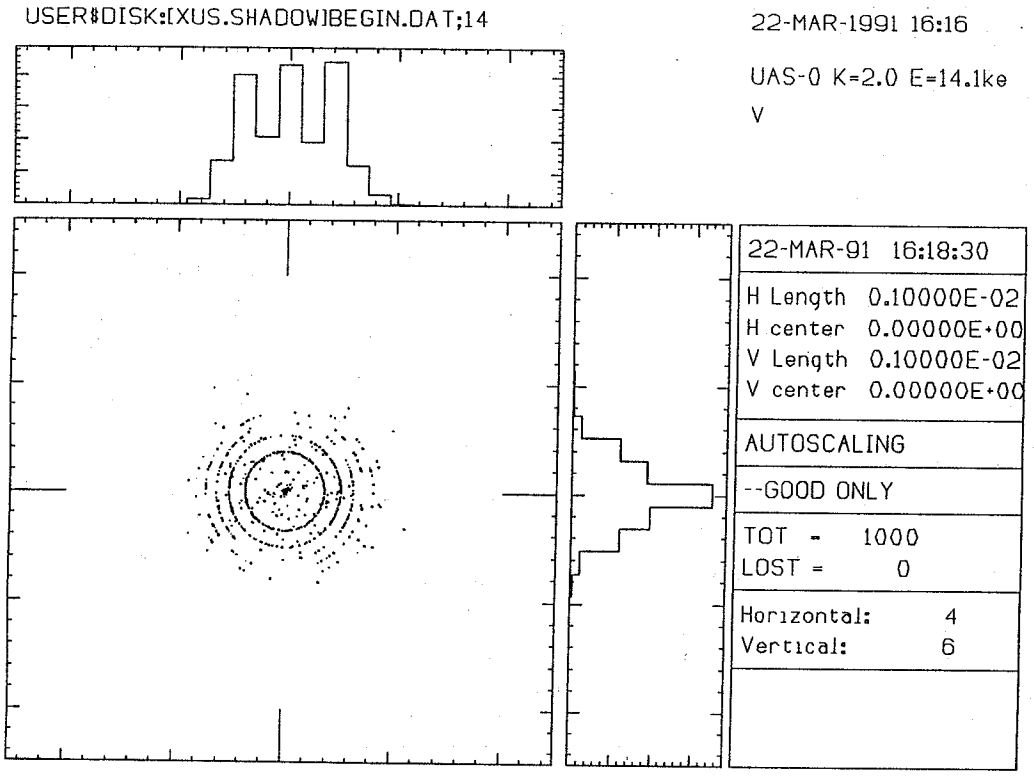


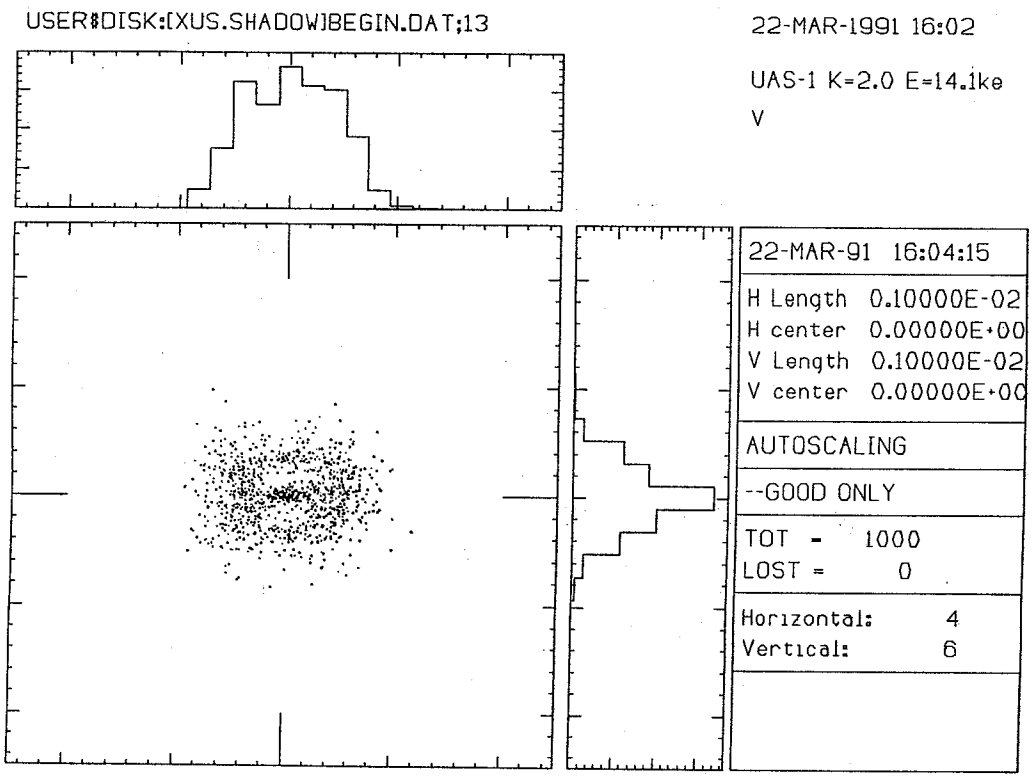


**Fig. UA-6. K = 2.0, third harmonic.**

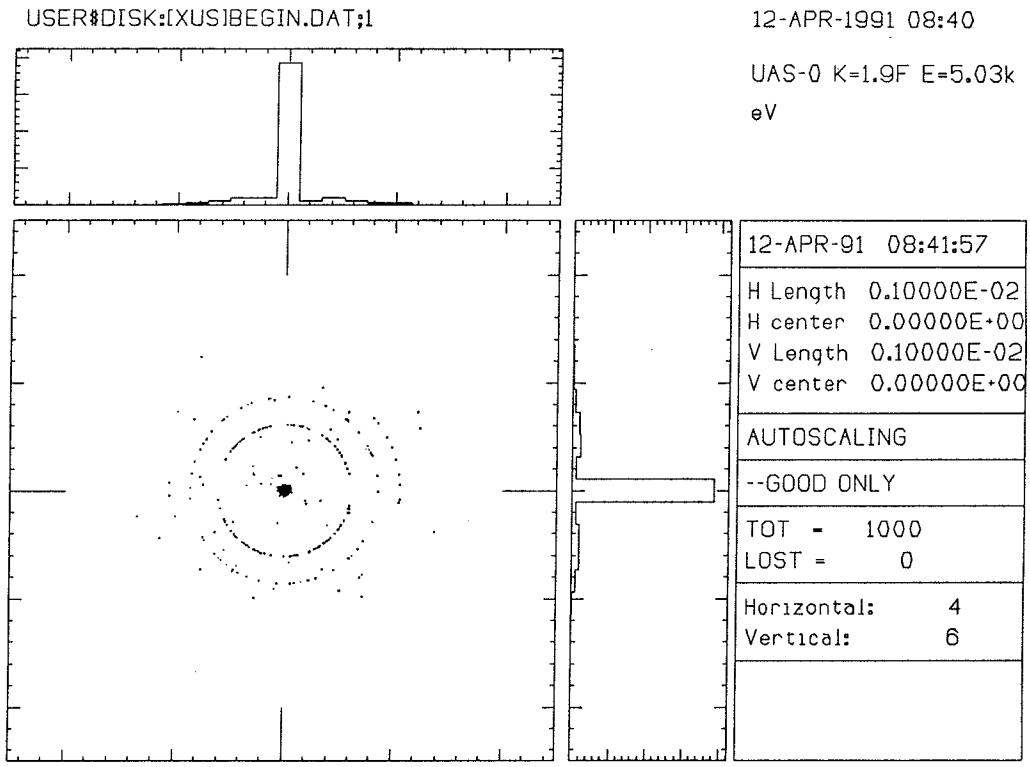


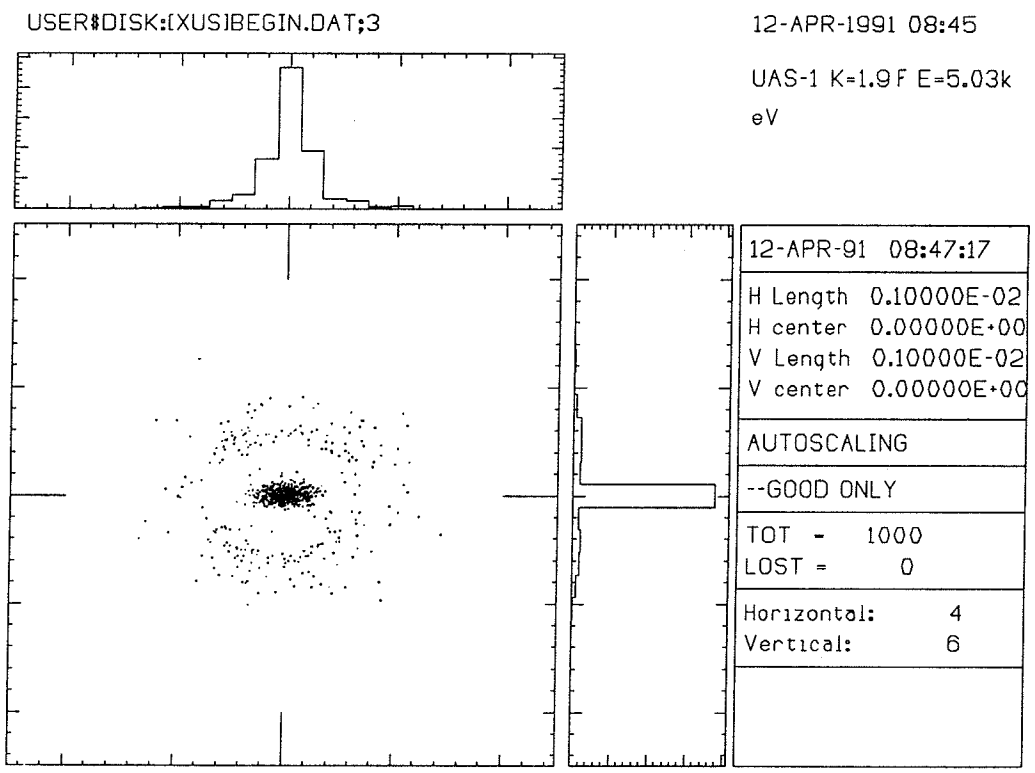


Fig. UA-7. K = 1.9, first harmonic.

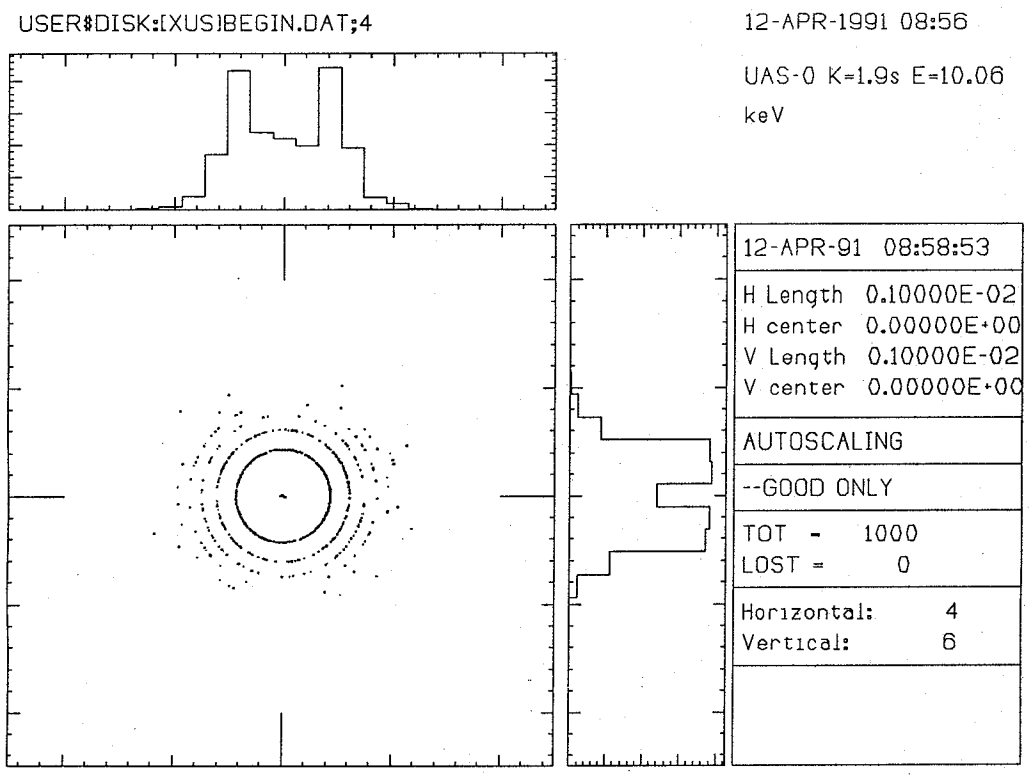


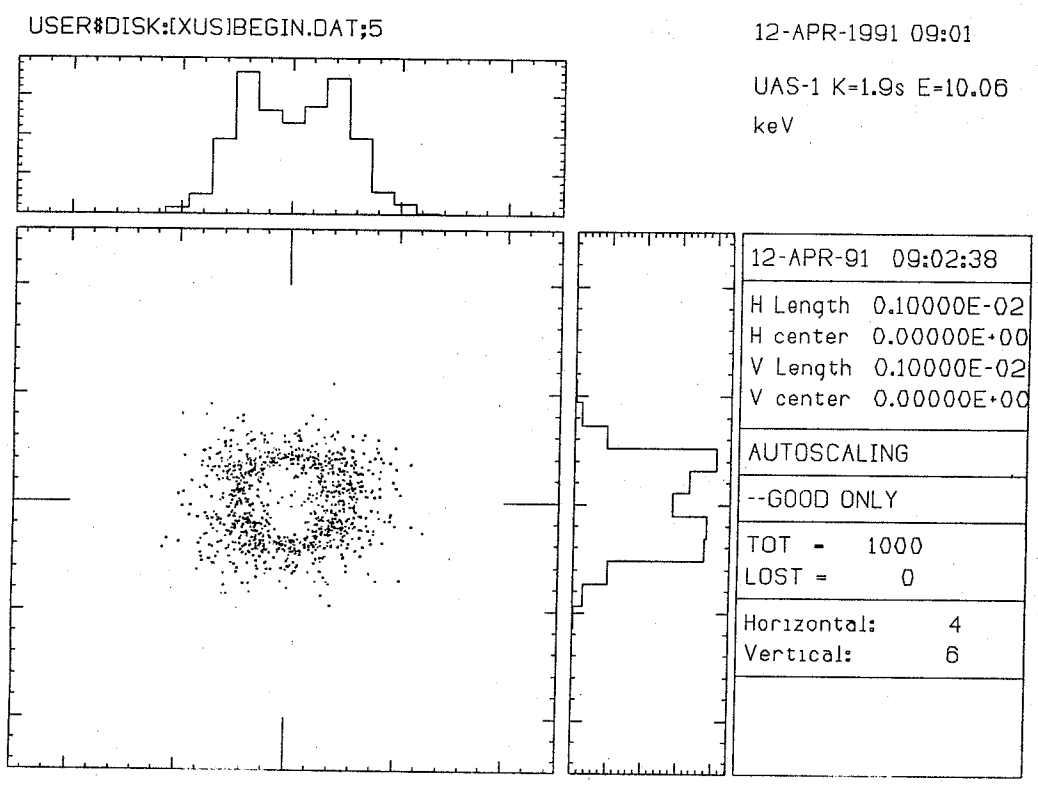


Fig. UA-8. K = 1.9, second harmonic.

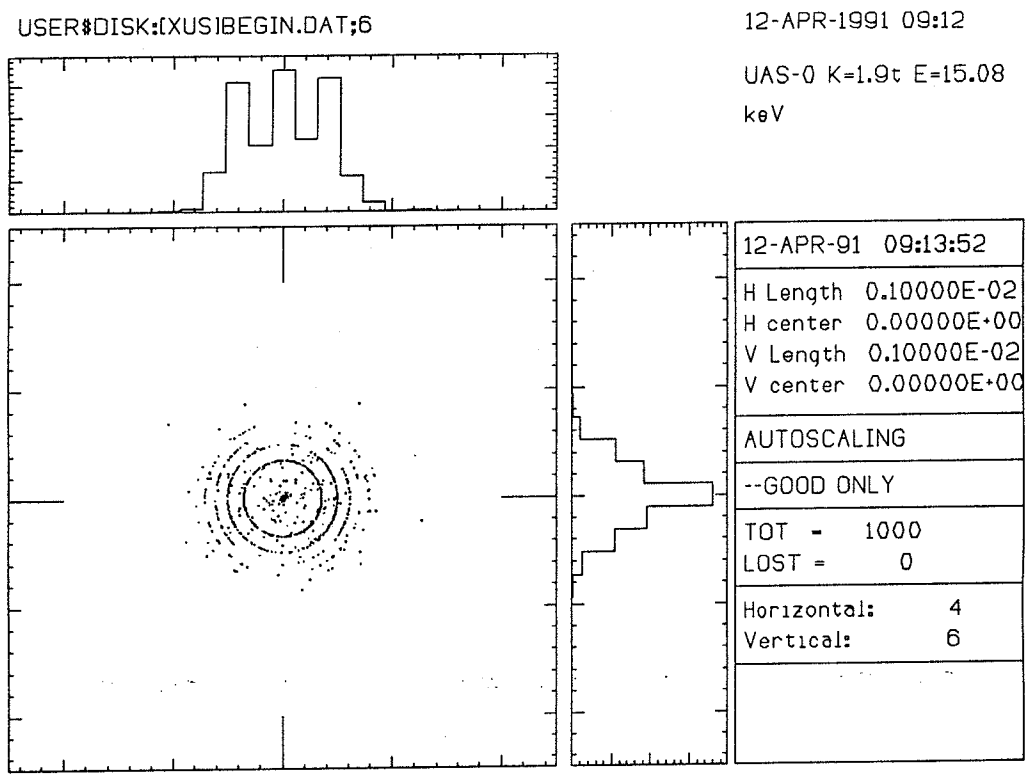


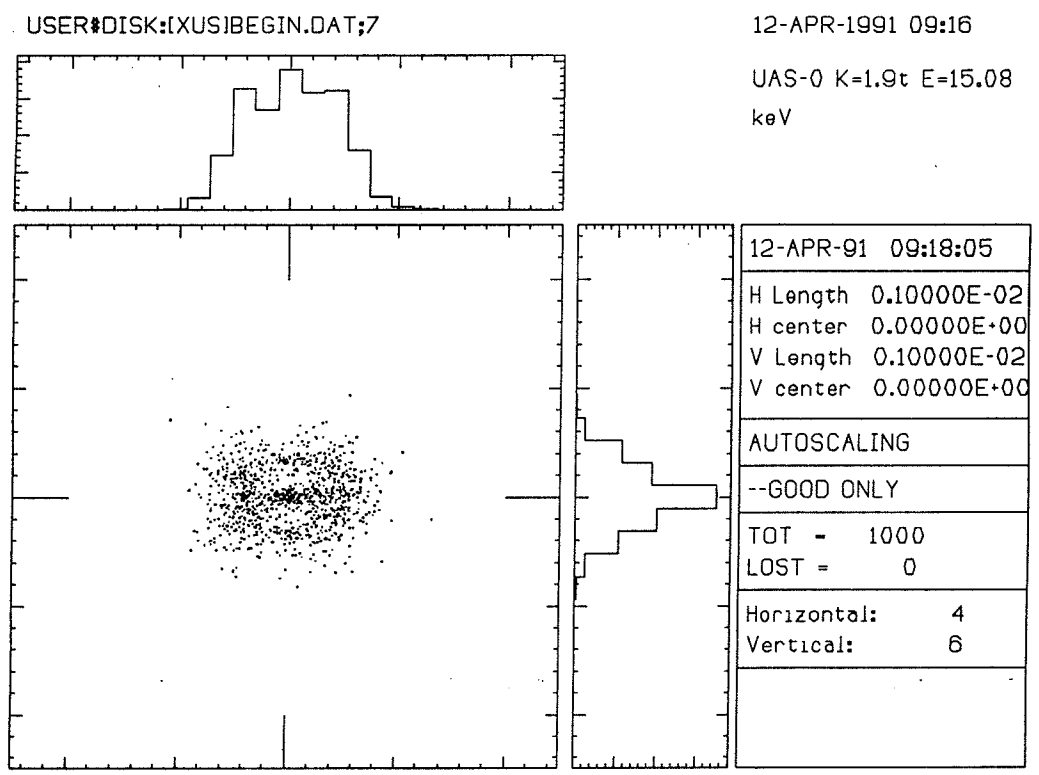


Fig. UA-9. K = 1.9, third harmonic.

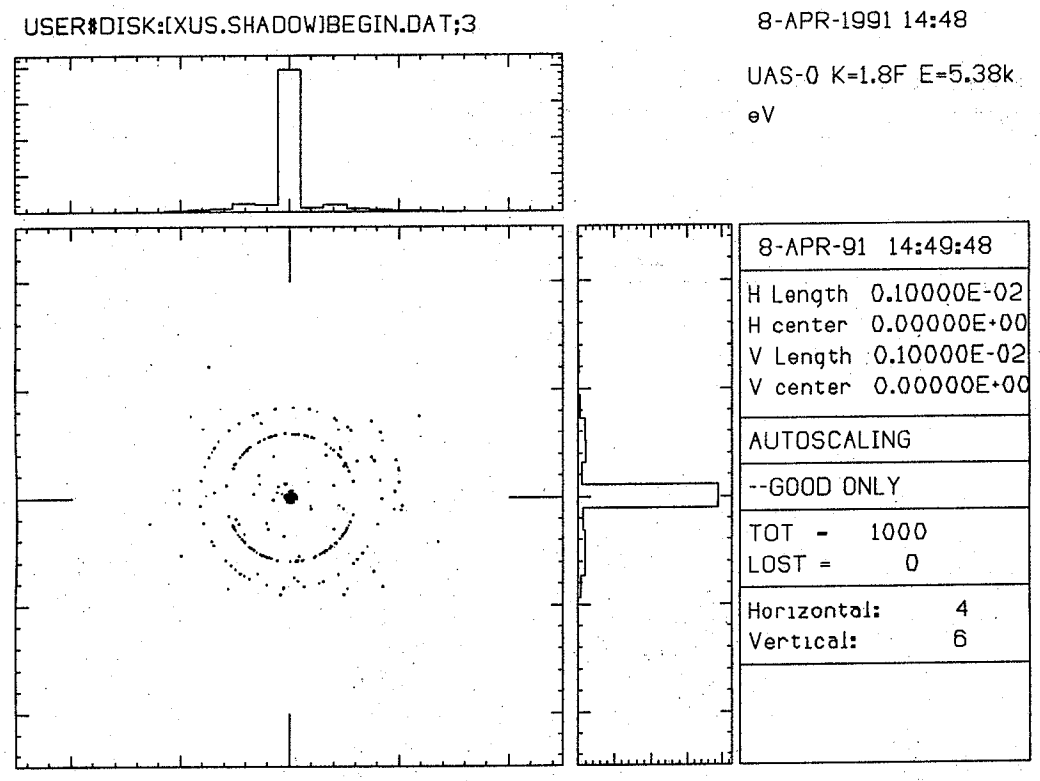


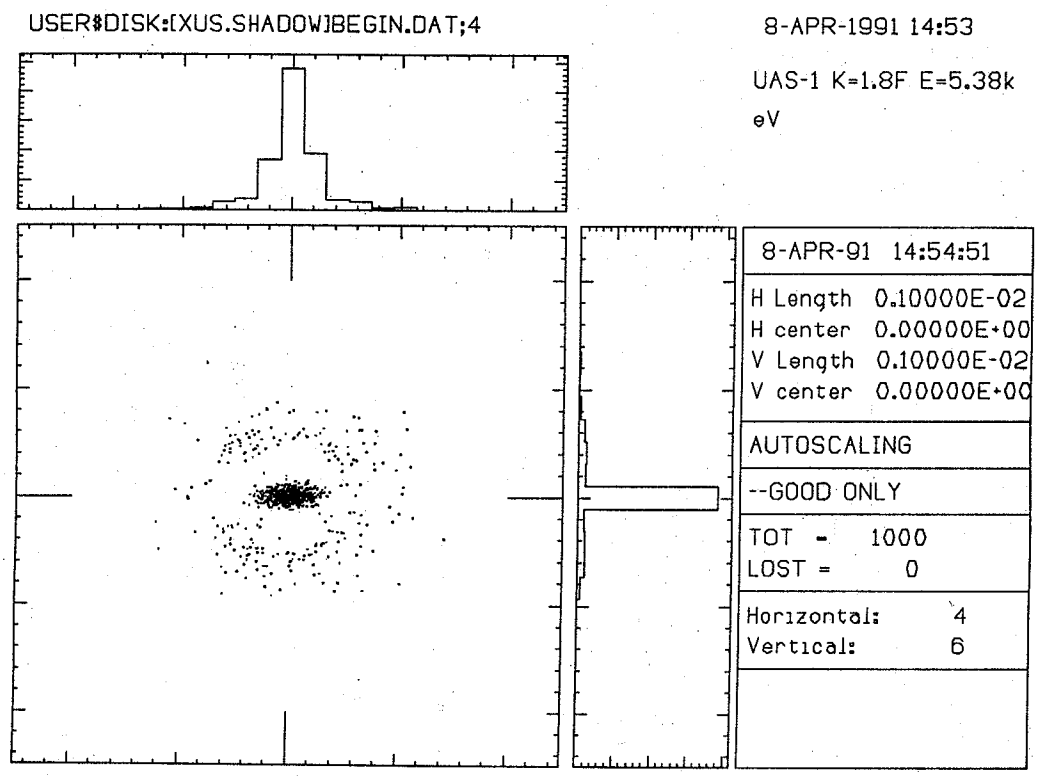


Fig. UA-10. K = 1.8, first harmonic.

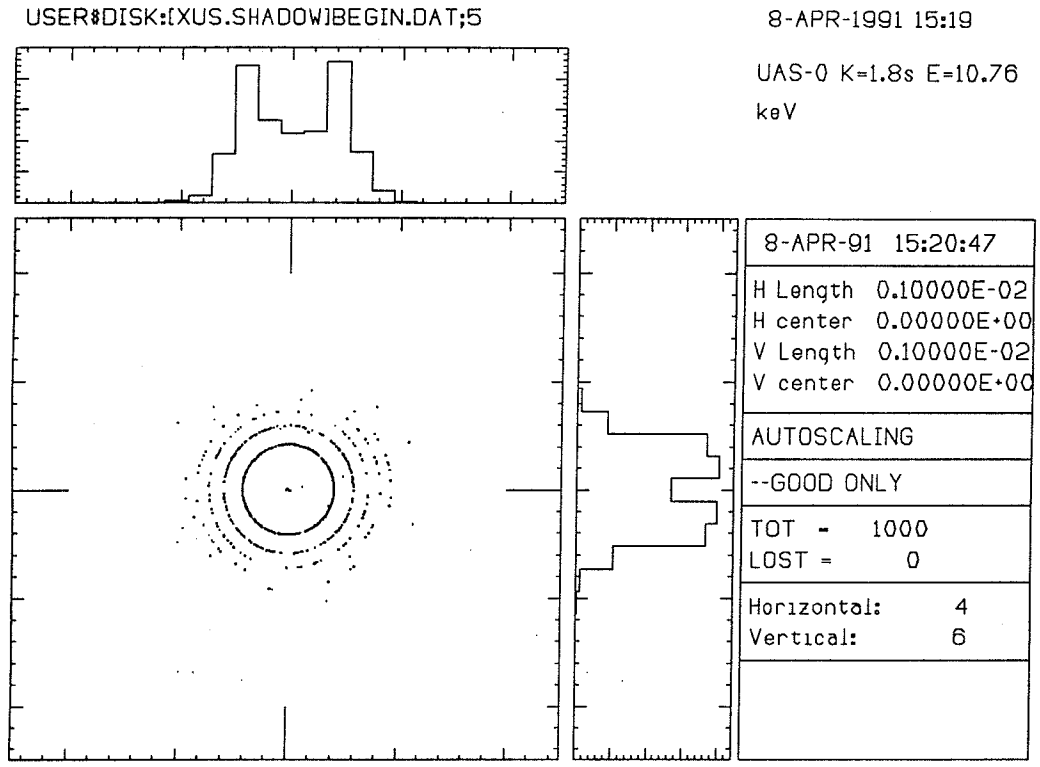


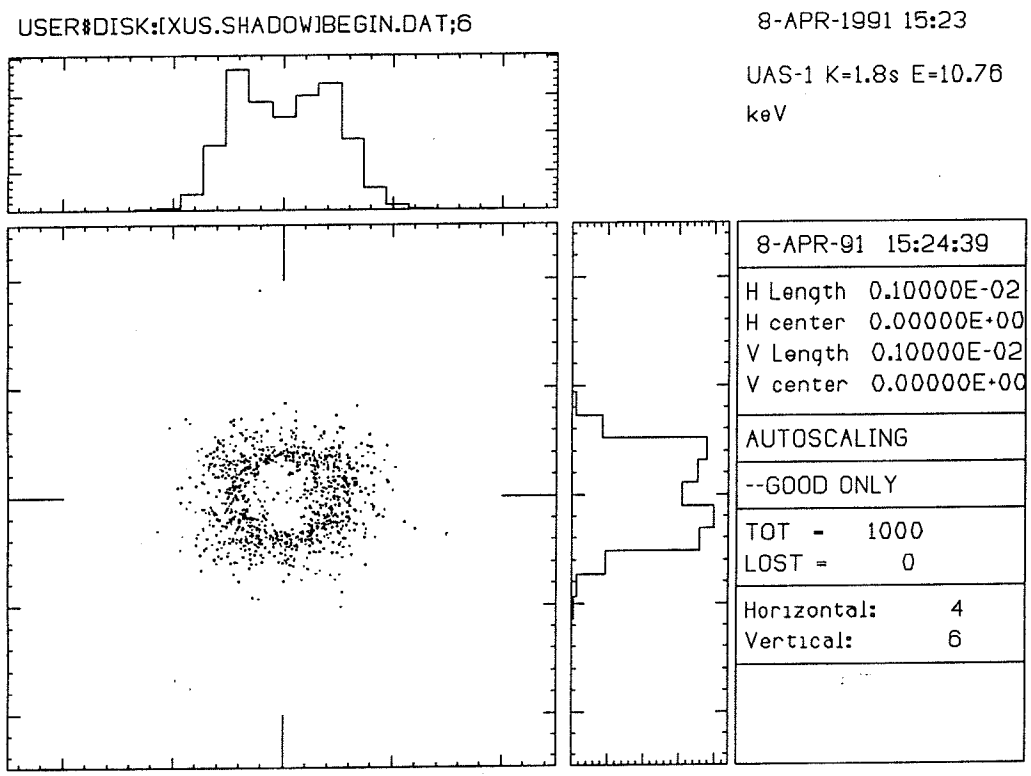


Fig. UA-11. K = 1.8, second harmonic.

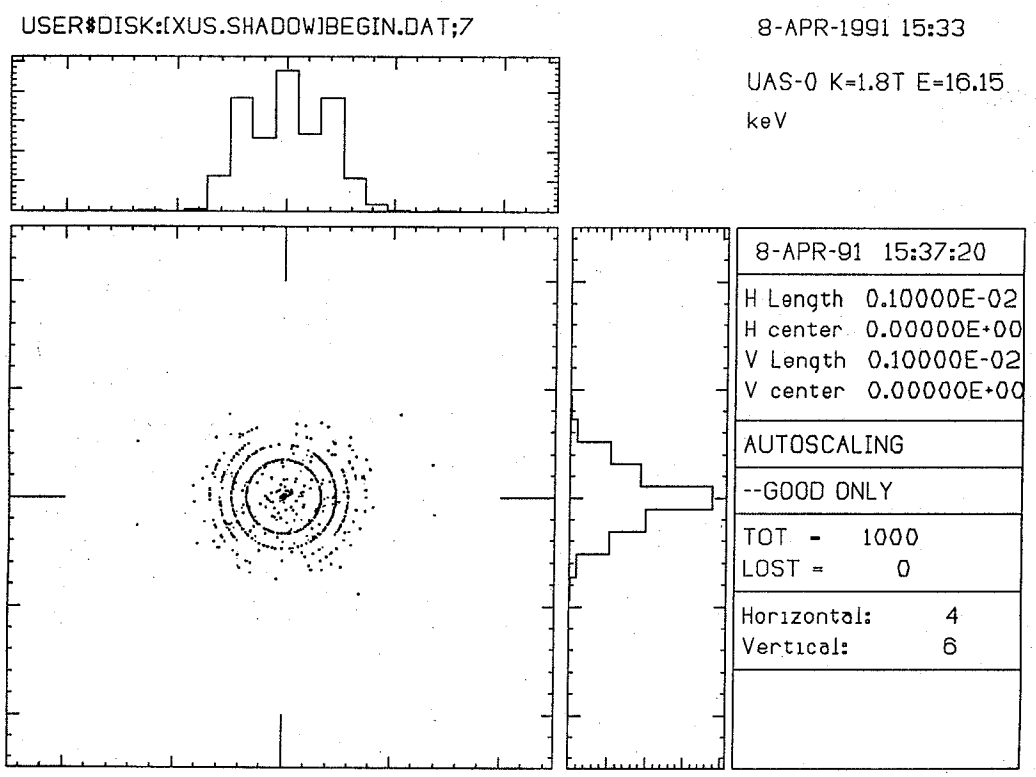


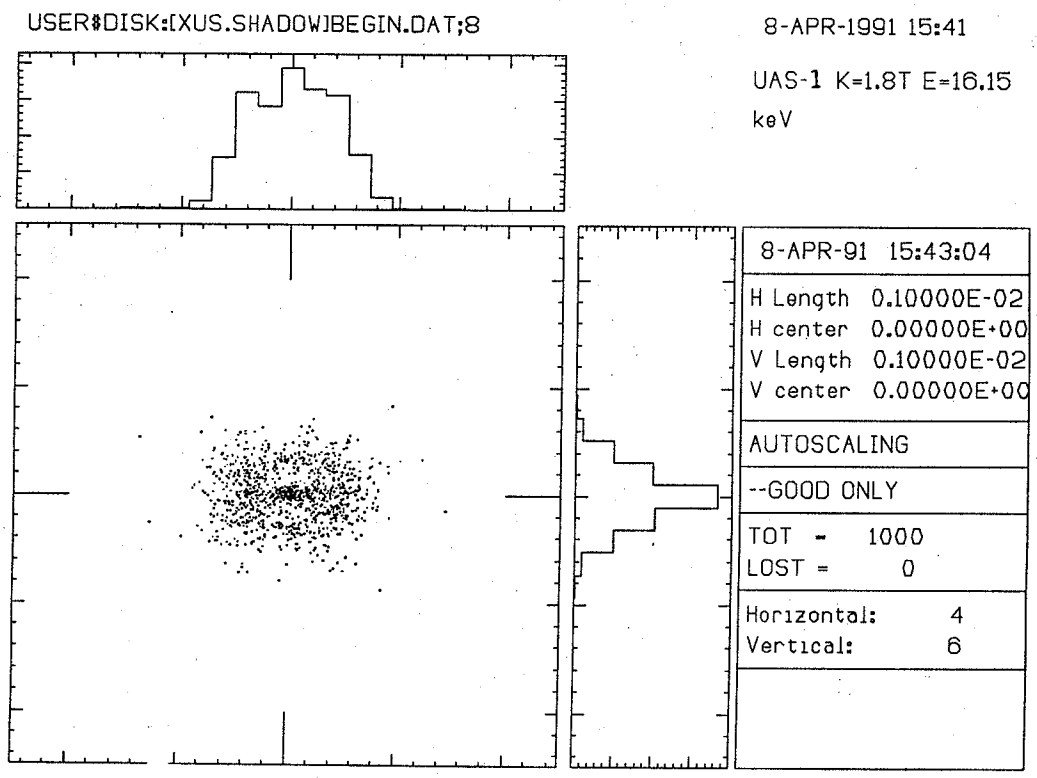


Fig. UA-12. K = 1.8, third harmonic.

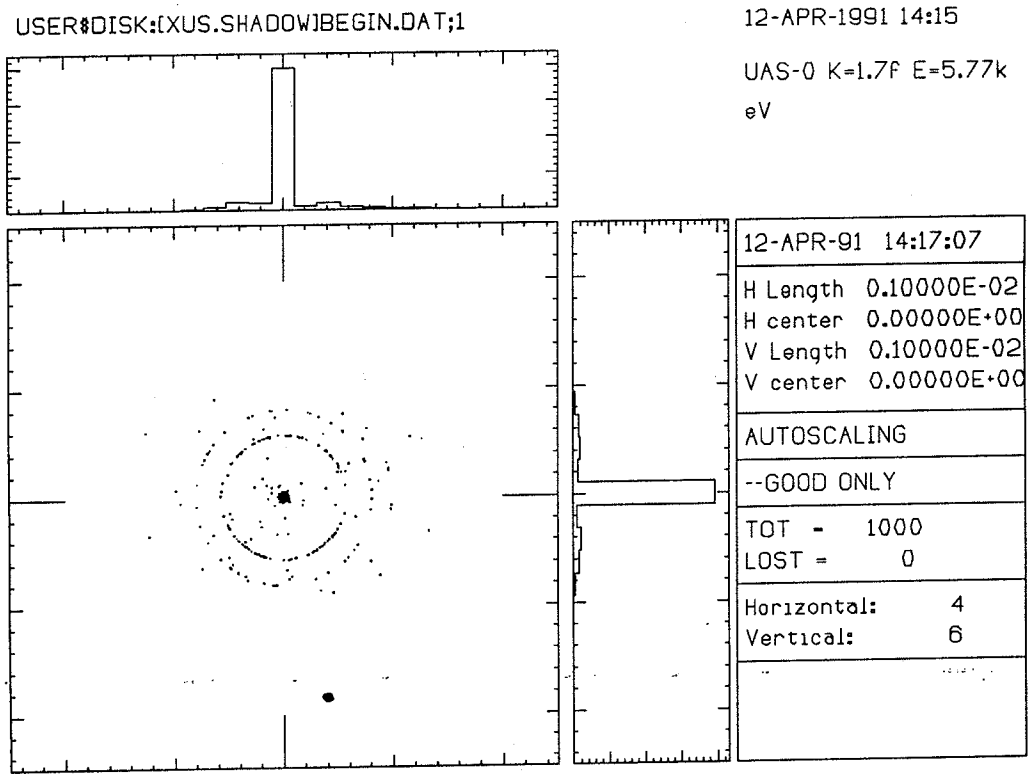


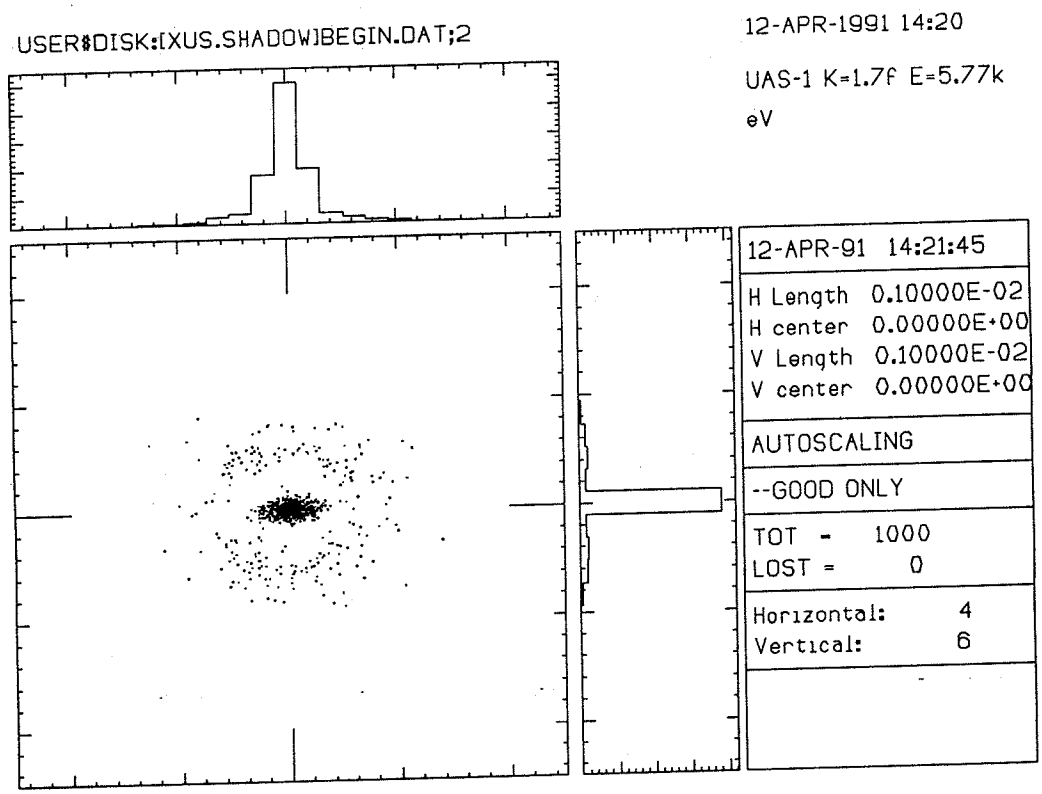


Fig. UA-13. K = 1.7, first harmonic.

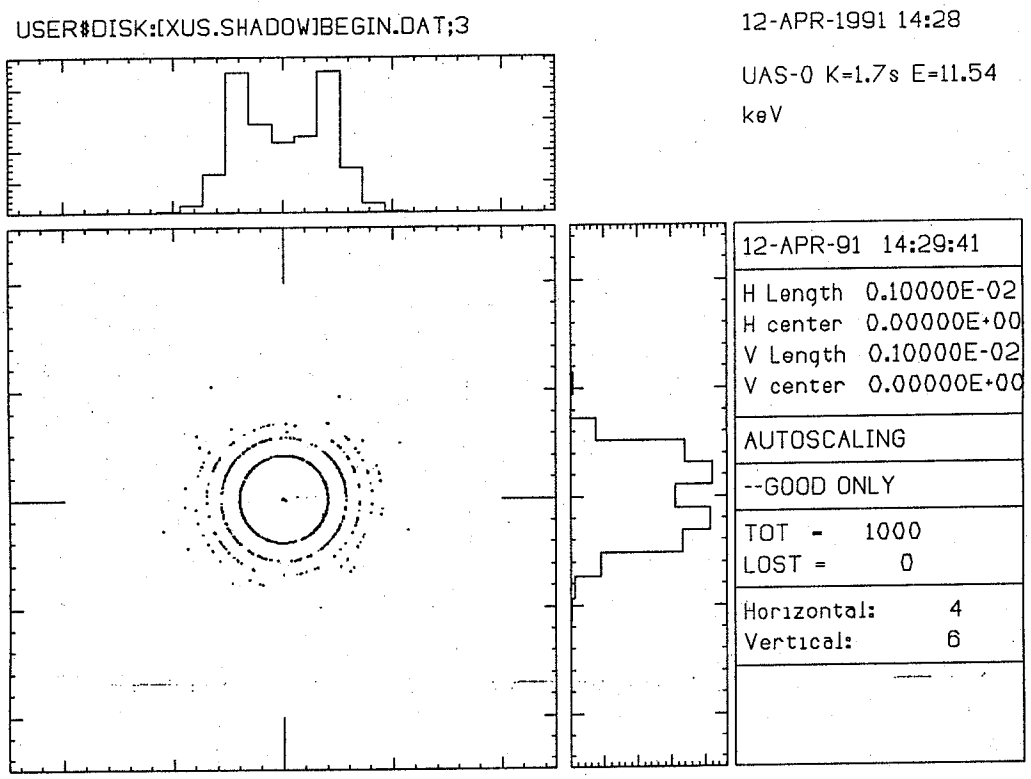


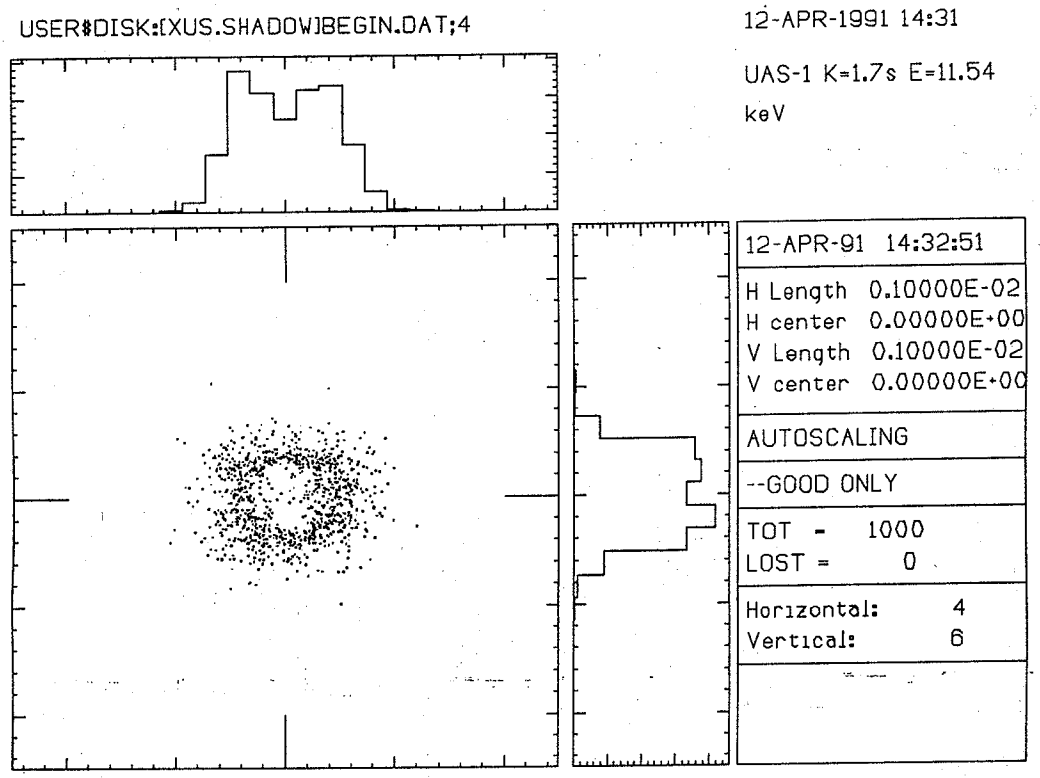


Fig. UA-14. K = 1.7, second harmonic.

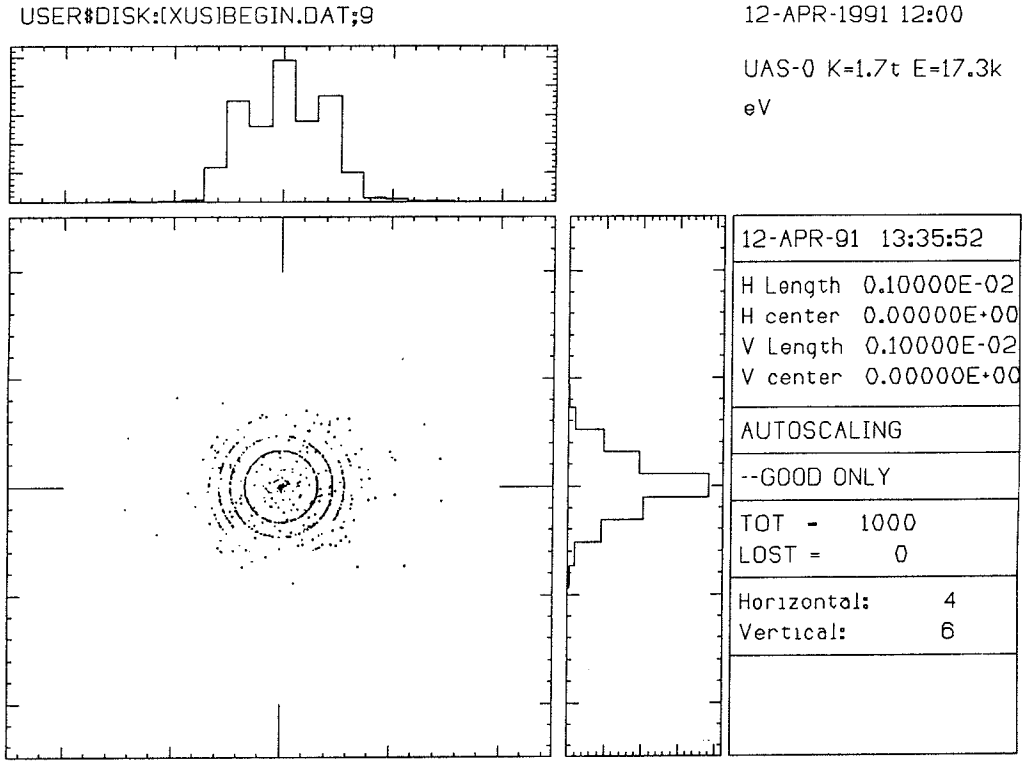


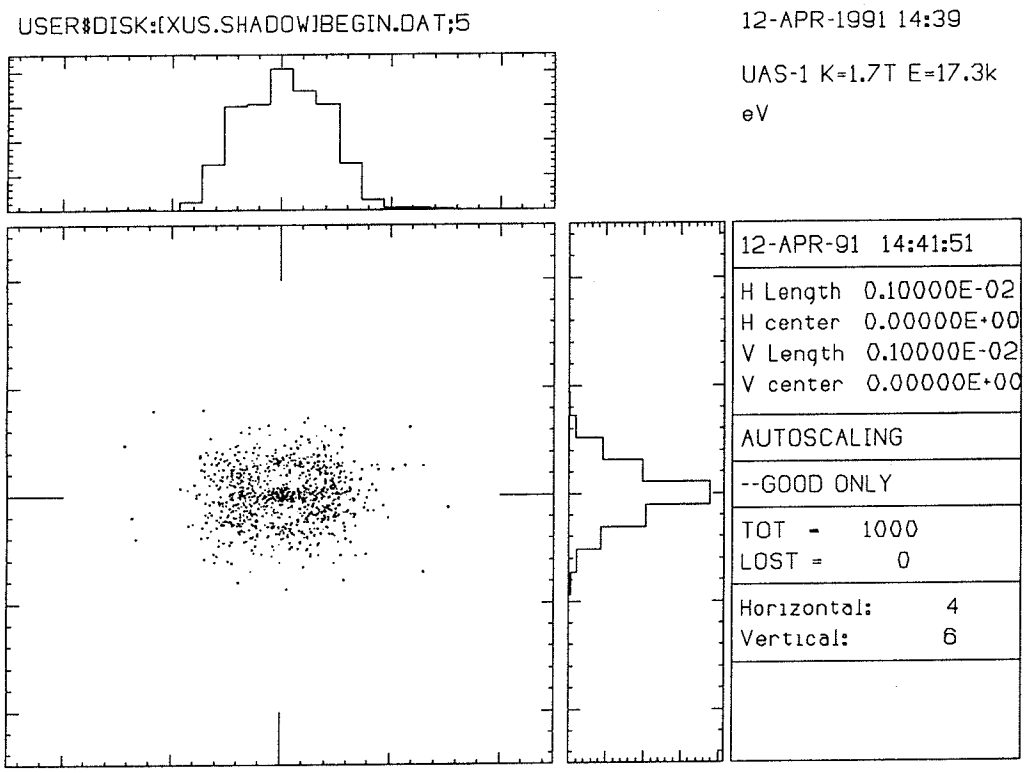


Fig. UA-15. K = 1.7, third harmonic.

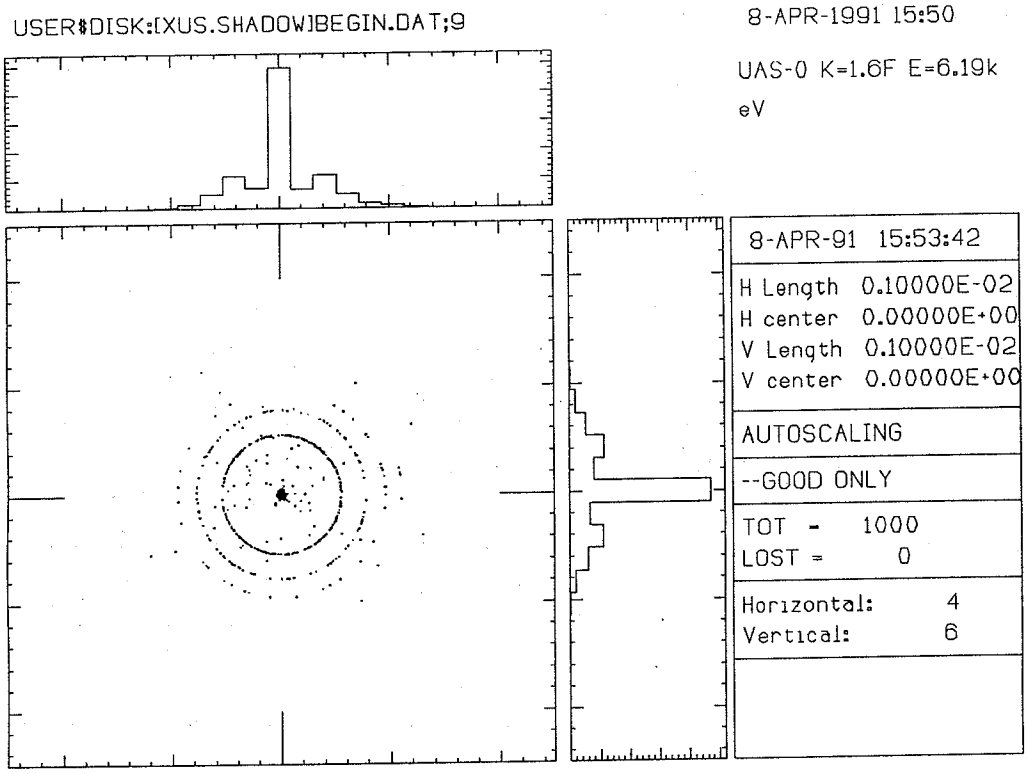


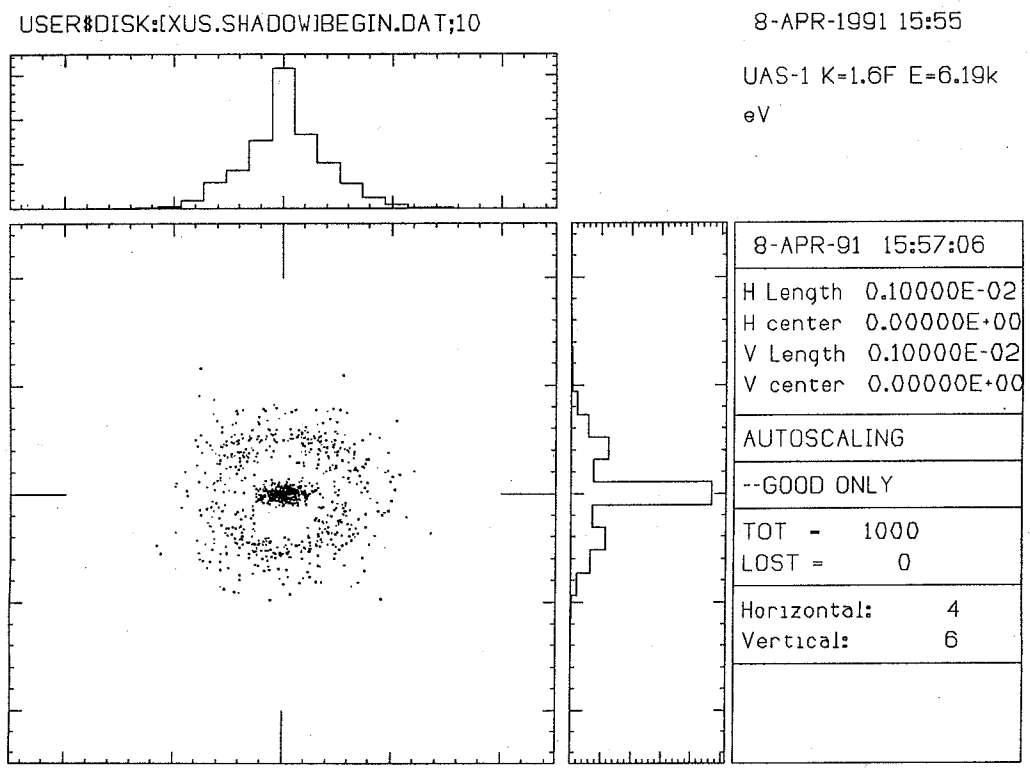


Fig. UA-16. K = 1.6, first harmonic.

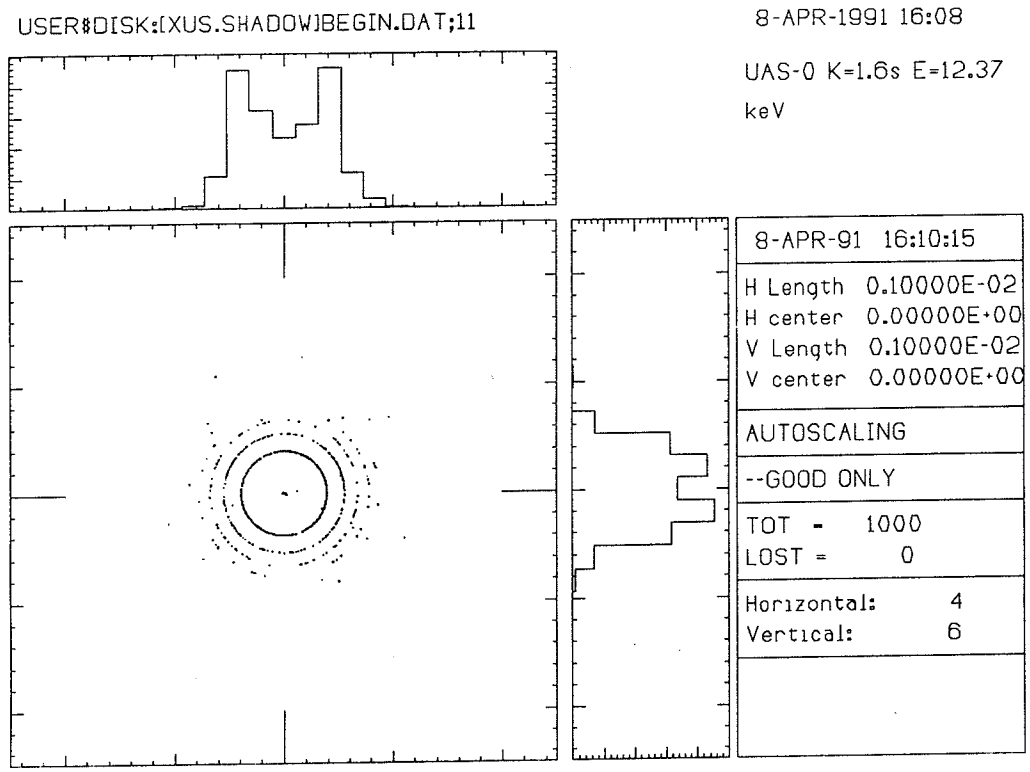


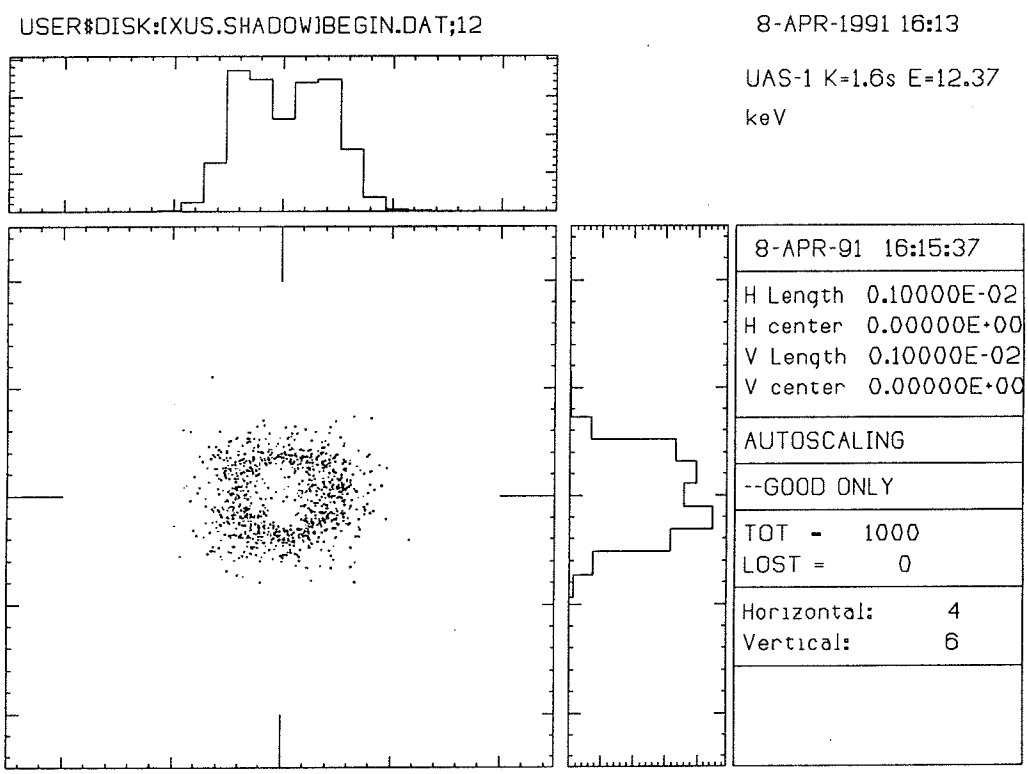


Fig. UA-17. K = 1.6, second harmonic.

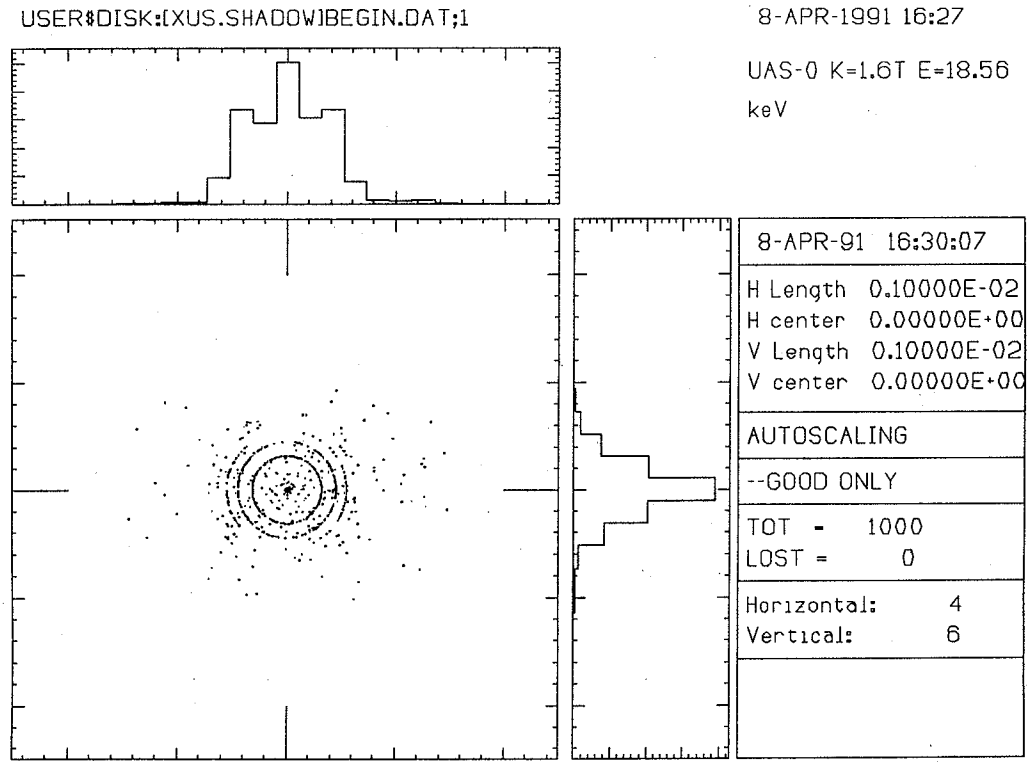


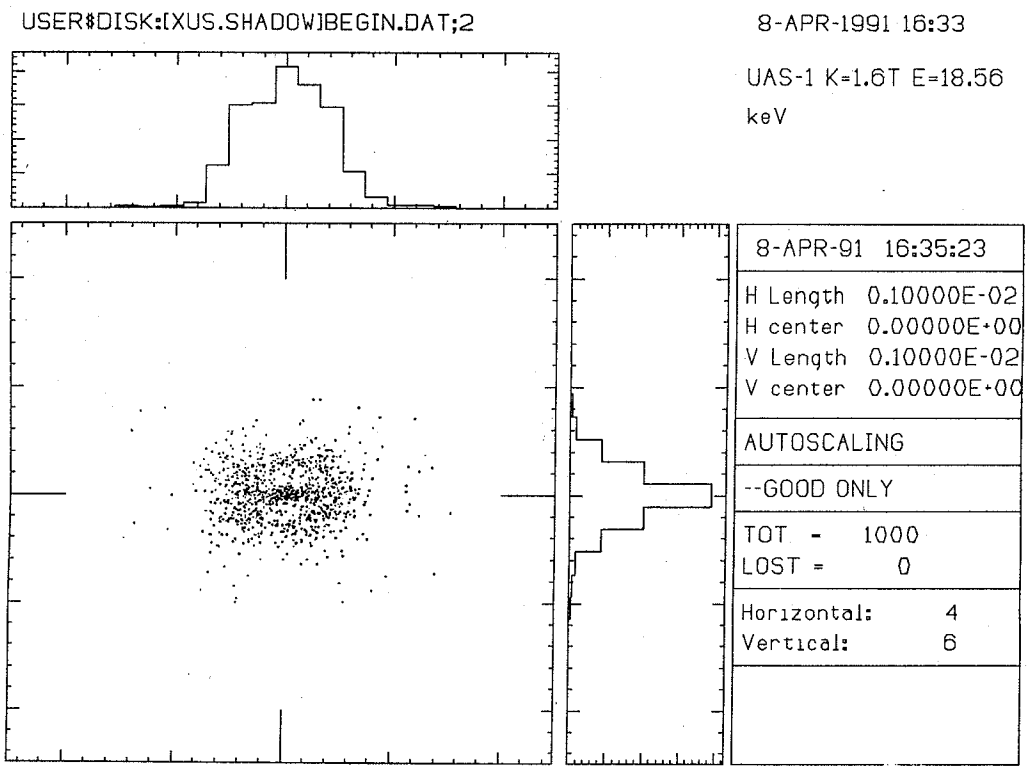


Fig. UA-18. K = 1.6, third harmonic.

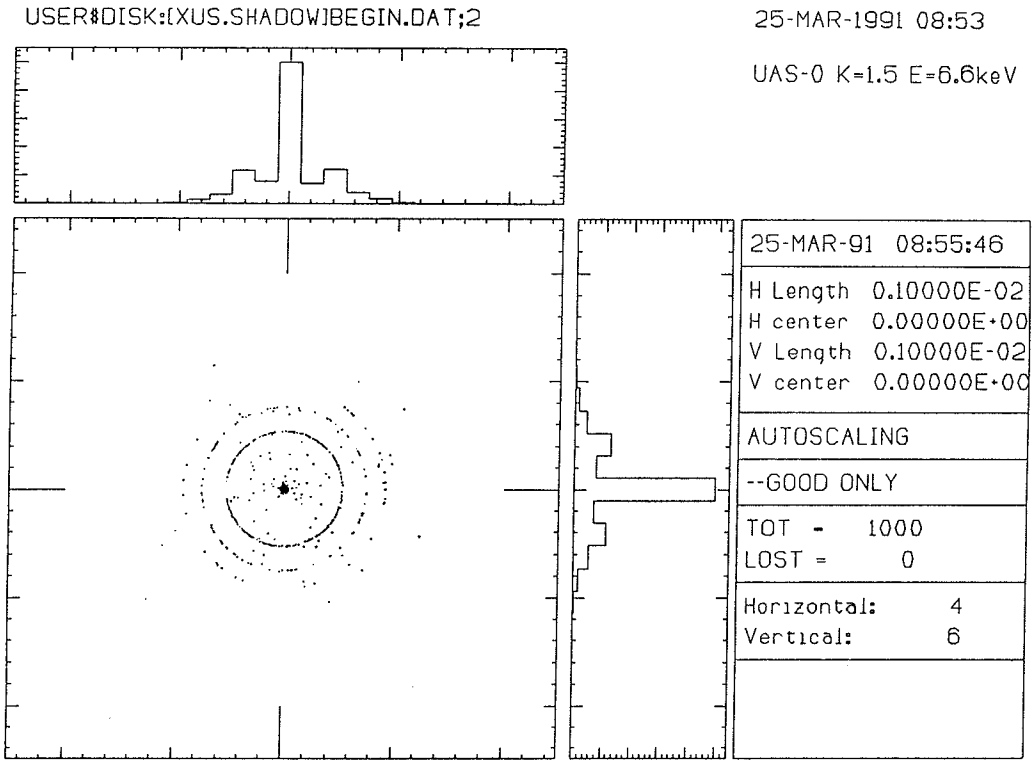


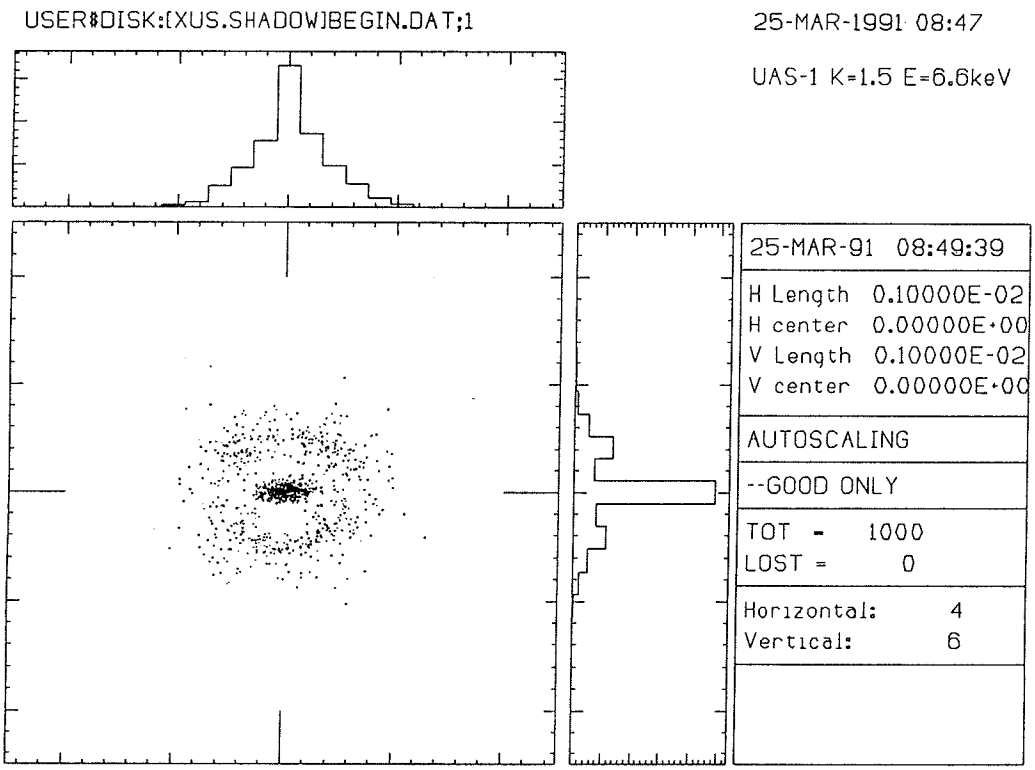


Fig. UA-19. K = 1.5, first harmonic.

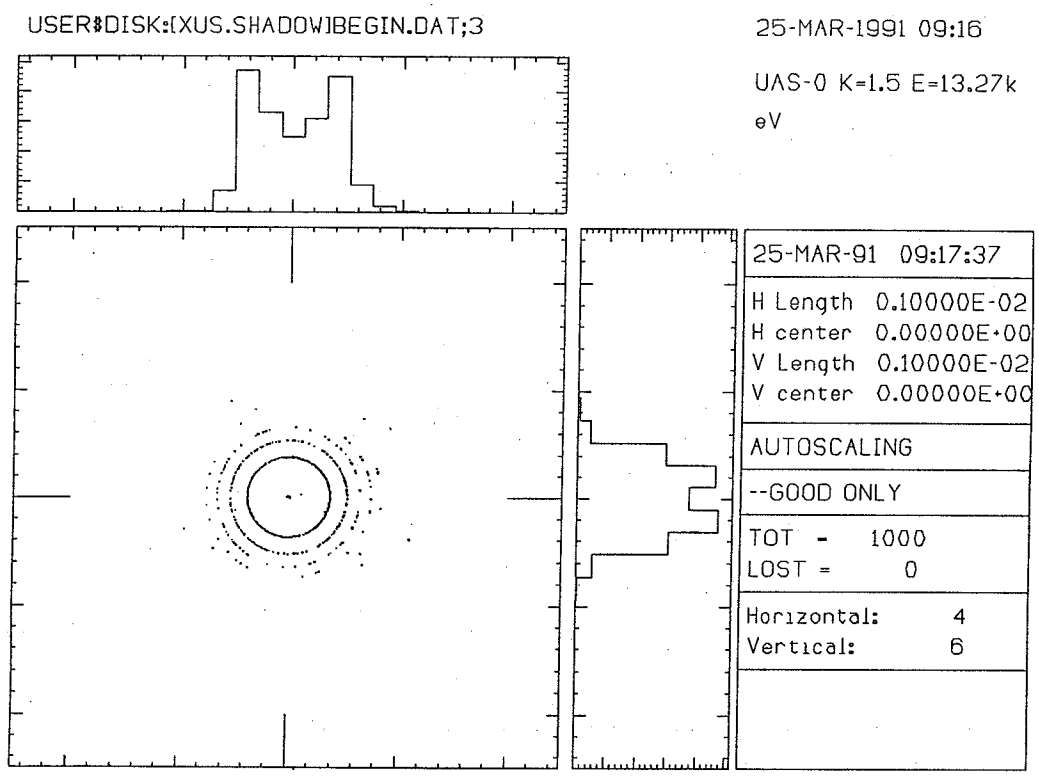


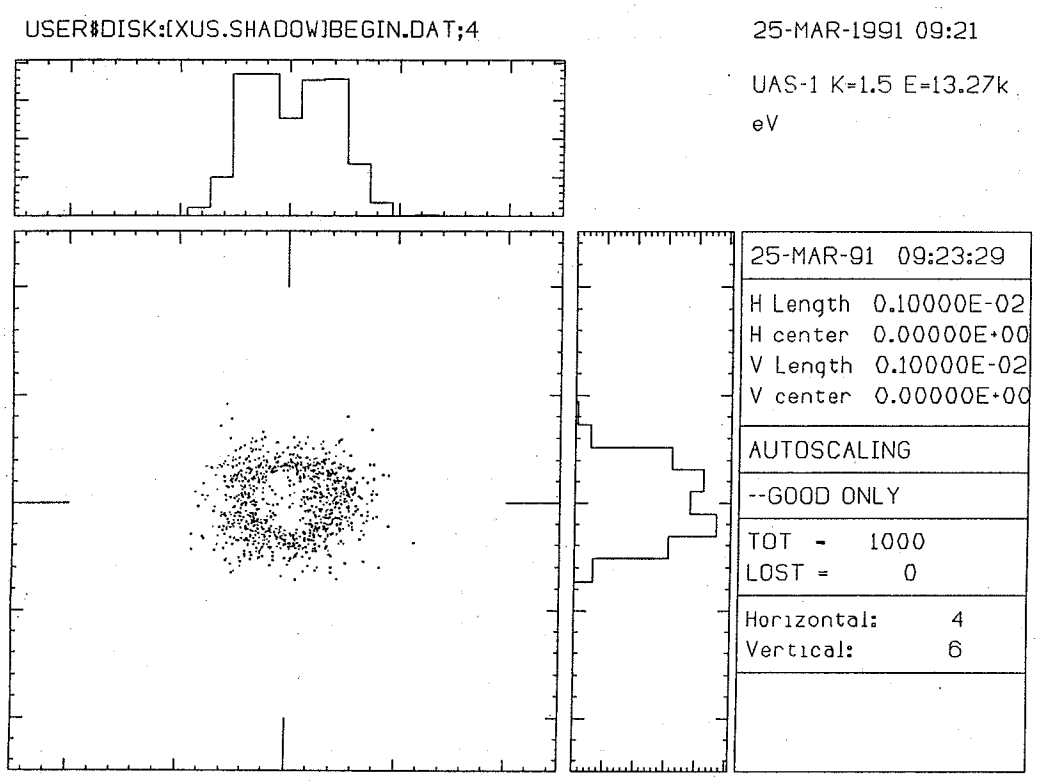


Fig. UA-20. K = 1.5, second harmonic.

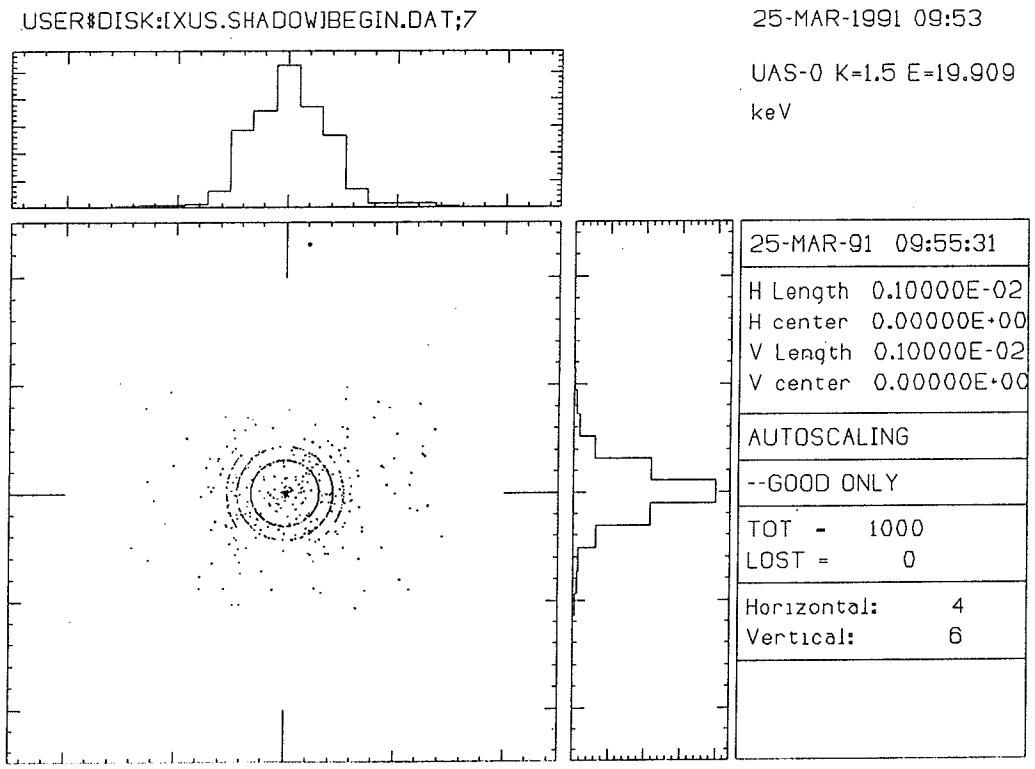


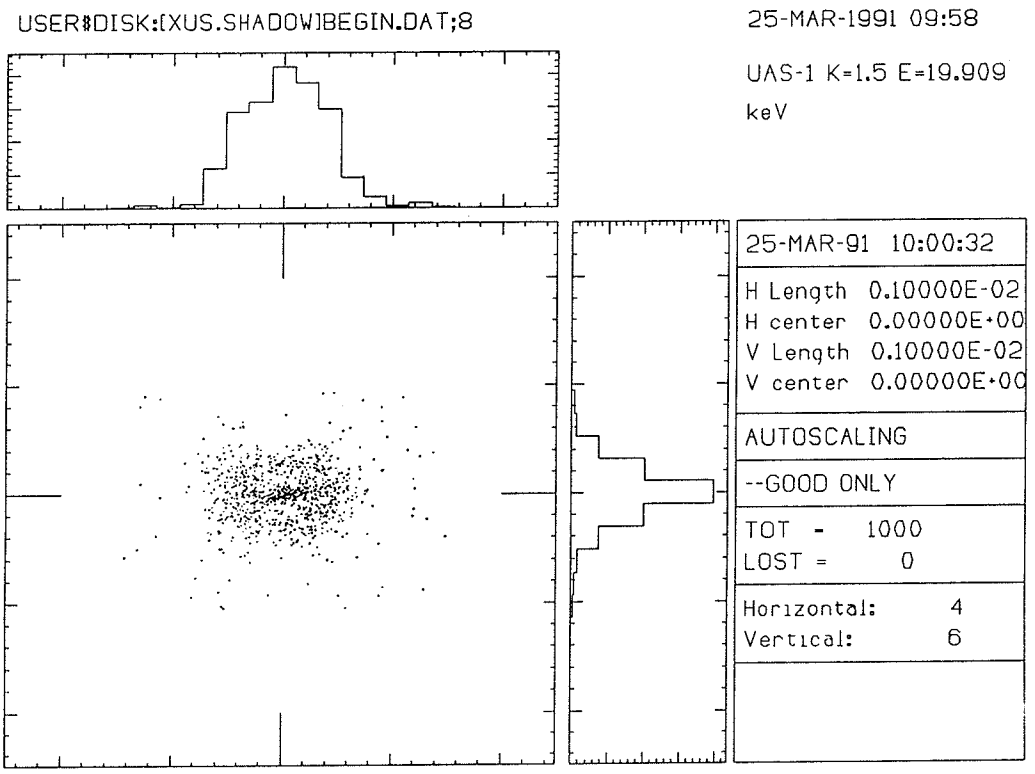


Fig. UA-21. K = 1.5, third harmonic.

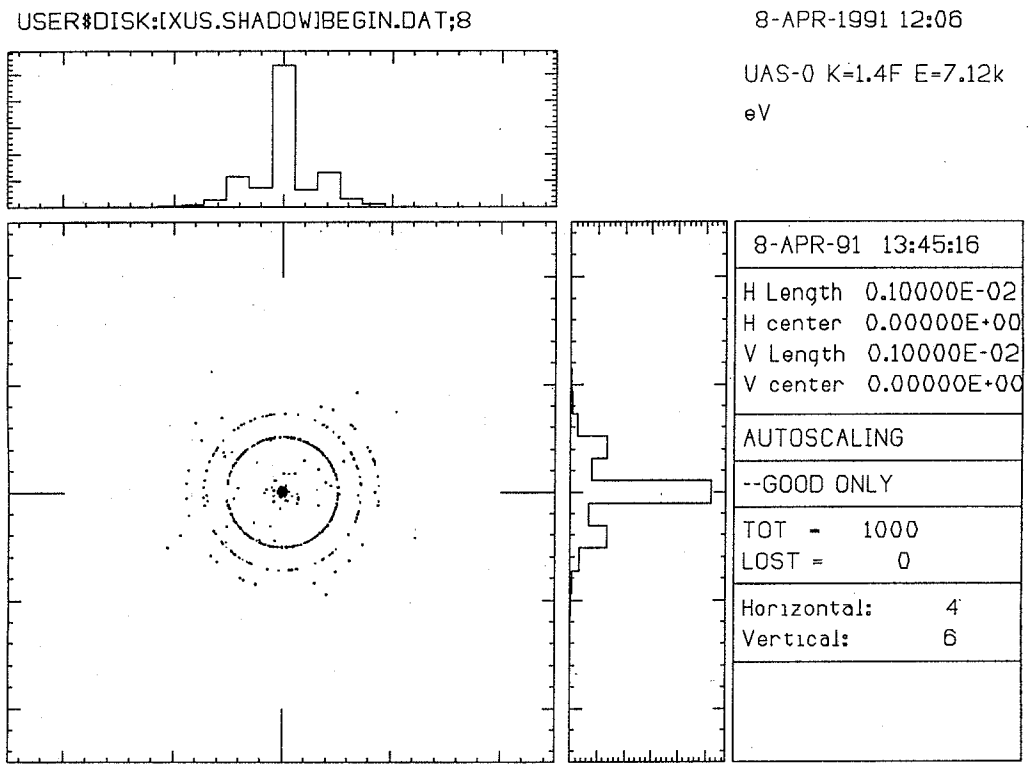


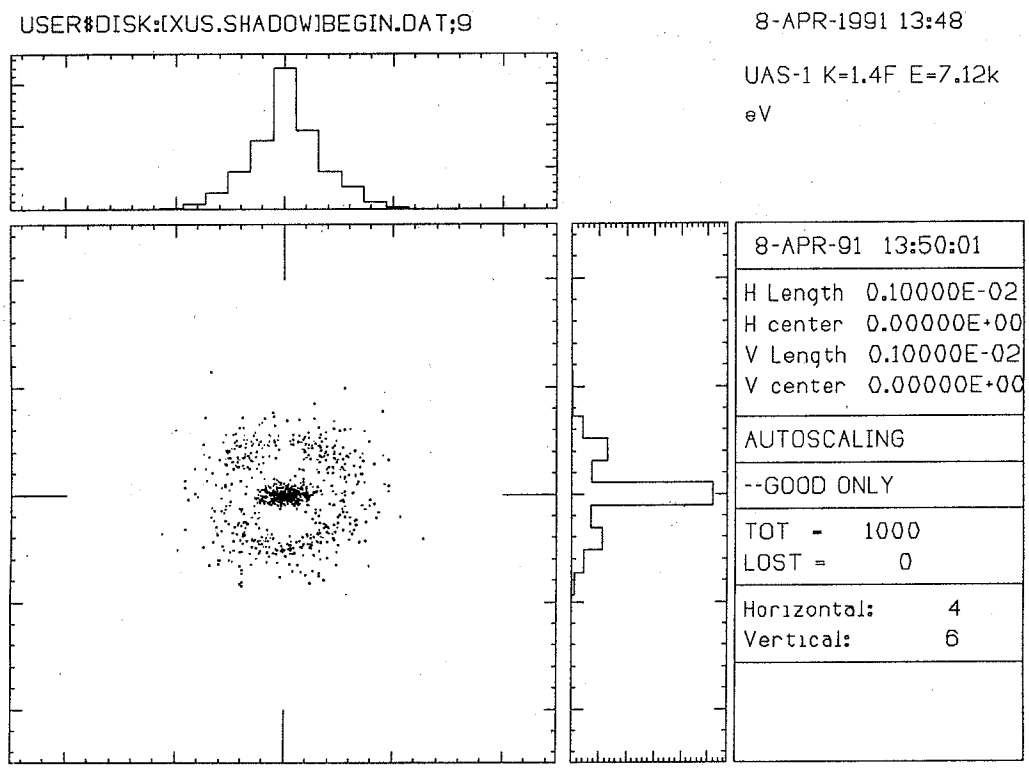


Fig. UA-22. K = 1.4, first harmonic.

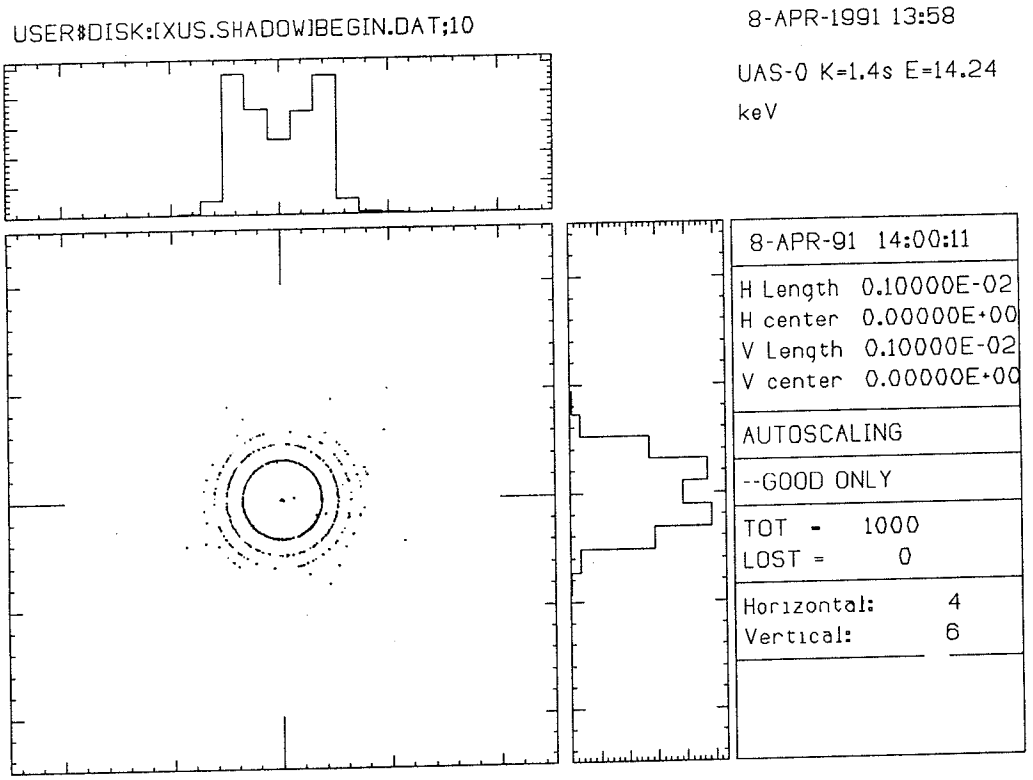


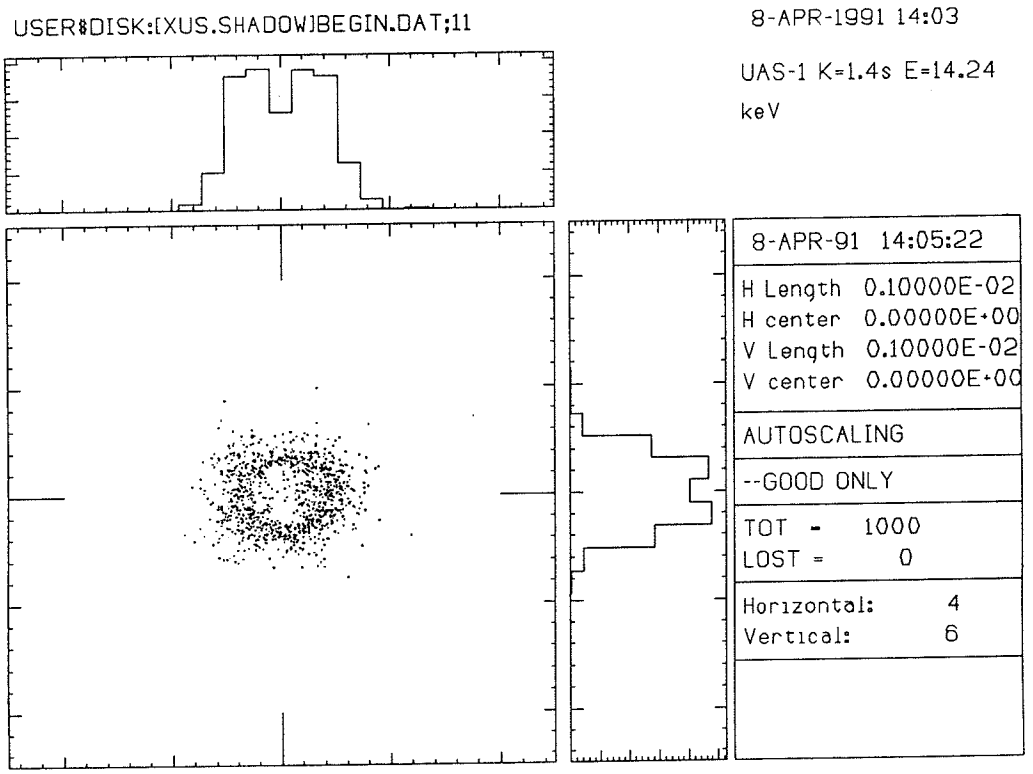


Fig. UA-23. K = 1.4, second harmonic.

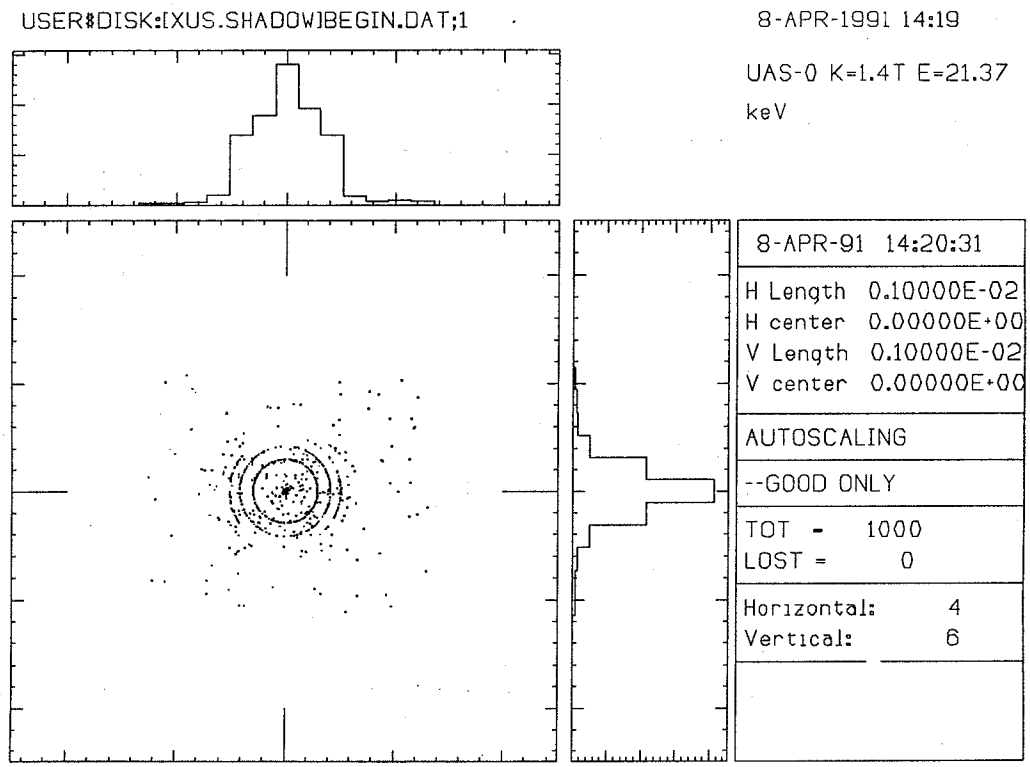


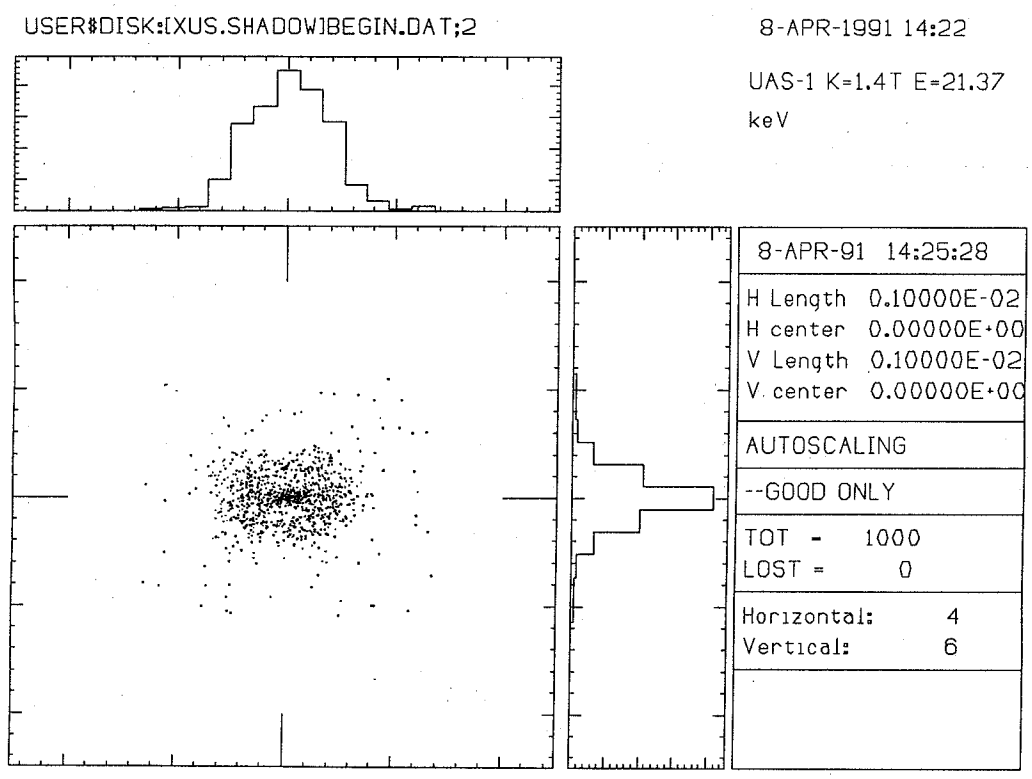


Fig. UA-24. K = 1.4, third harmonic.

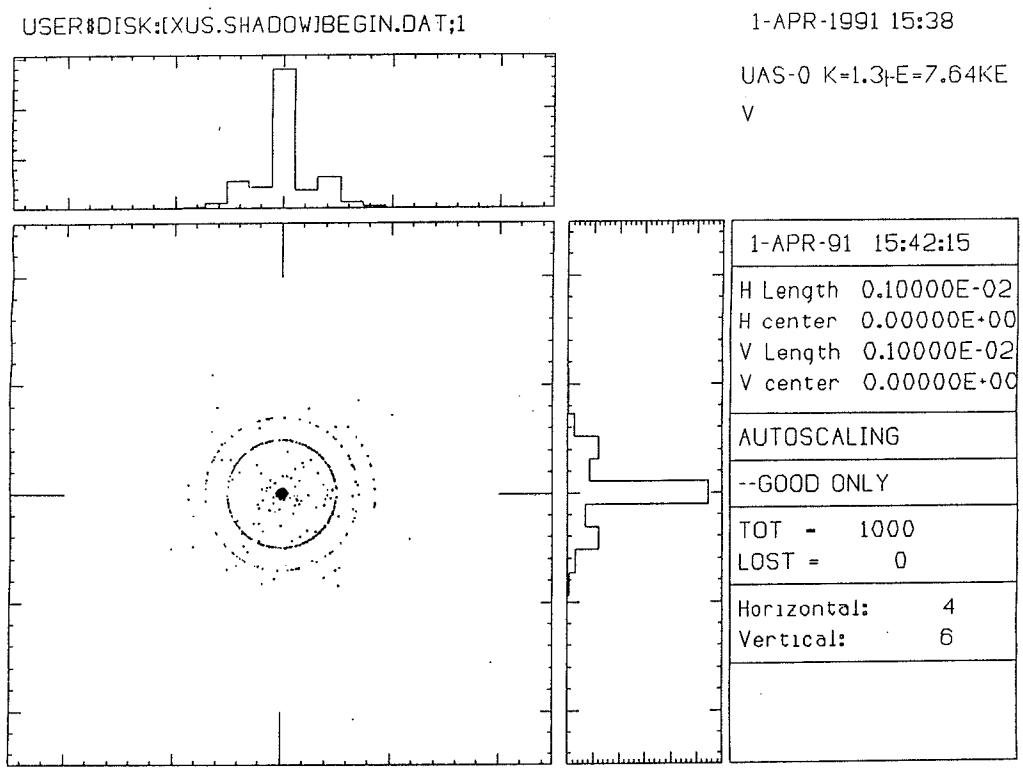


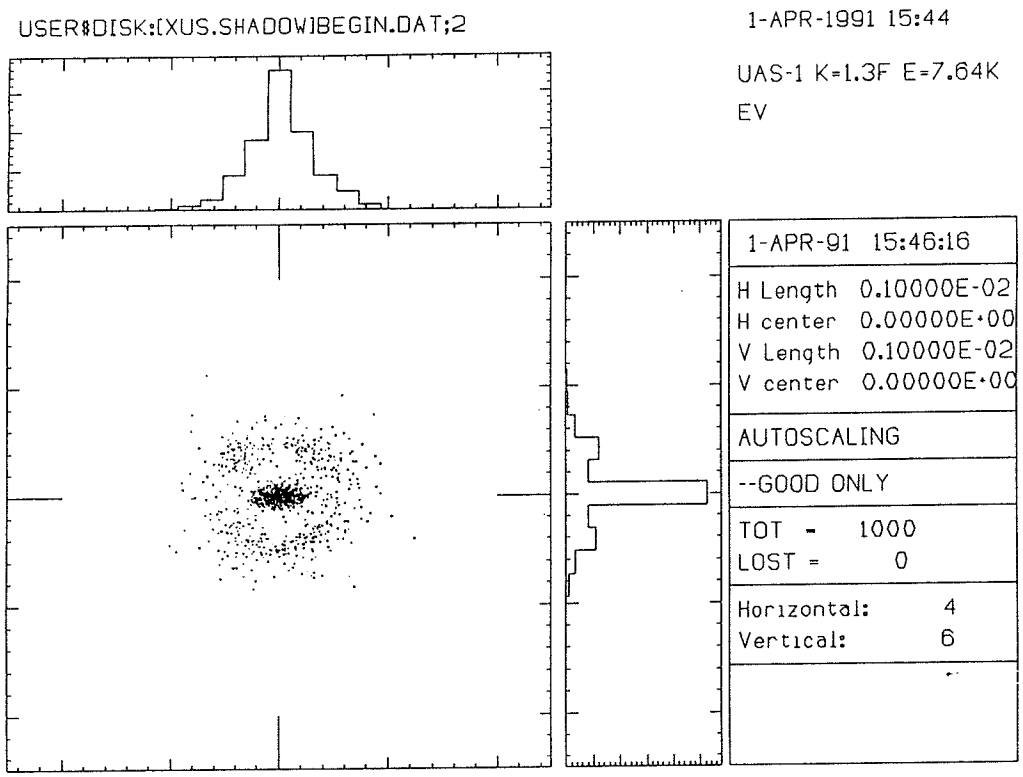


Fig. UA-25. K = 1.3, first harmonic.

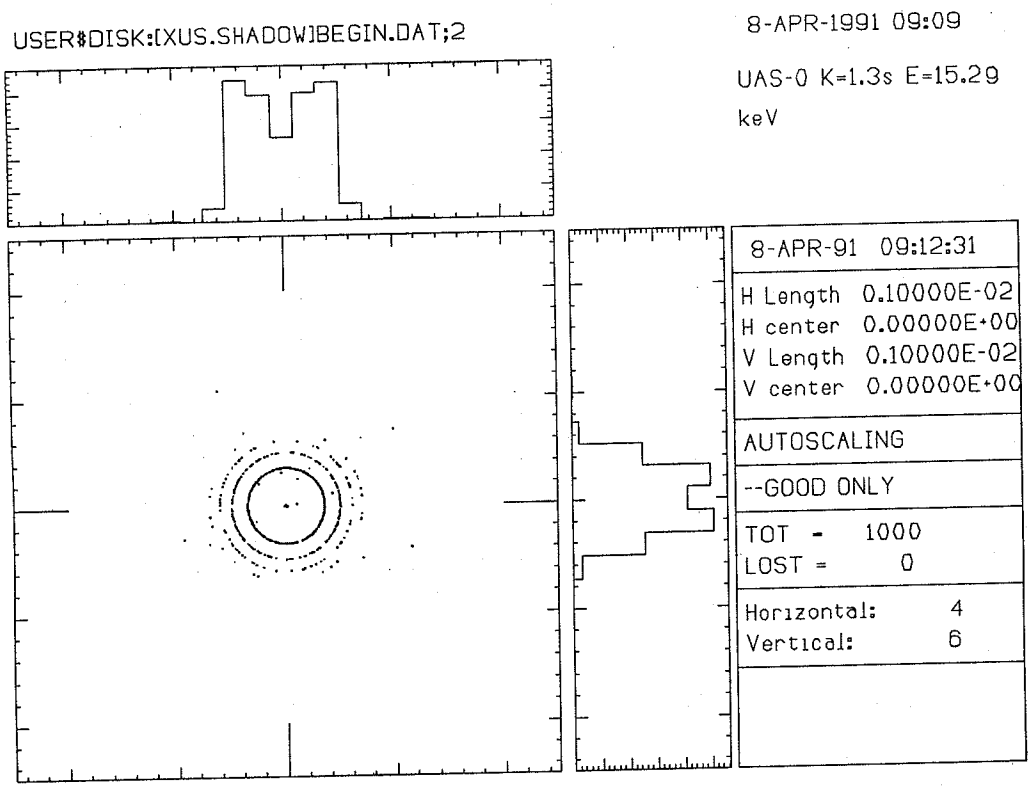


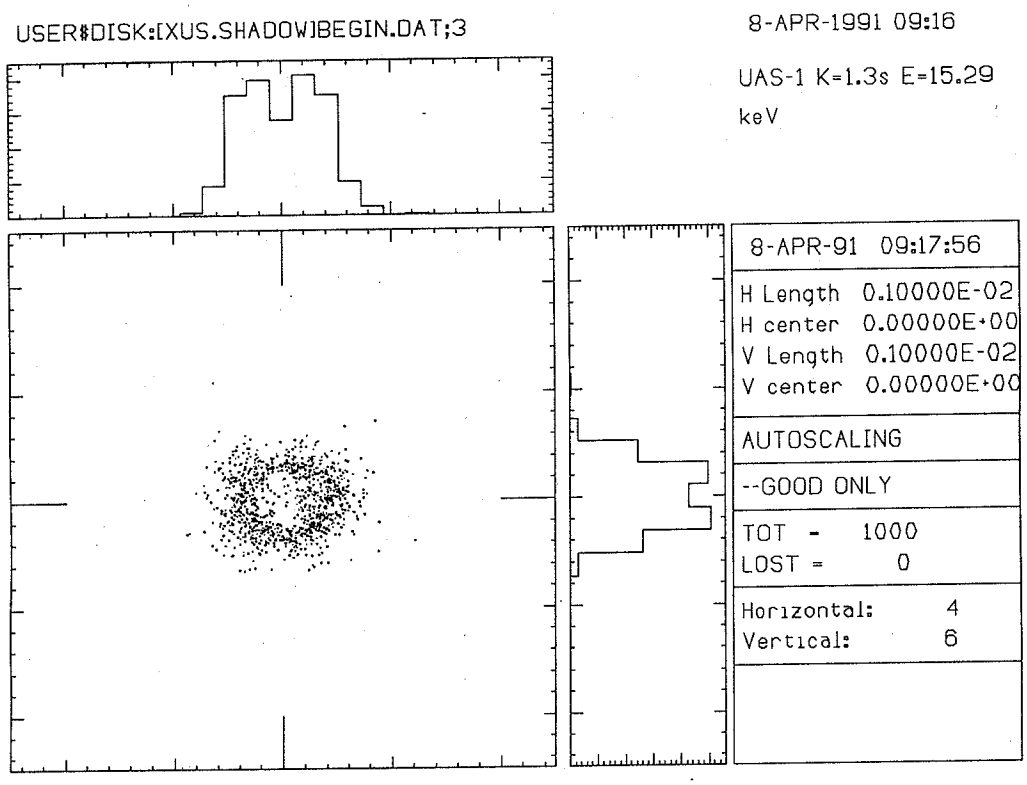


Fig. UA-26. K = 1.3, second harmonic.

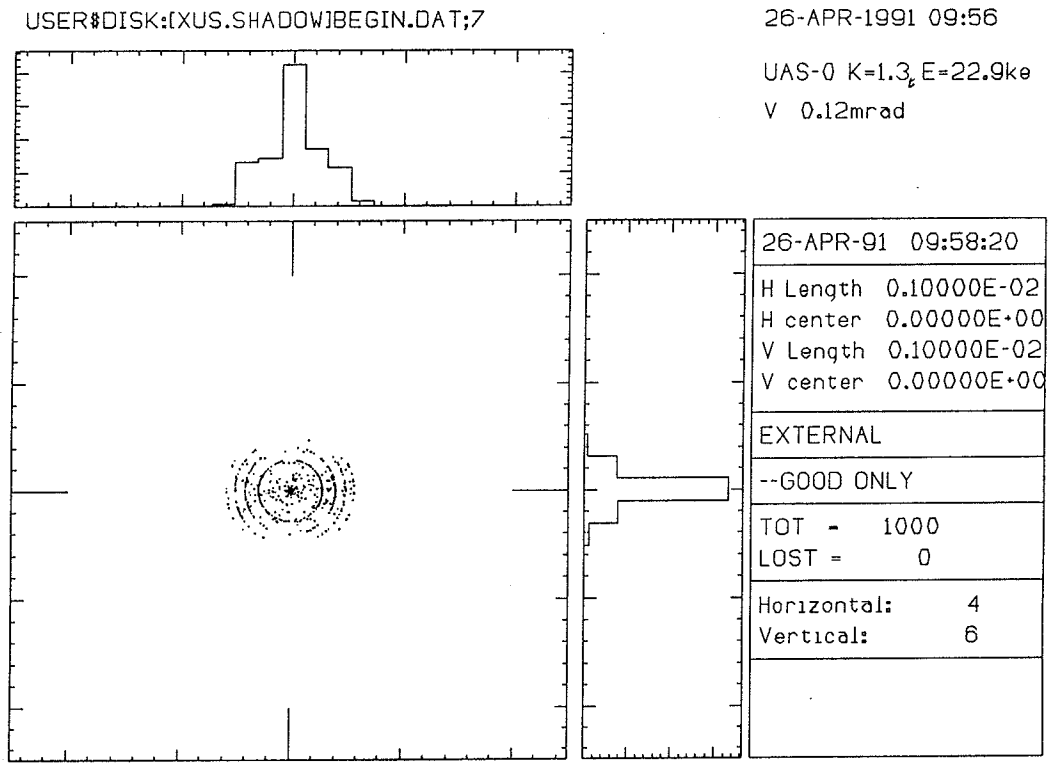


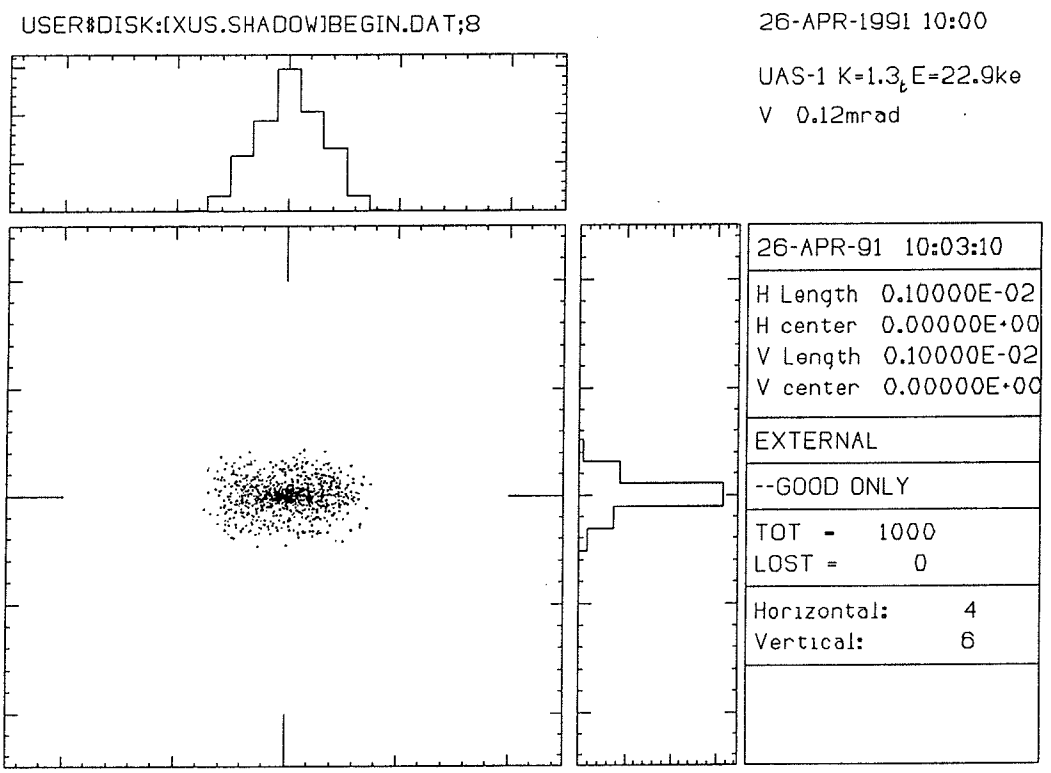


Fig. UA-27. K = 1.3, third harmonic.

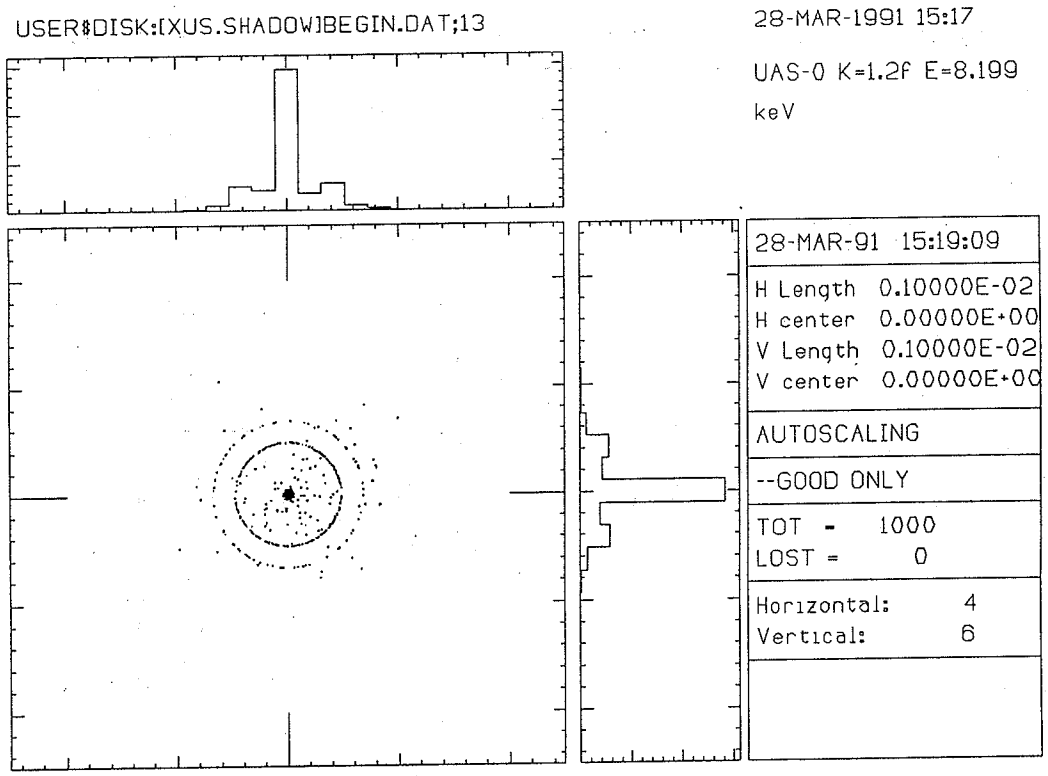


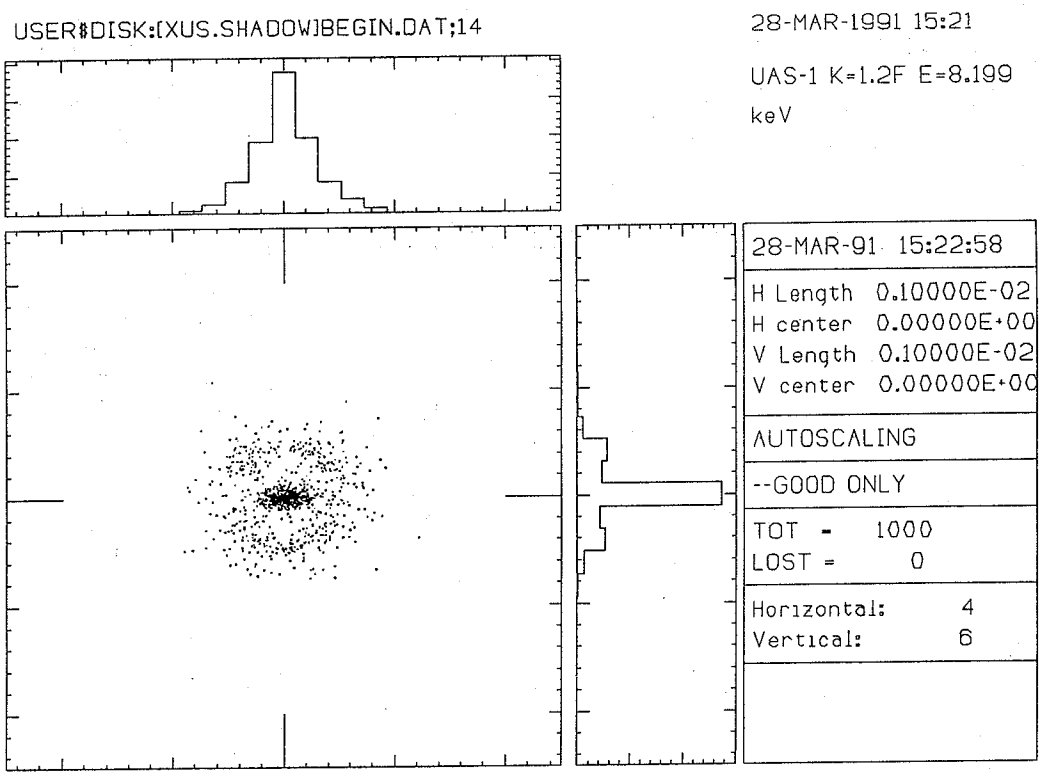


Fig. UA-28. K = 1.2, first harmonic.

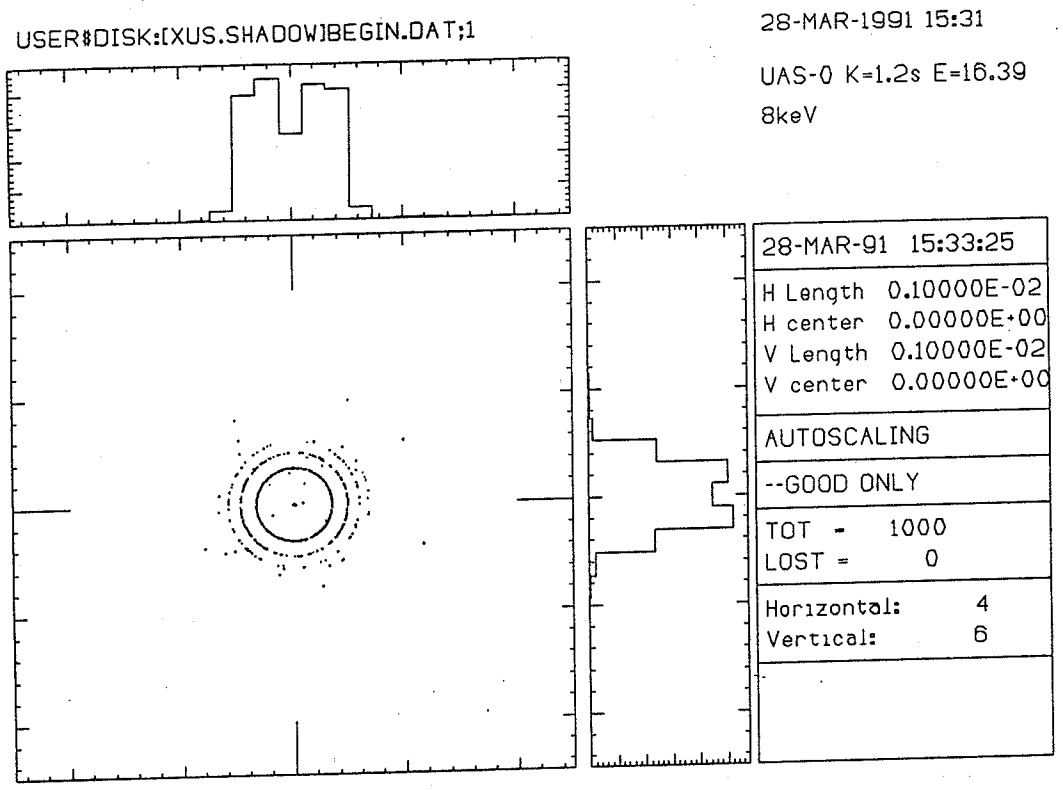


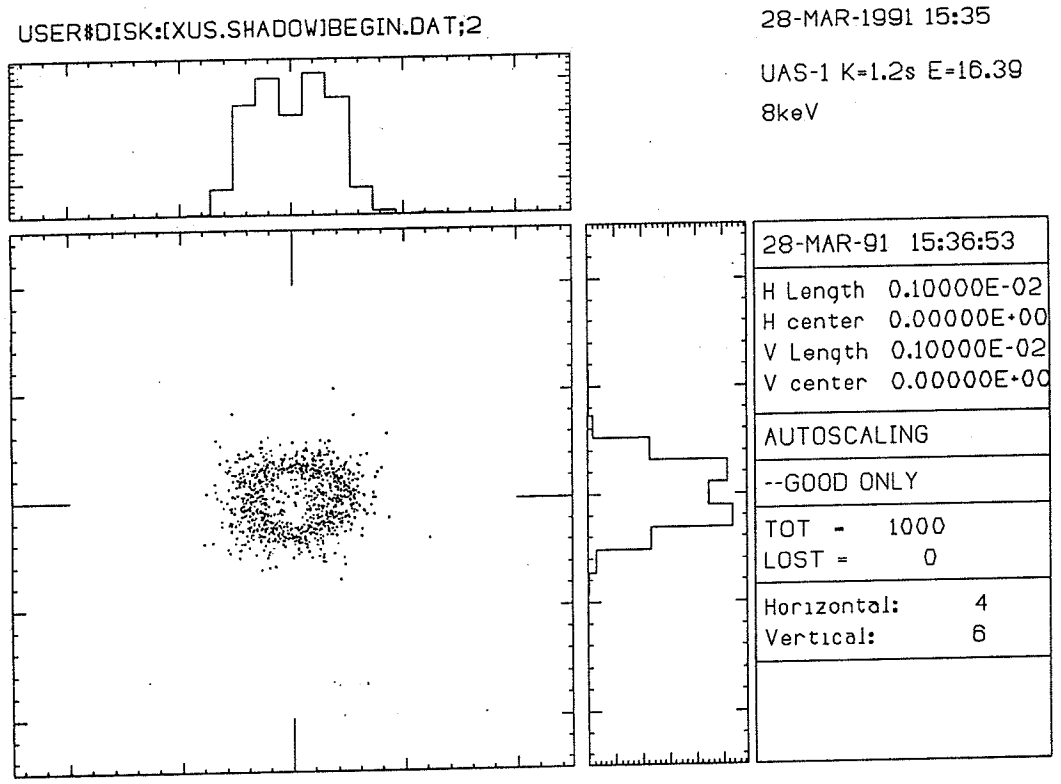


Fig. UA-29. K = 1.2, second harmonic.

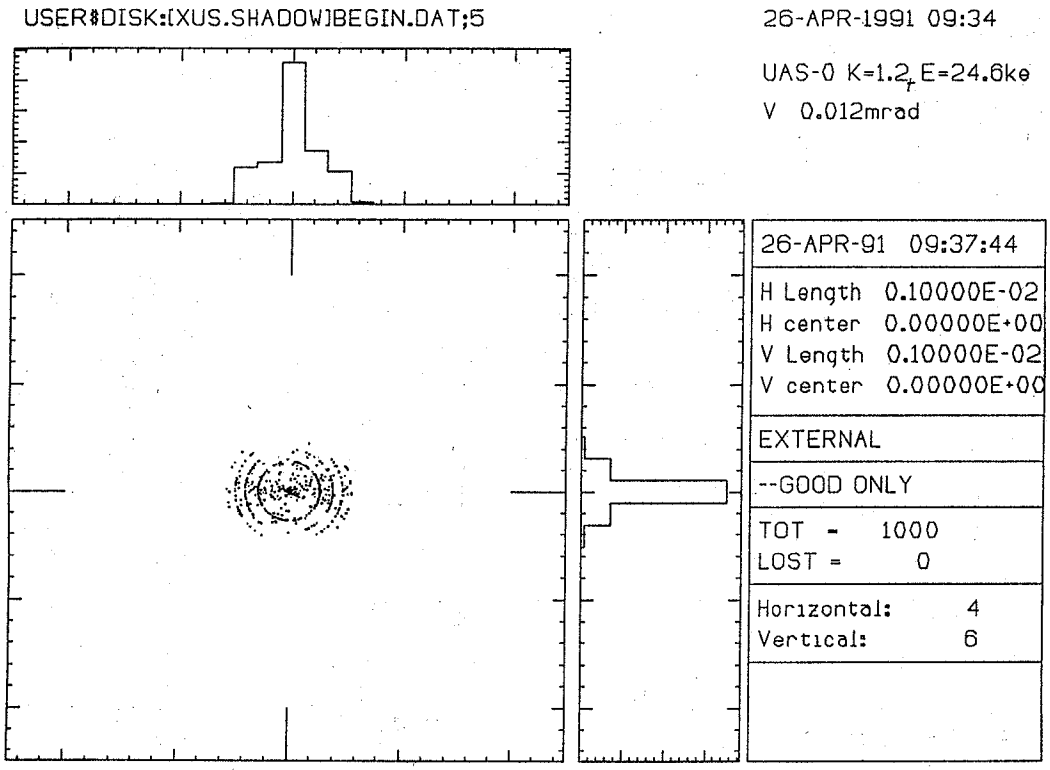


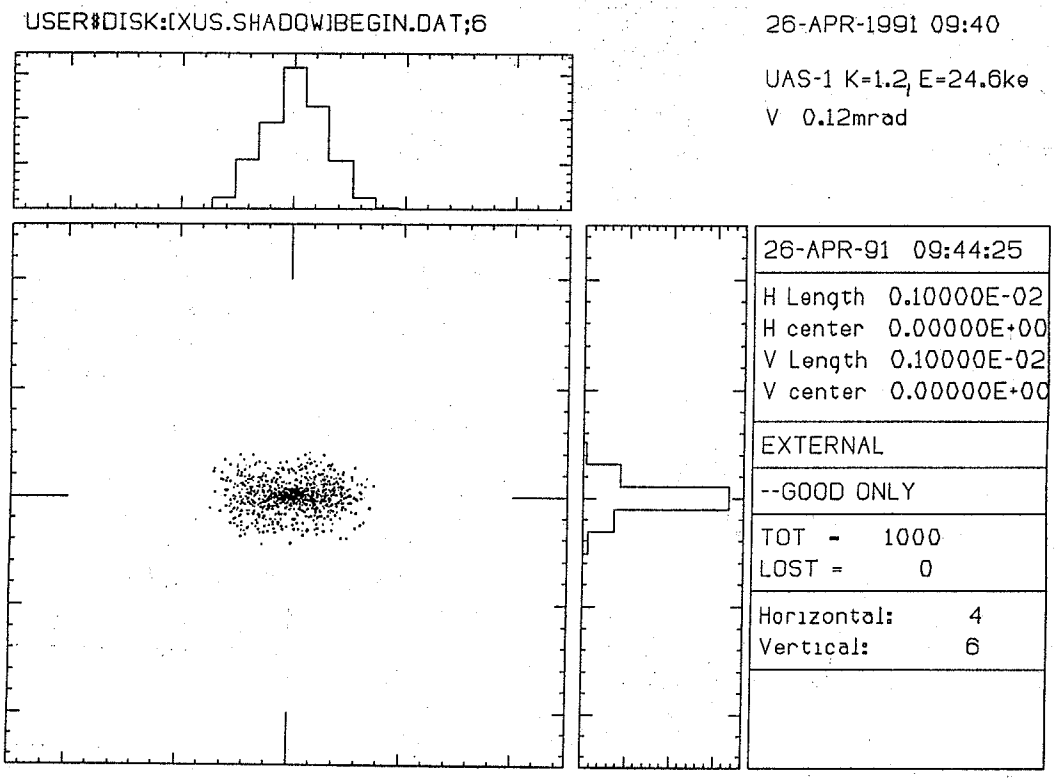


Fig. UA-30. K = 1.2, third harmonic.

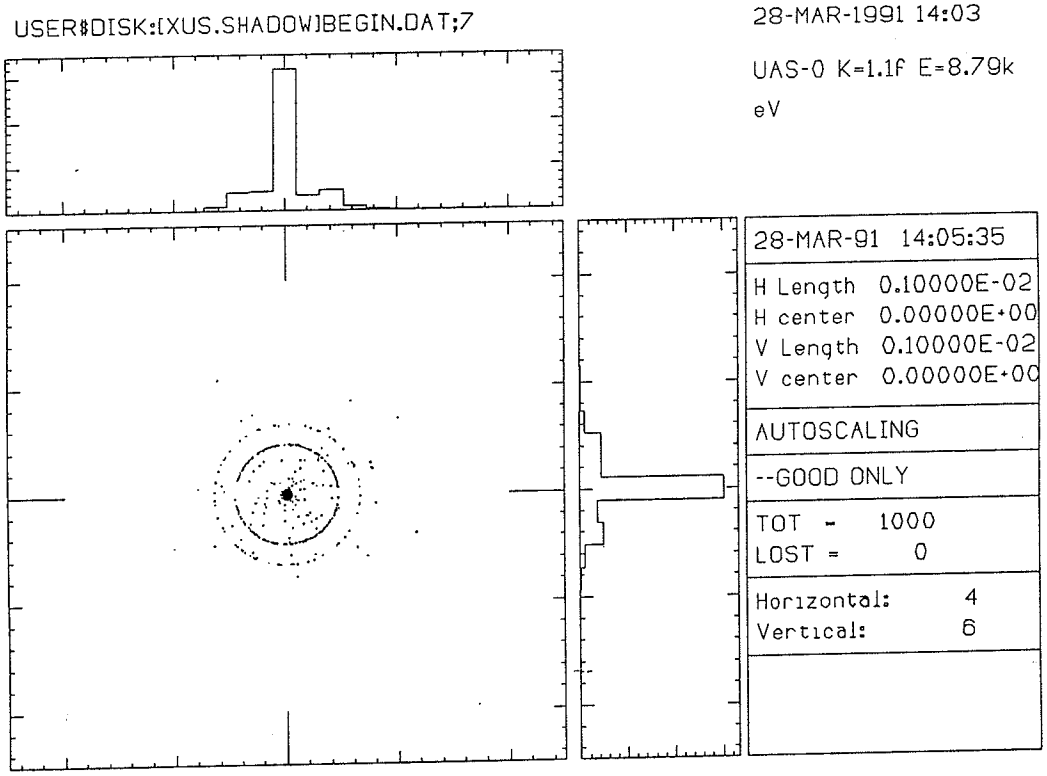


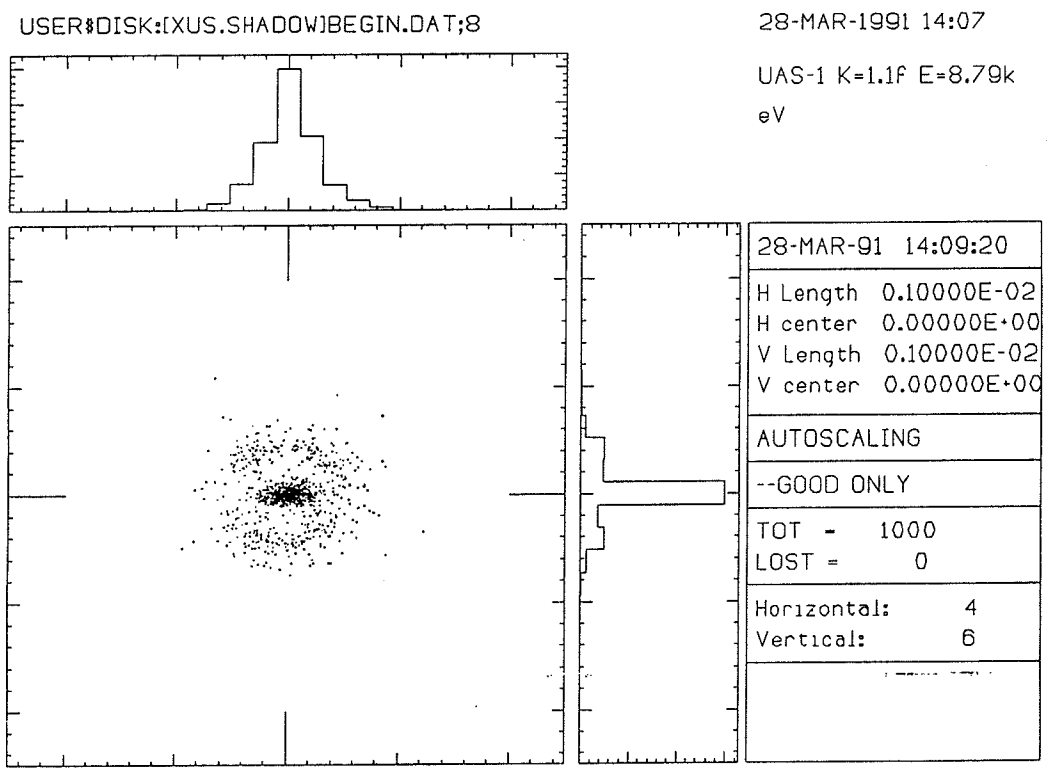


Fig. UA-31. K = 1.1, first harmonic.

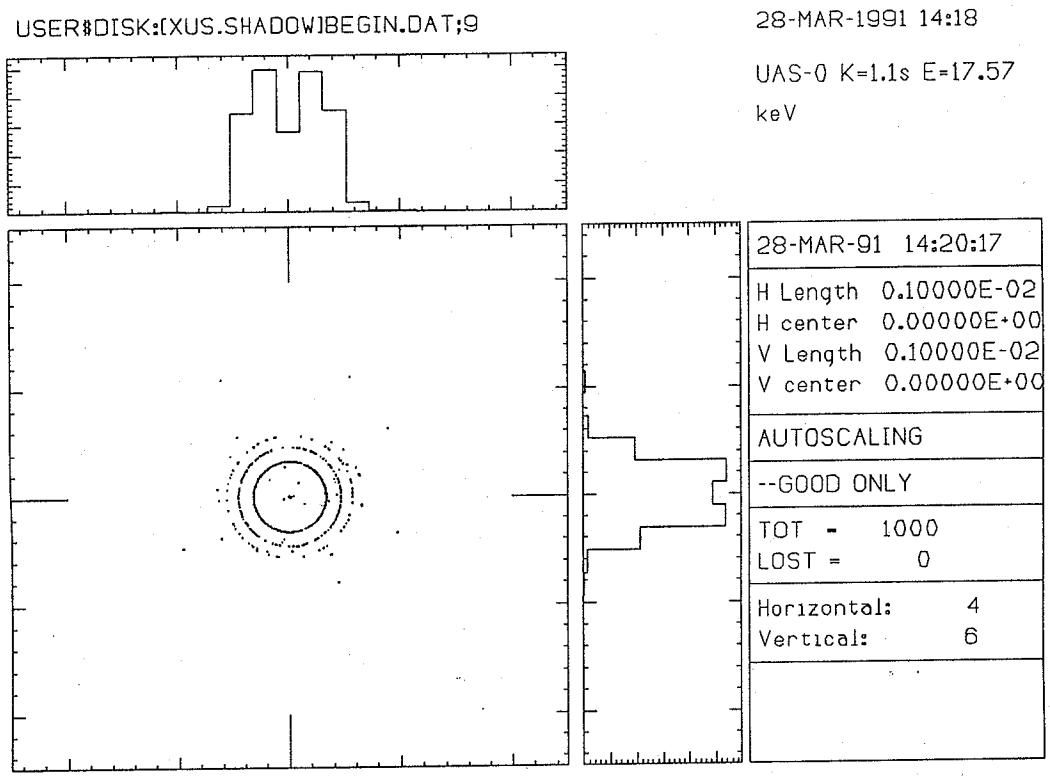


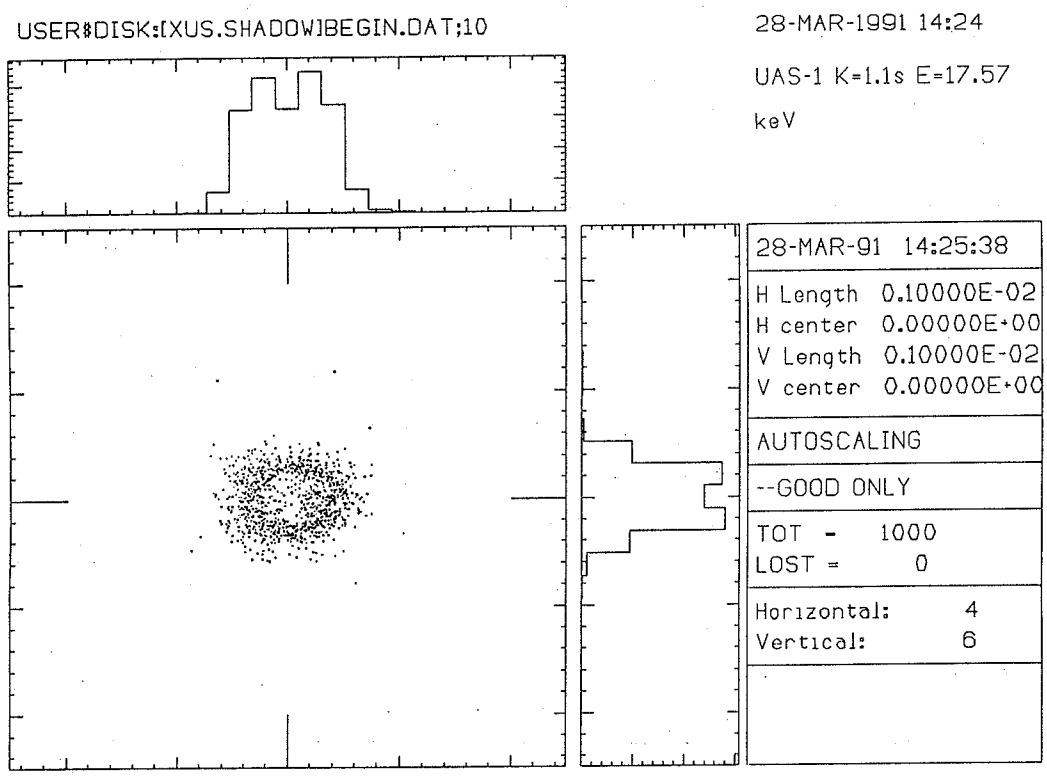


Fig. UA-32. K = 1.1, second harmonic.

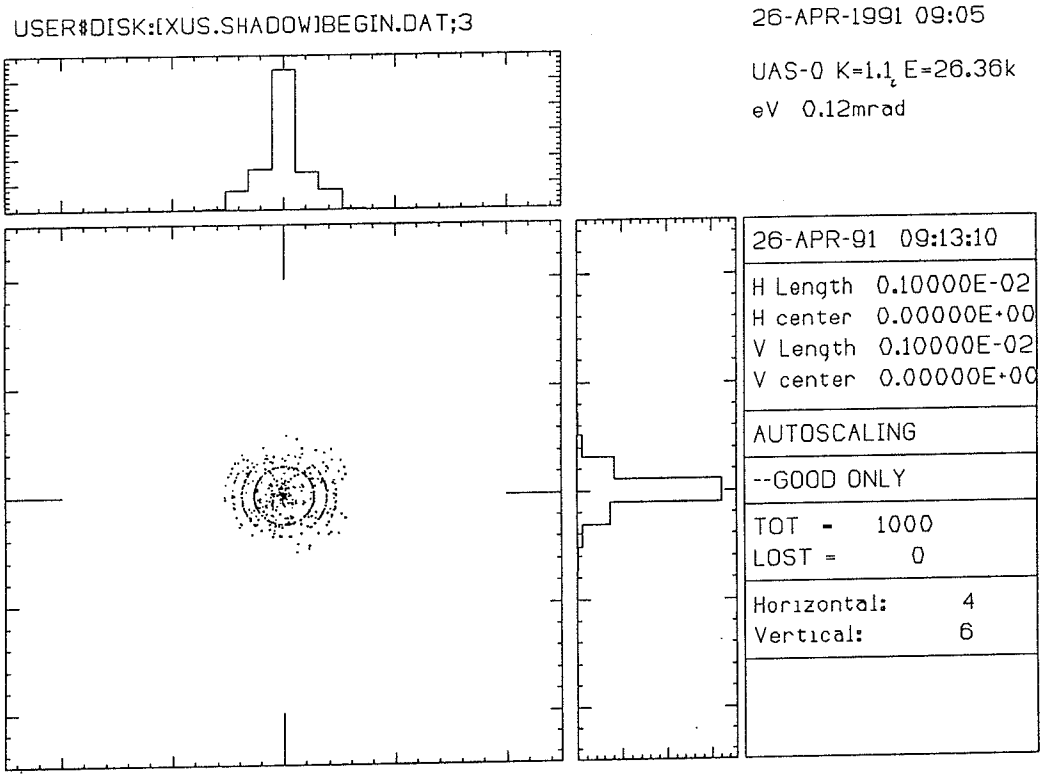


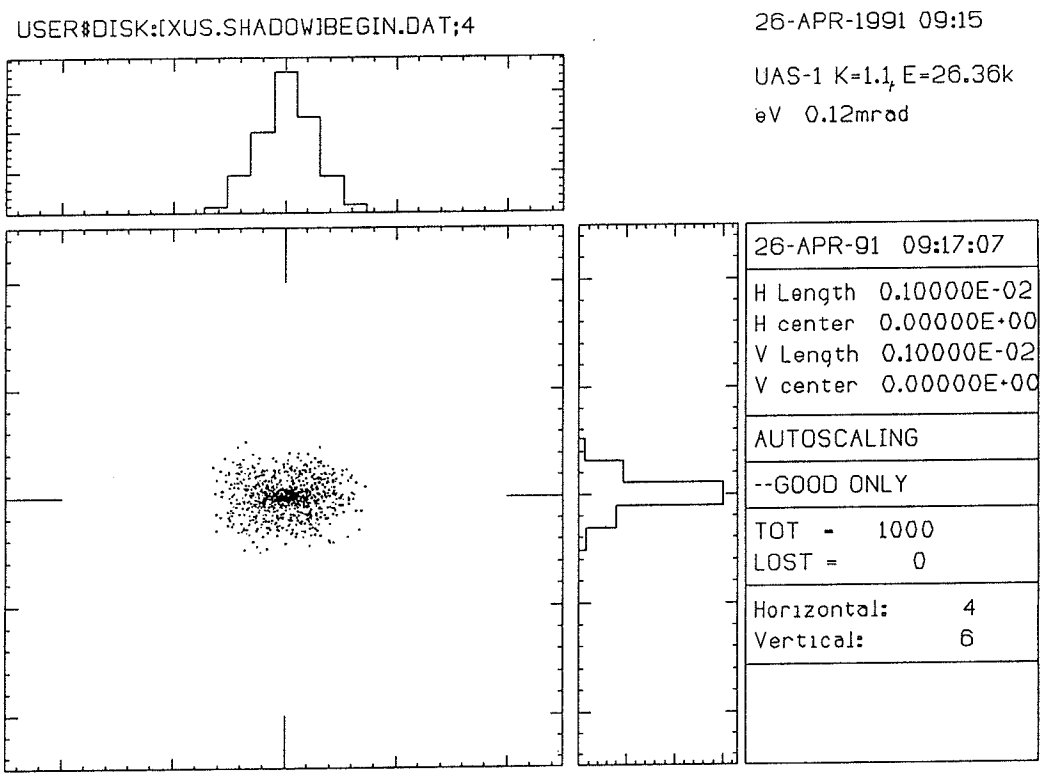


Fig. UA-33. K = 1.1, third harmonic.

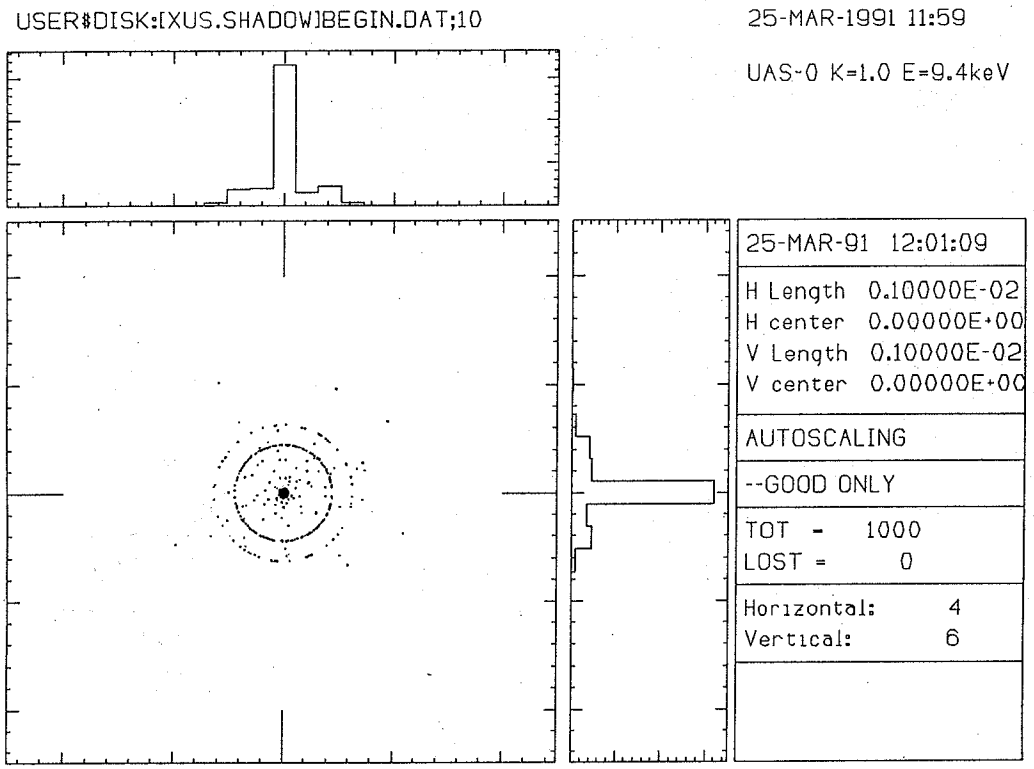


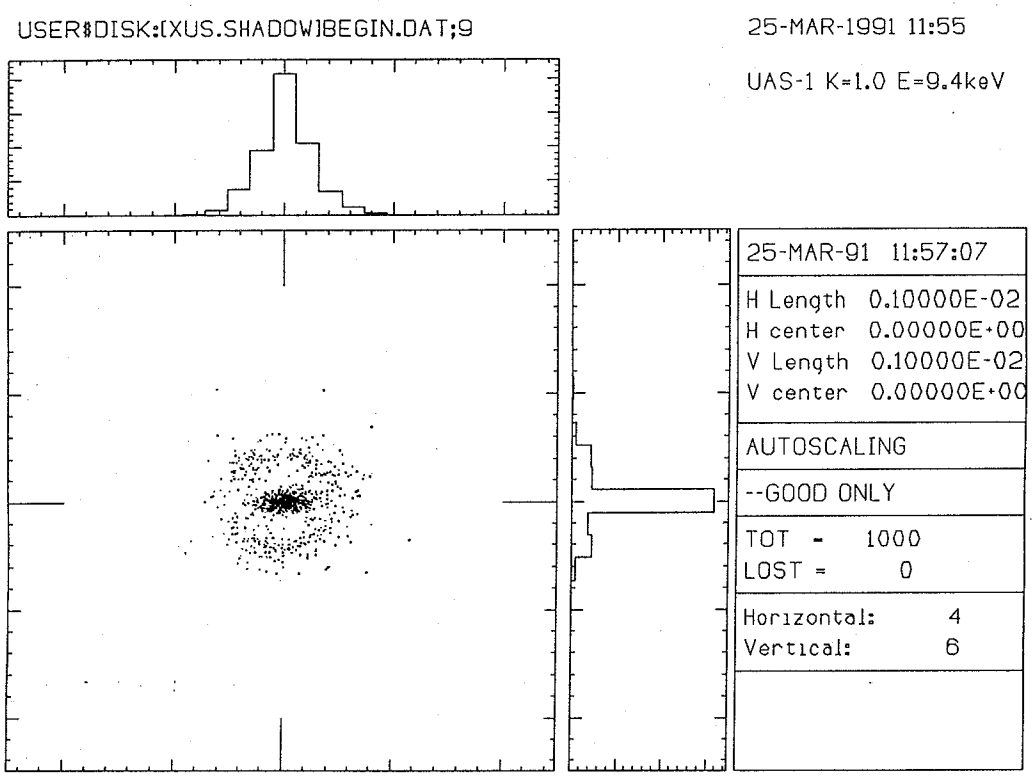


Fig. UA-34. K = 1.0, first harmonic.

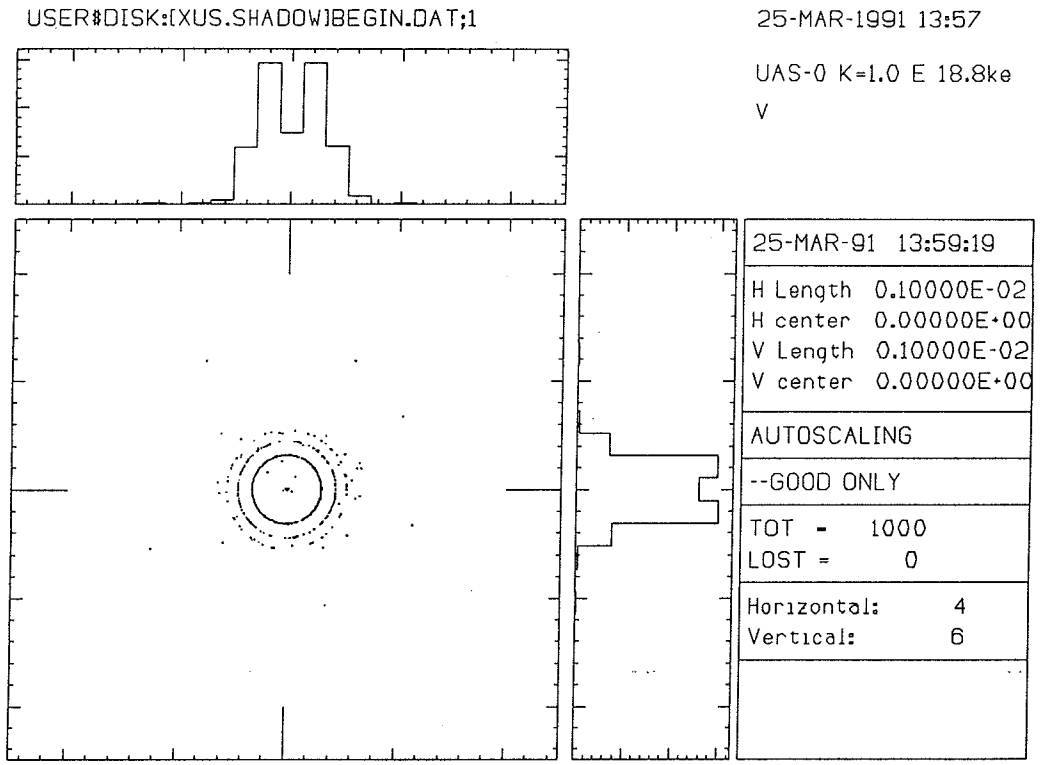


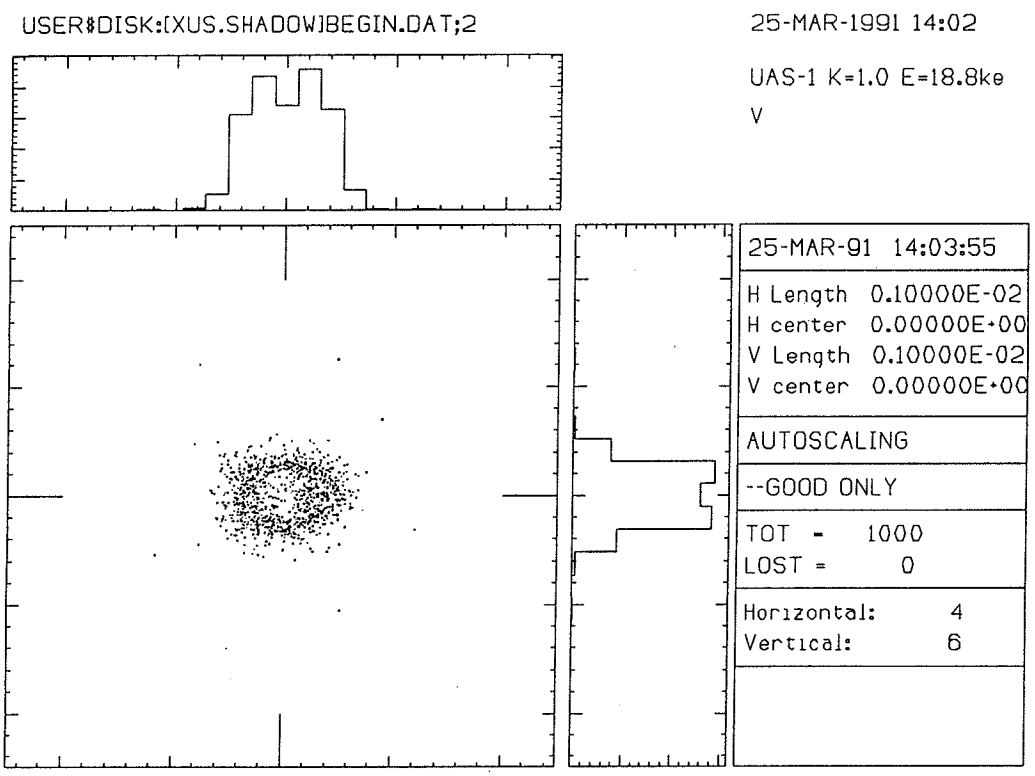


Fig. UA-35. K = 1.0, second harmonic.

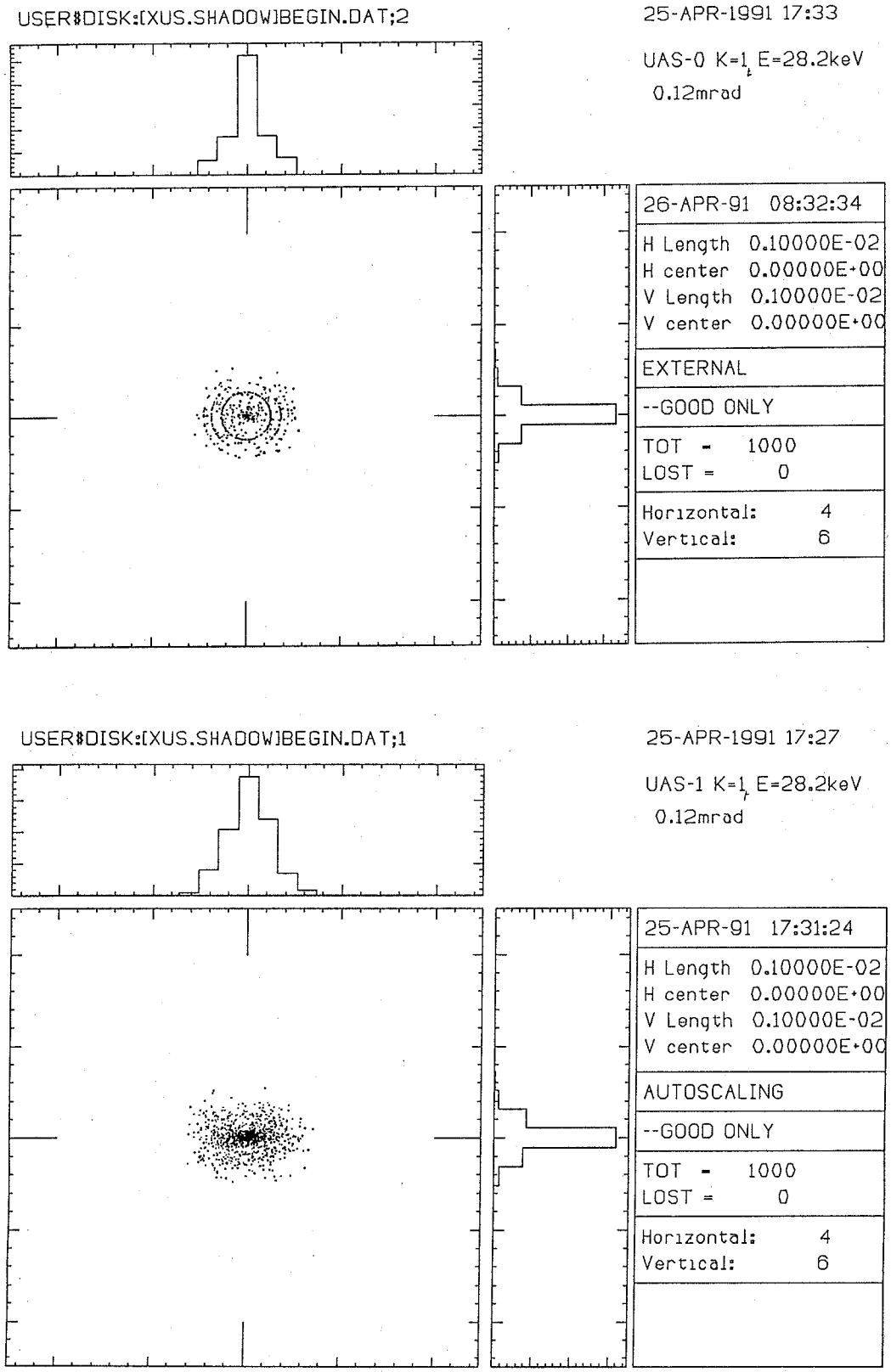


Fig. UA-36. K = 1.0, third harmonic.

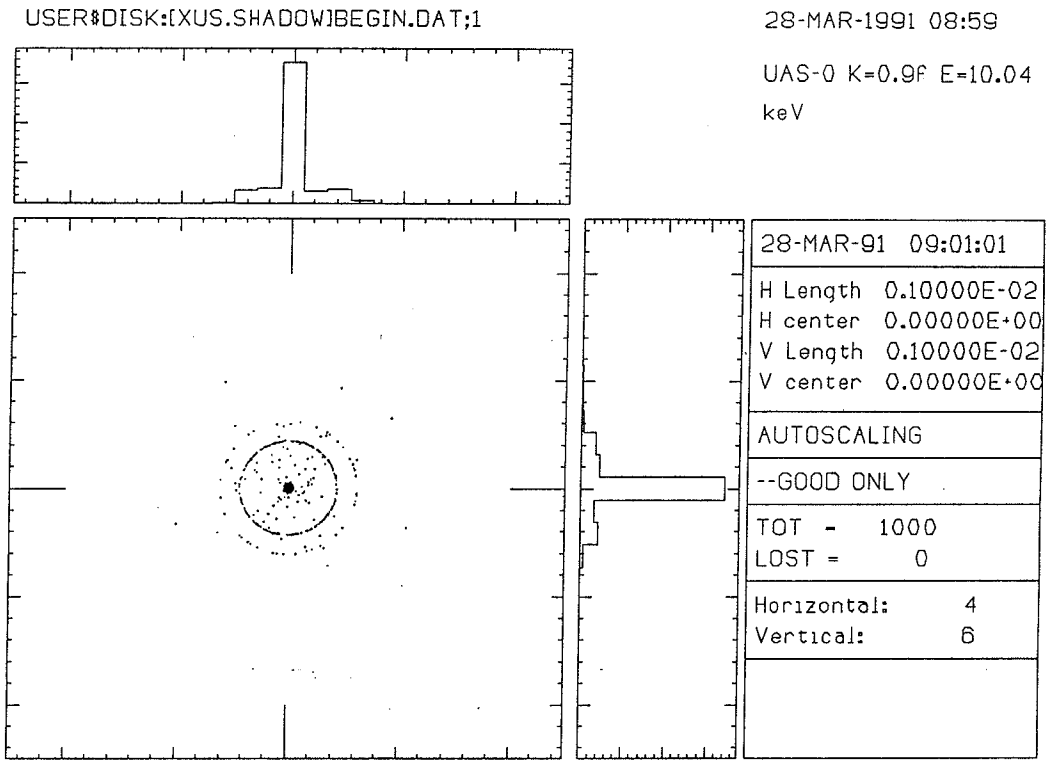


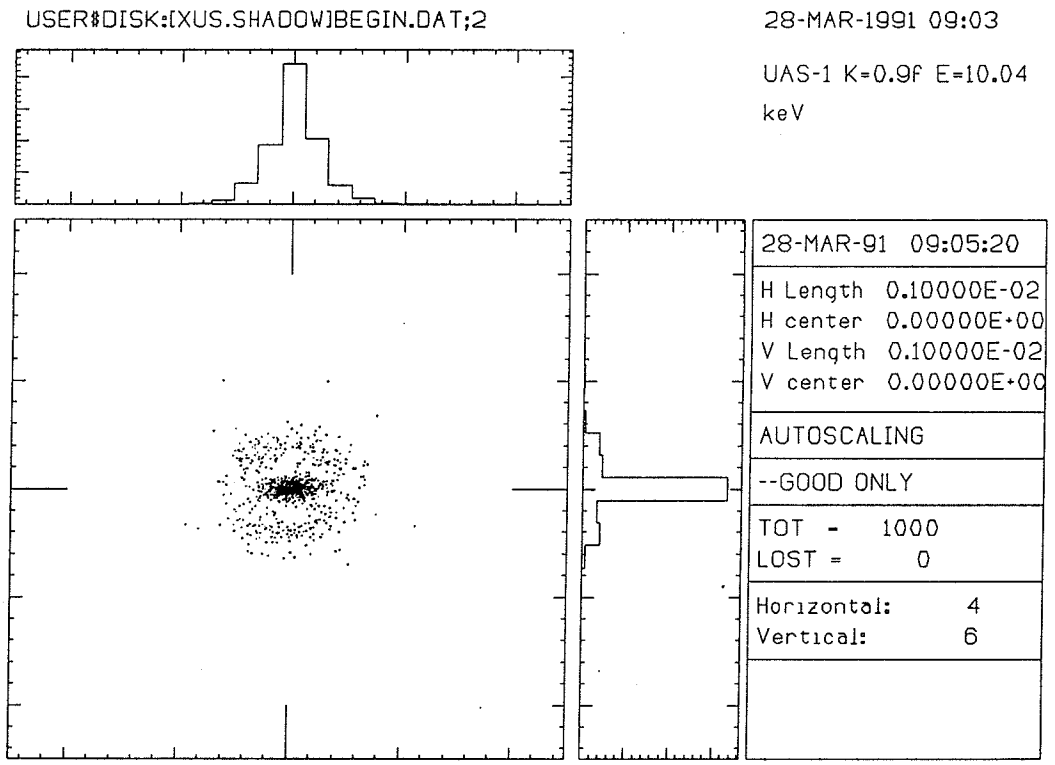


Fig. UA-37. K = 0.9, first harmonic.

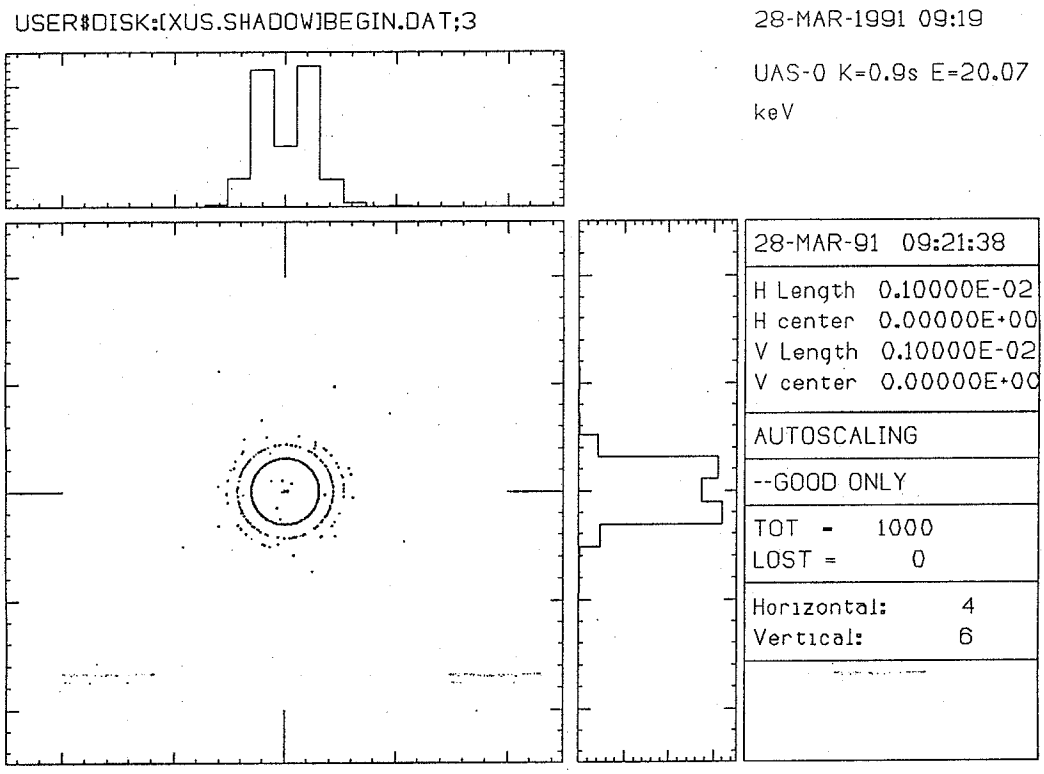


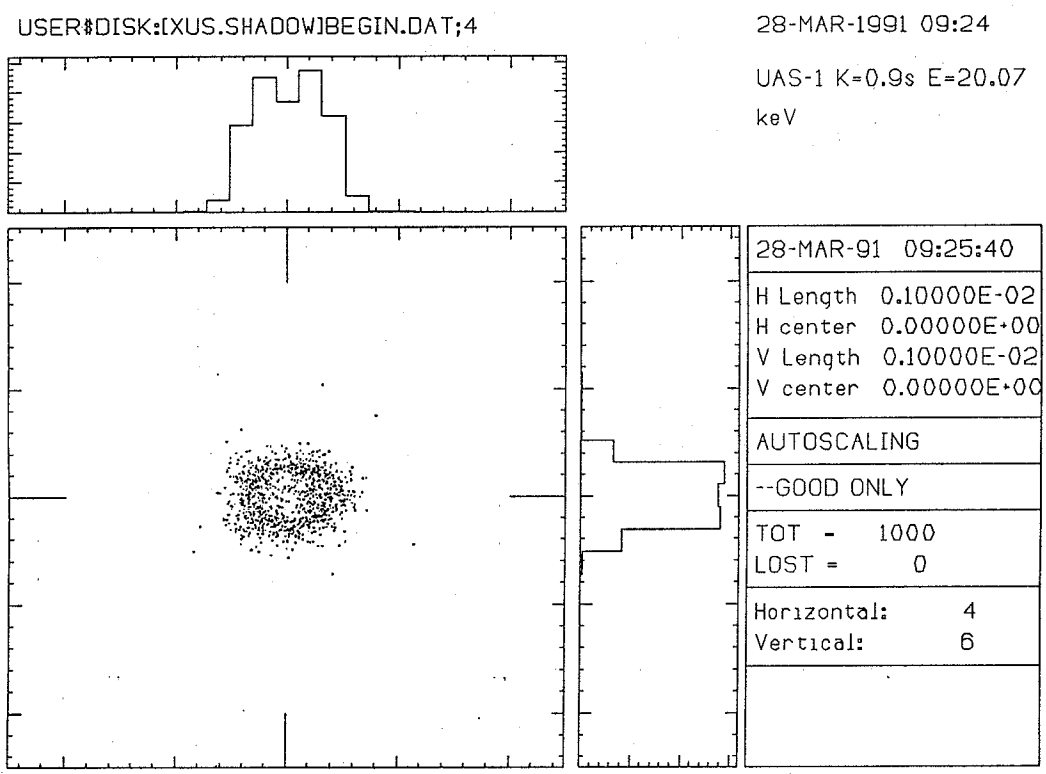


Fig. UA-38. K = 0.9, second harmonic.

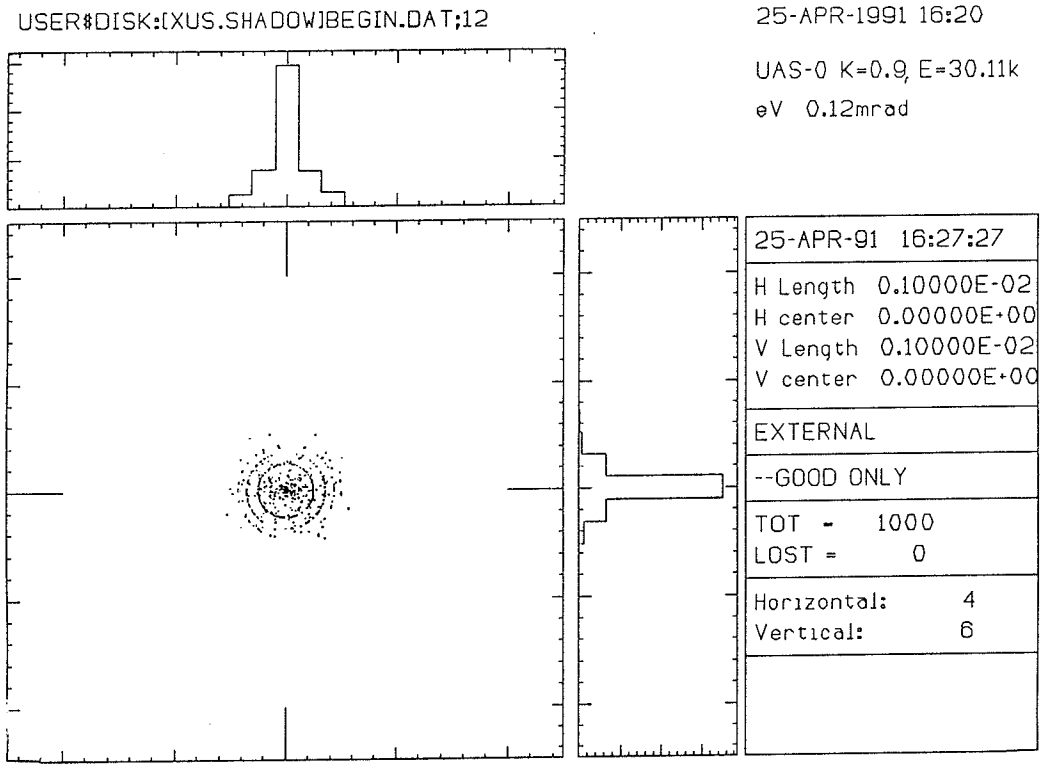


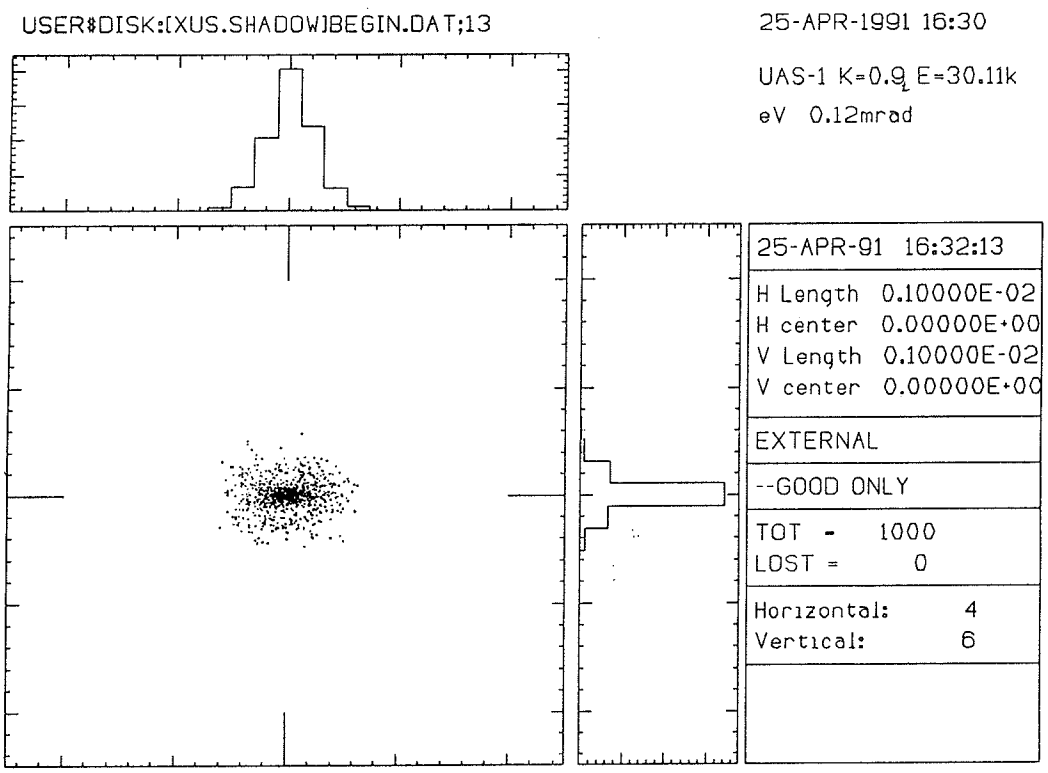


Fig. UA-39. K = 0.9, third harmonic.

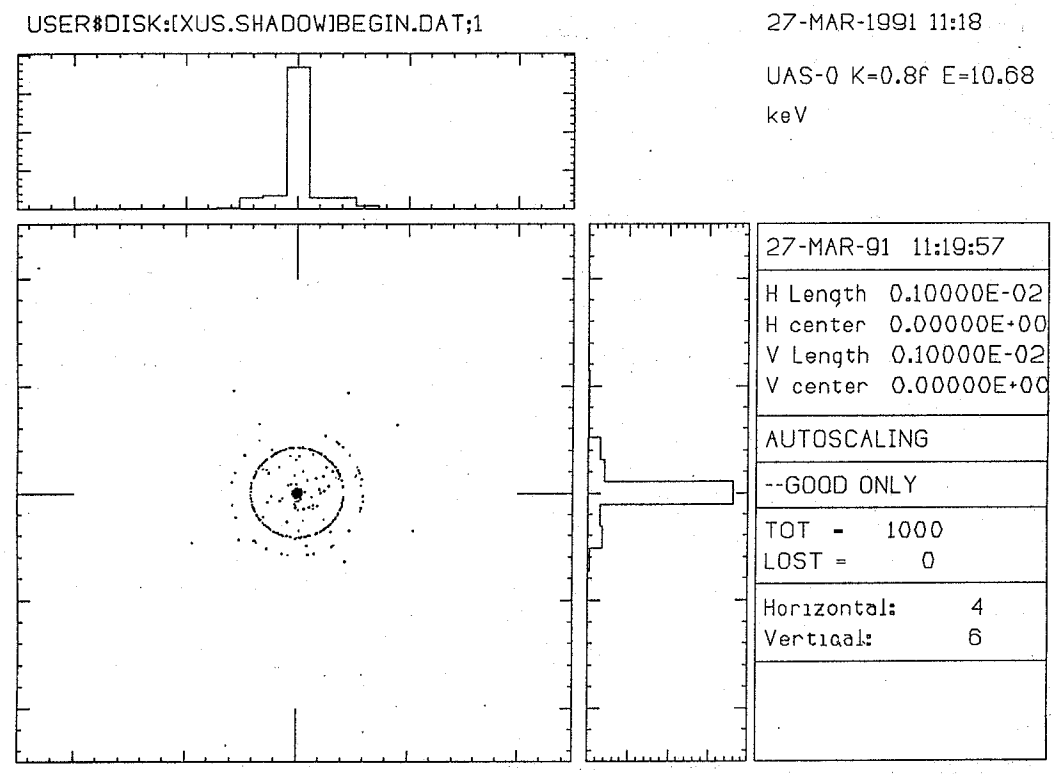


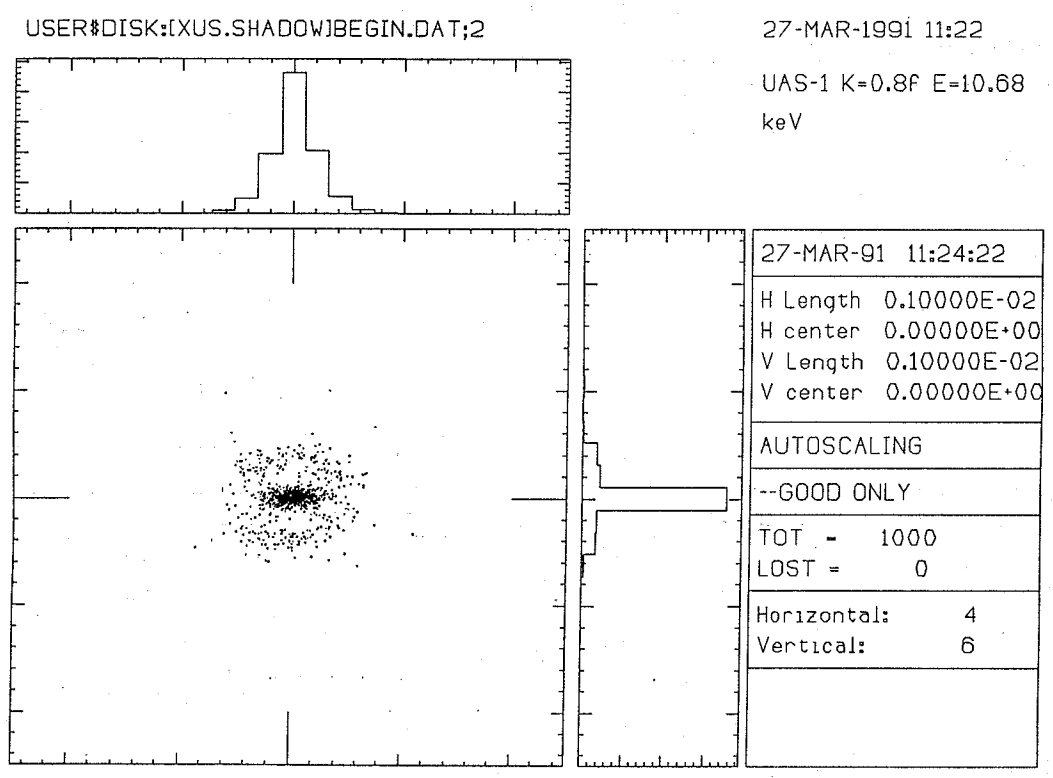


Fig. UA-40. K = 0.8, first harmonic.

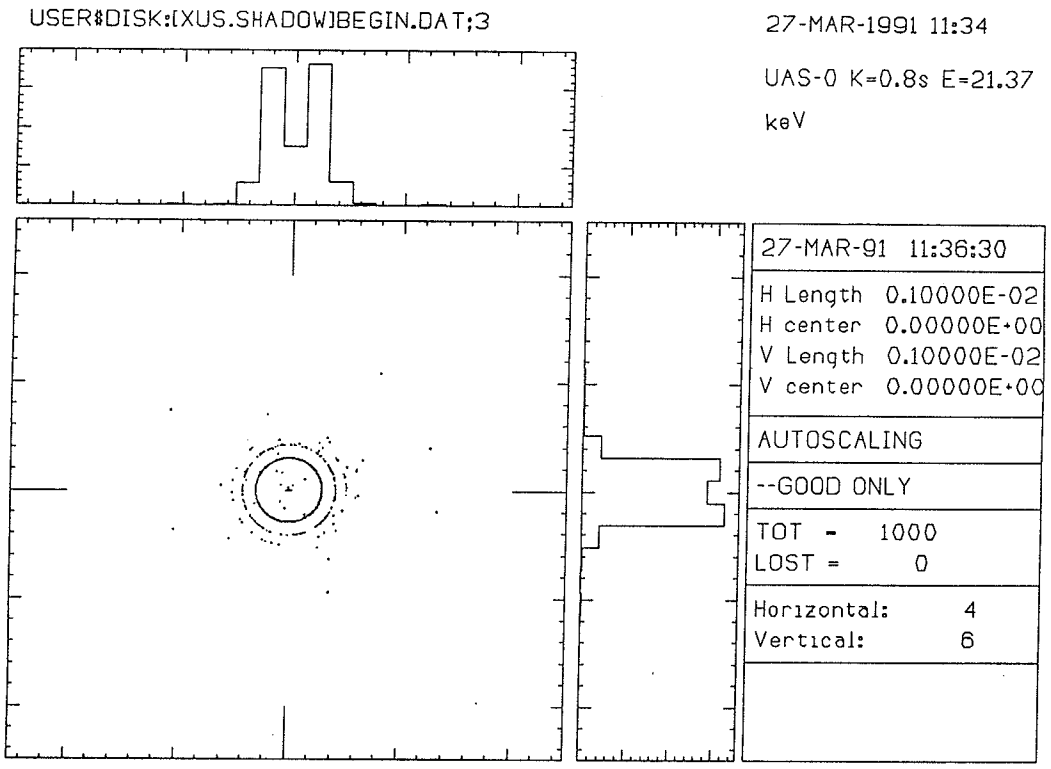


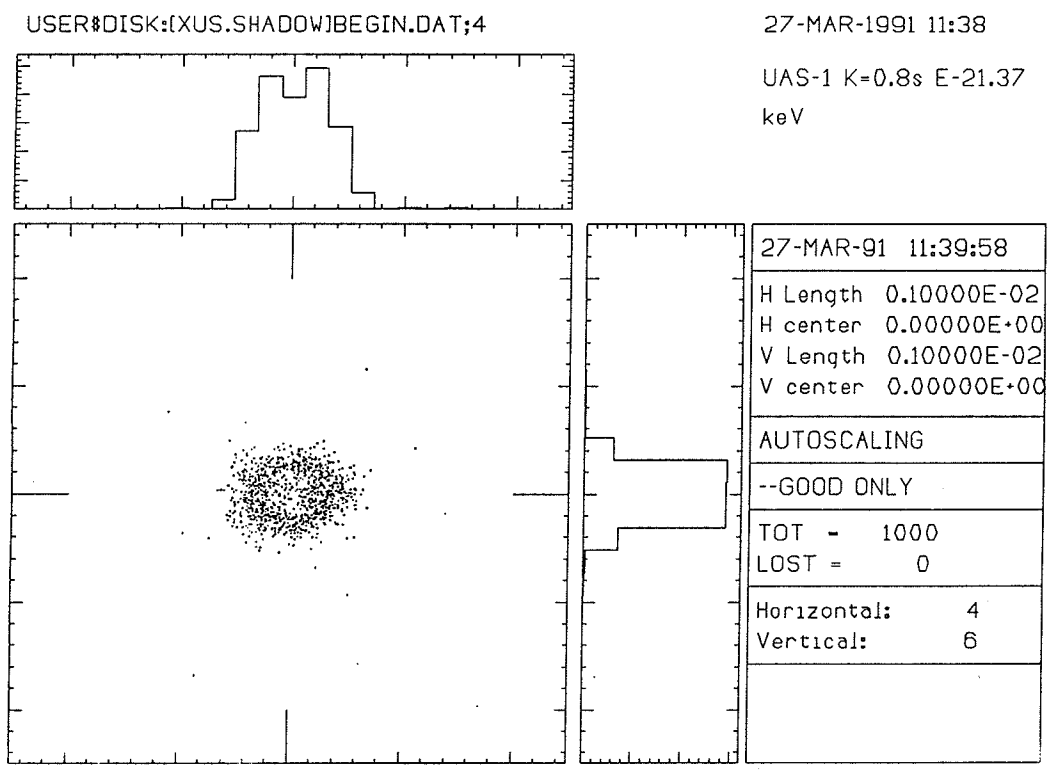


Fig. UA-41. K = 0.8, second harmonic.

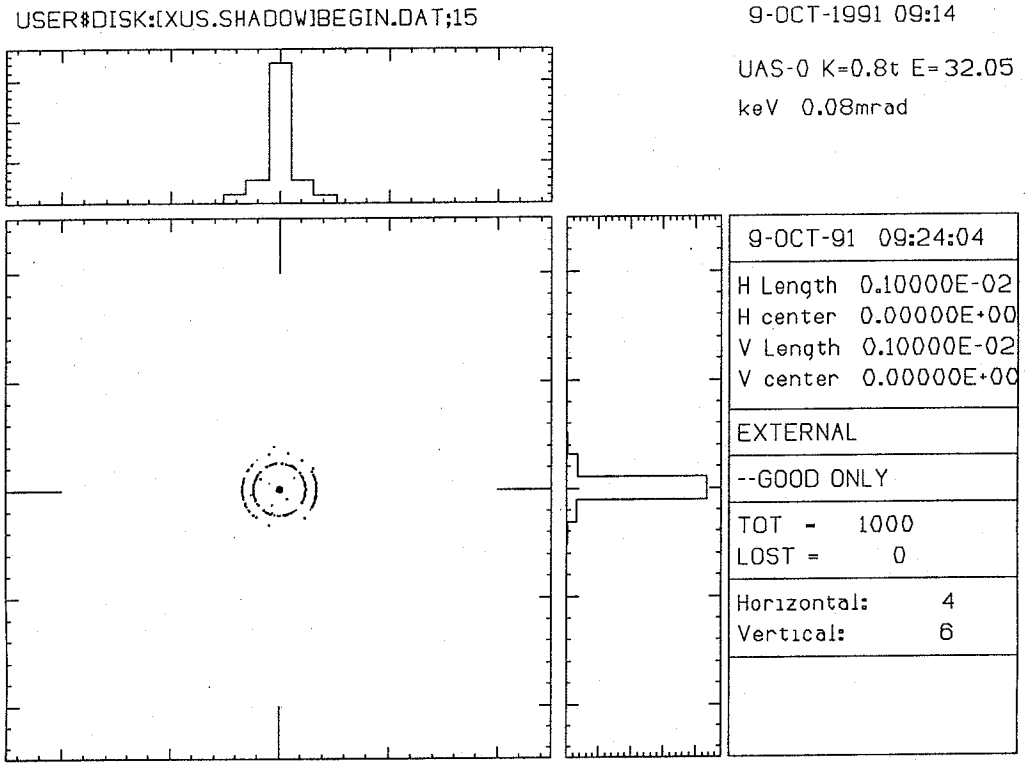


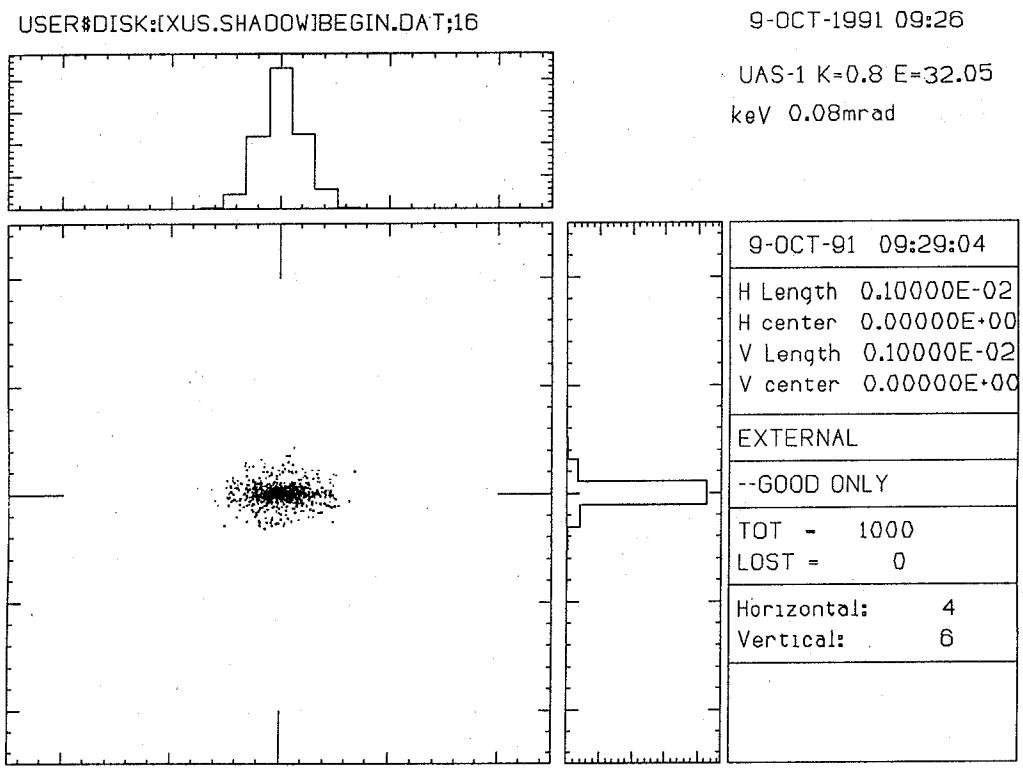


Fig. UA-42. K = 0.8, third harmonic.

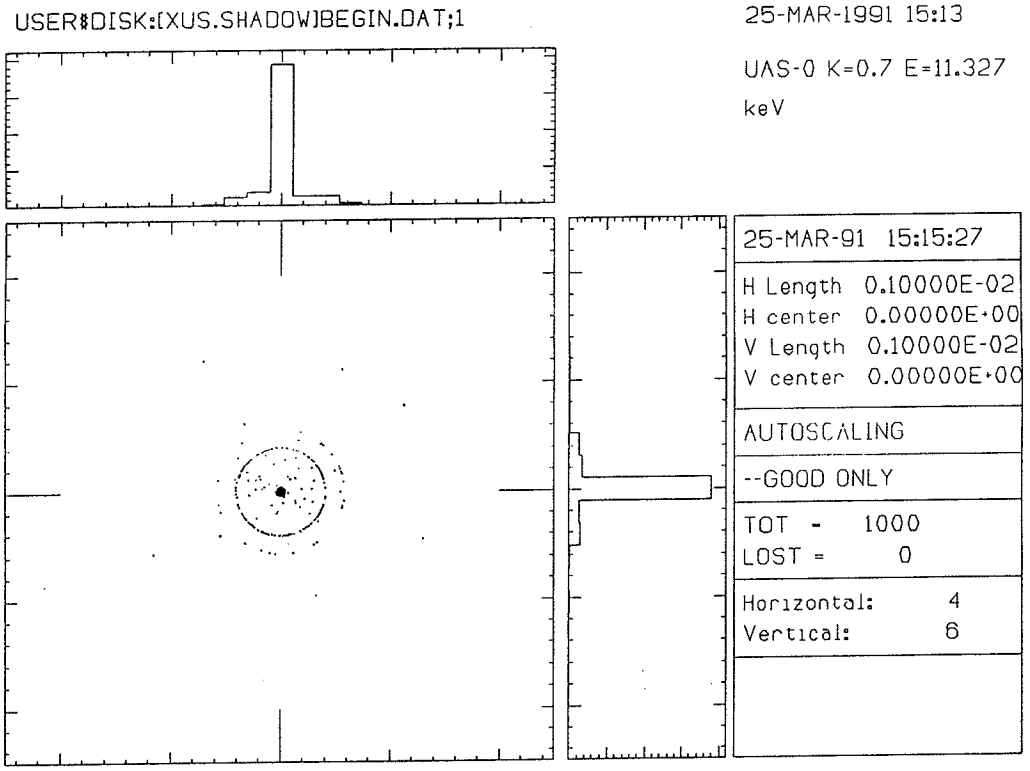


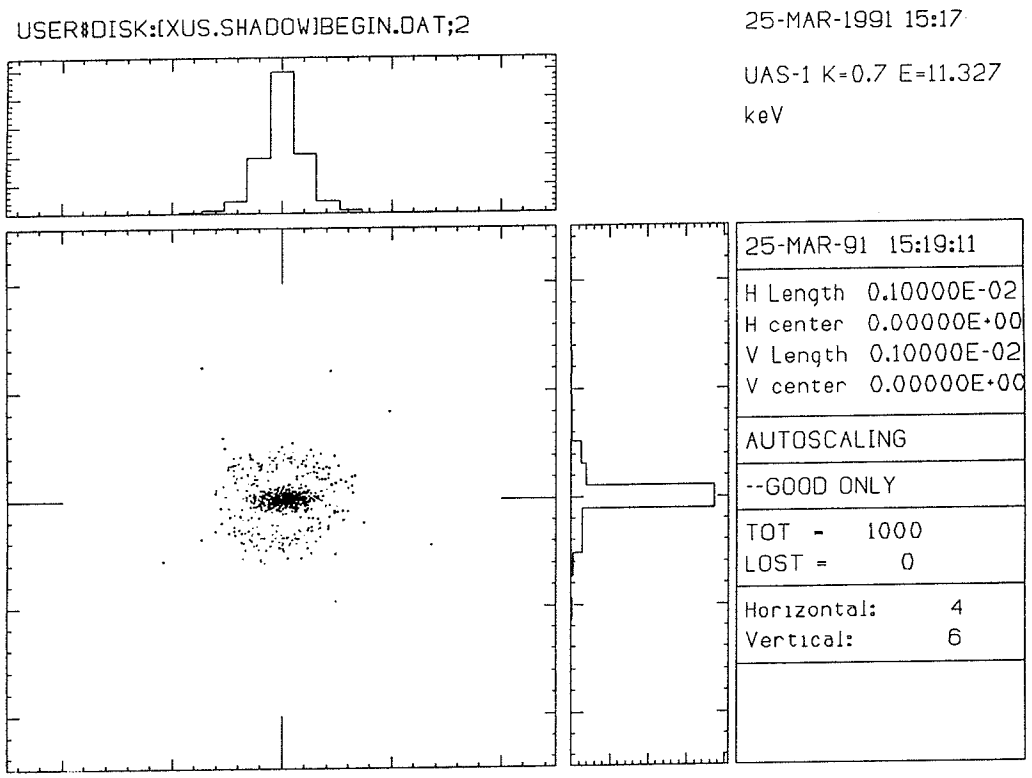


Fig. UA-43. K = 0.7, first harmonic.

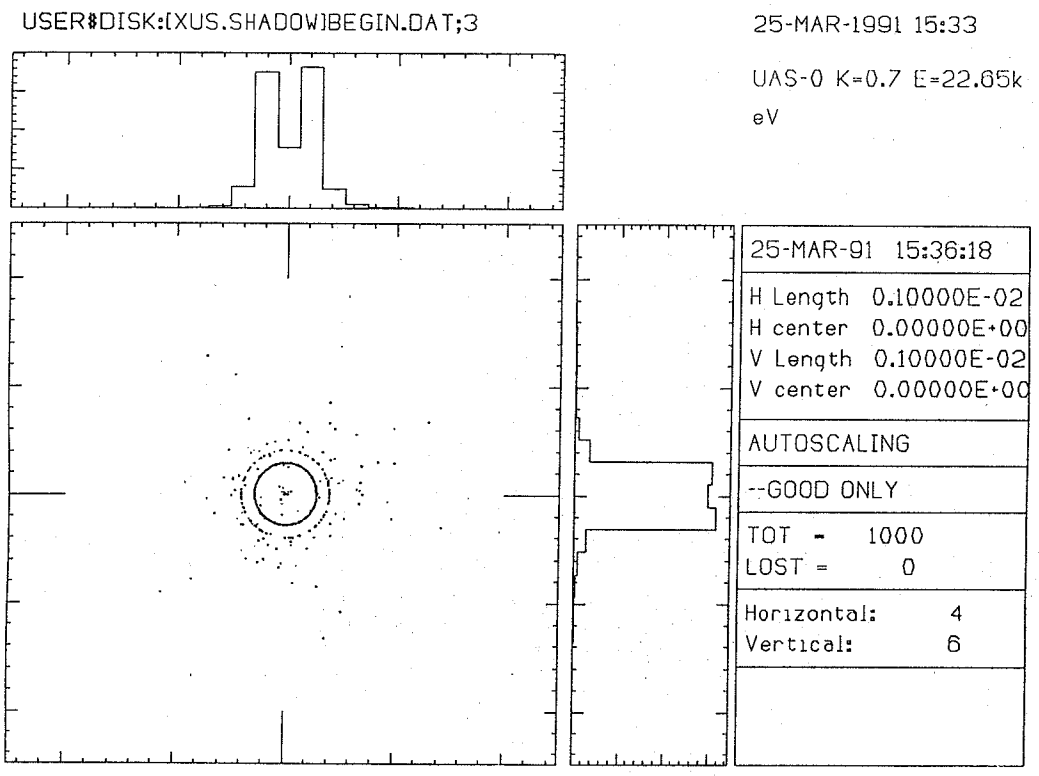


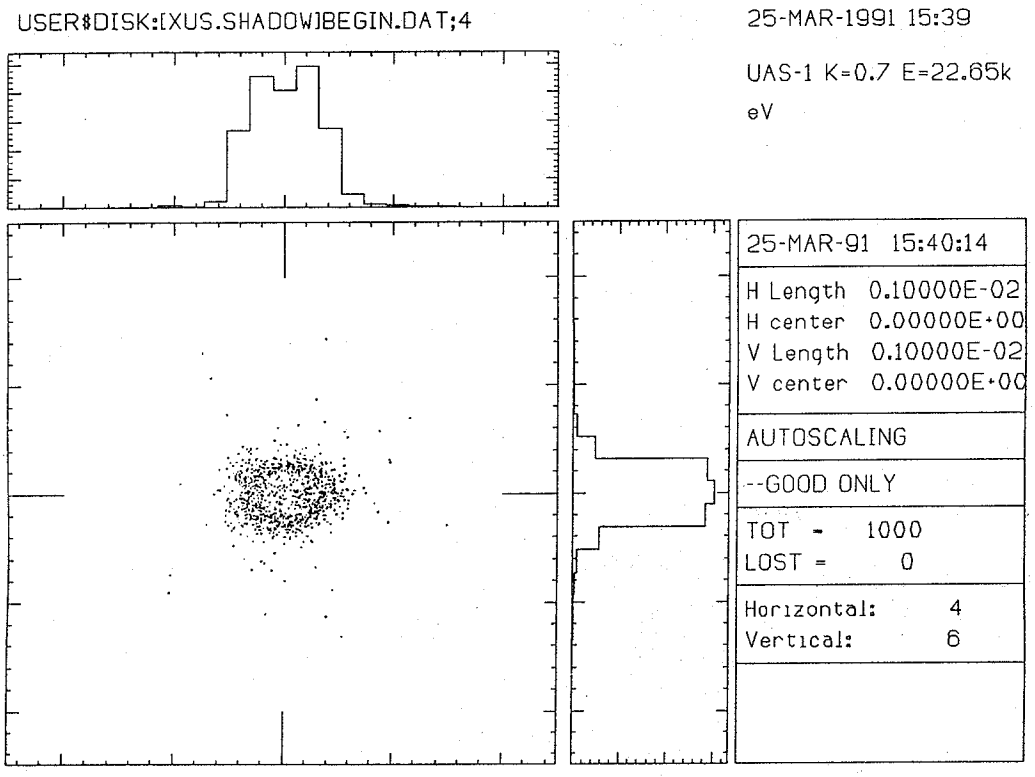


Fig. UA-44. K = 0.7, second harmonic.

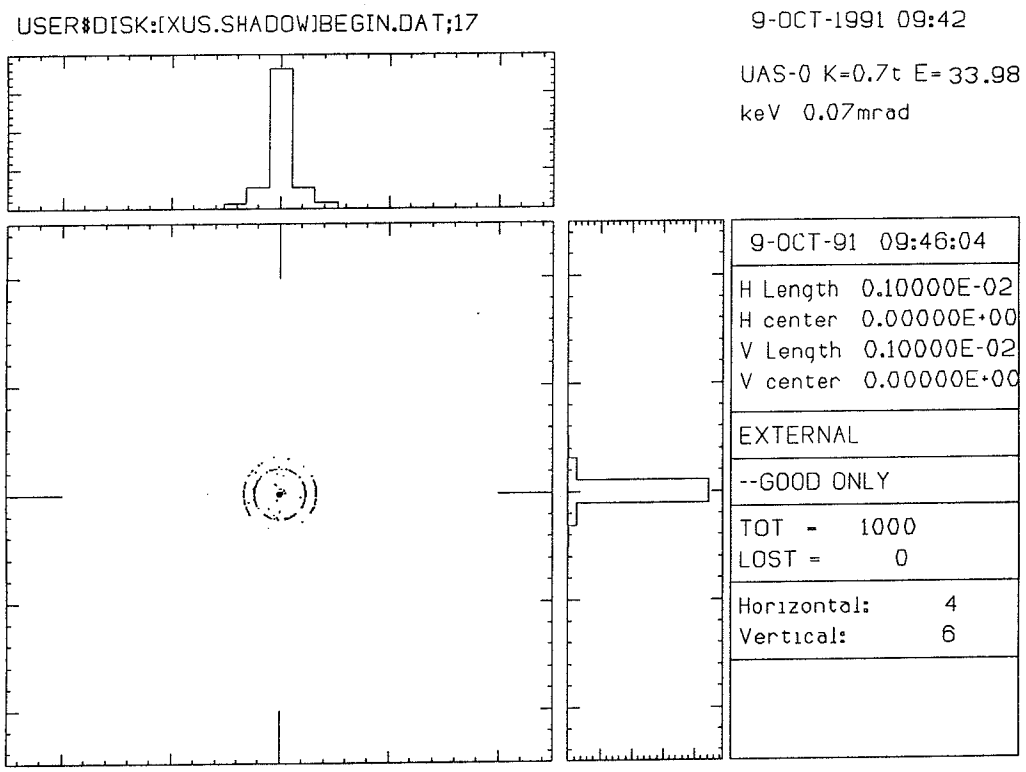


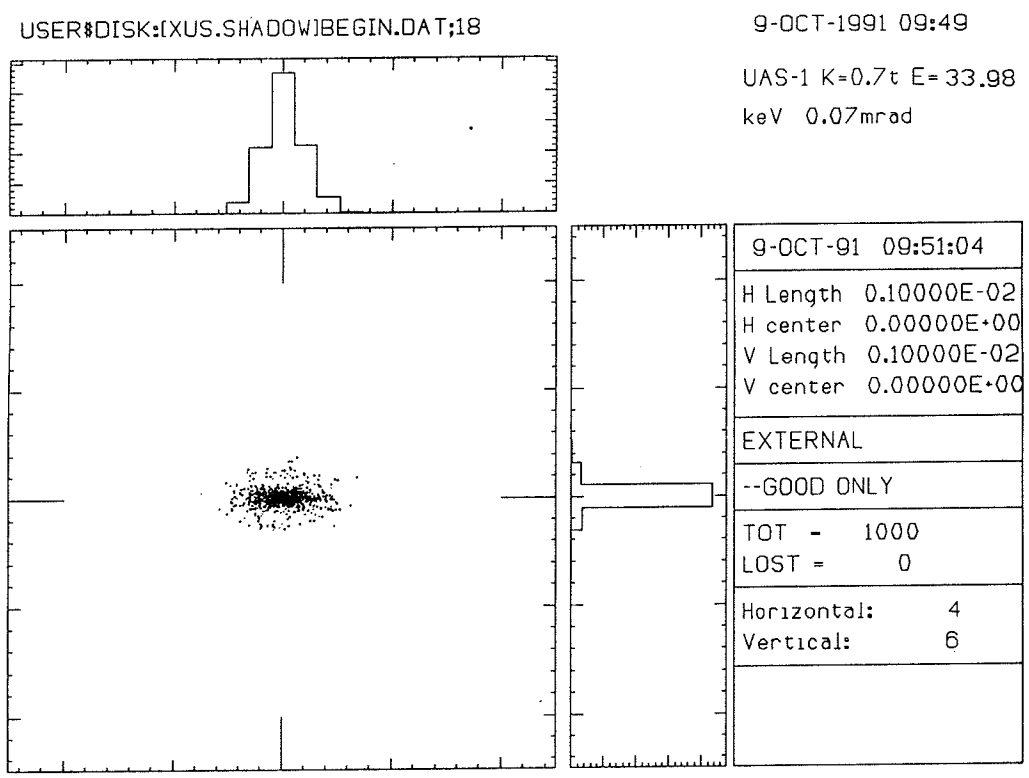


Fig. UA-45. K = 0.7, third harmonic.

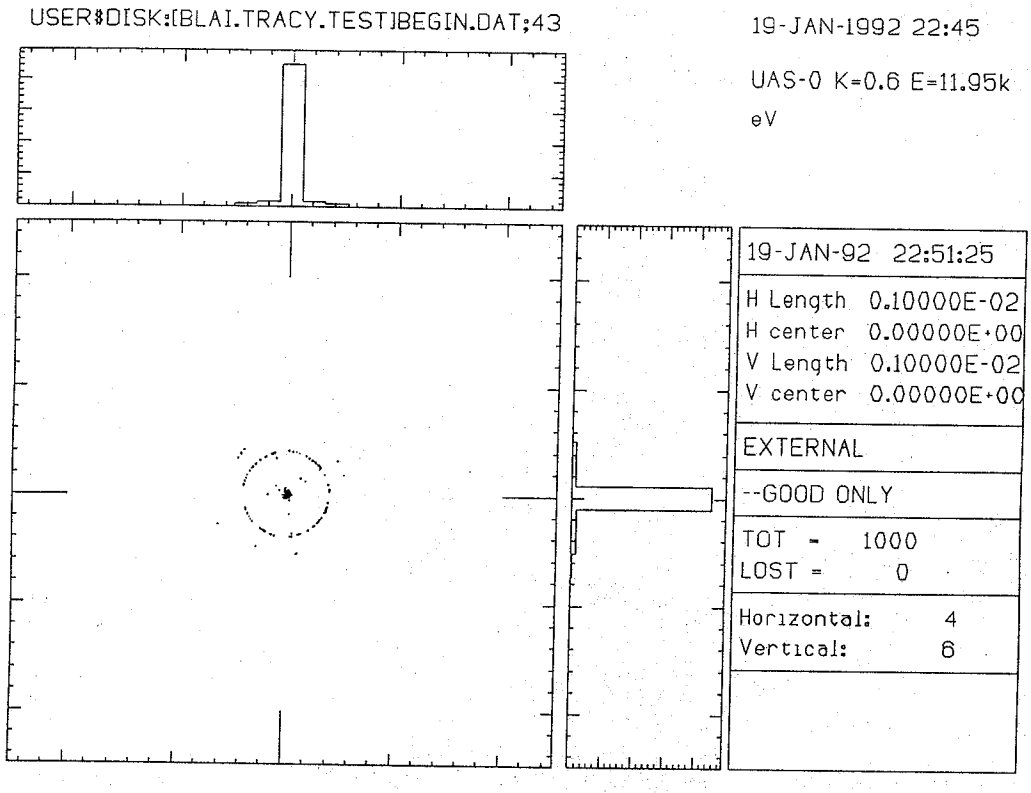


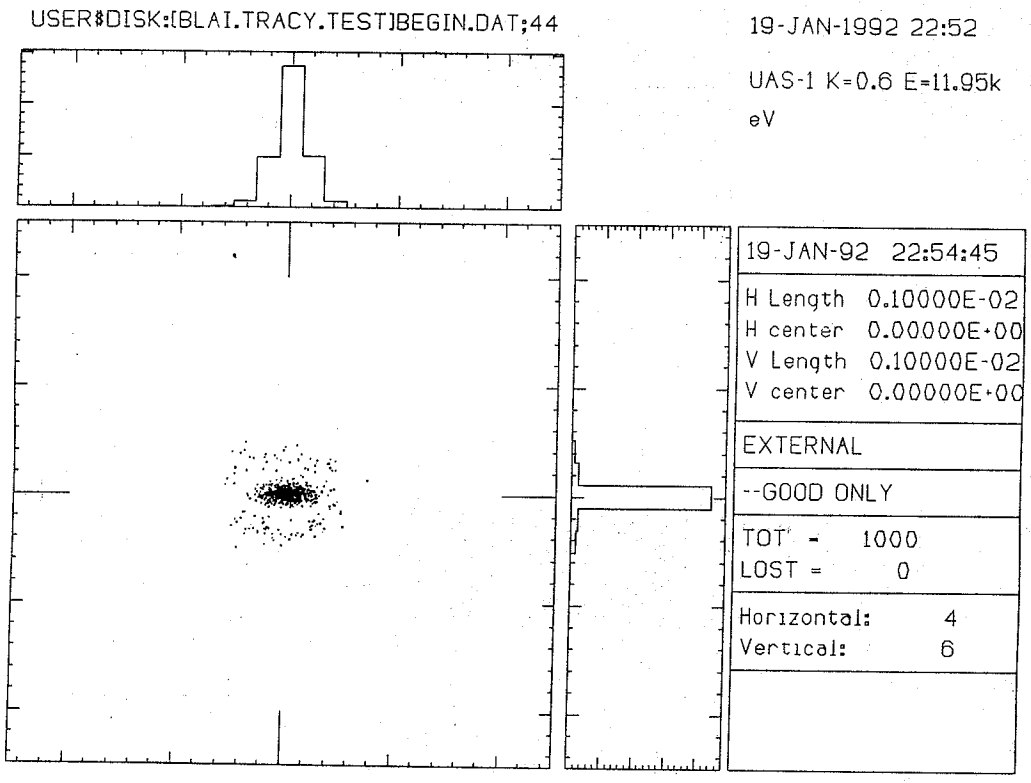


Fig. UA-46. K = 0.6, first harmonic.

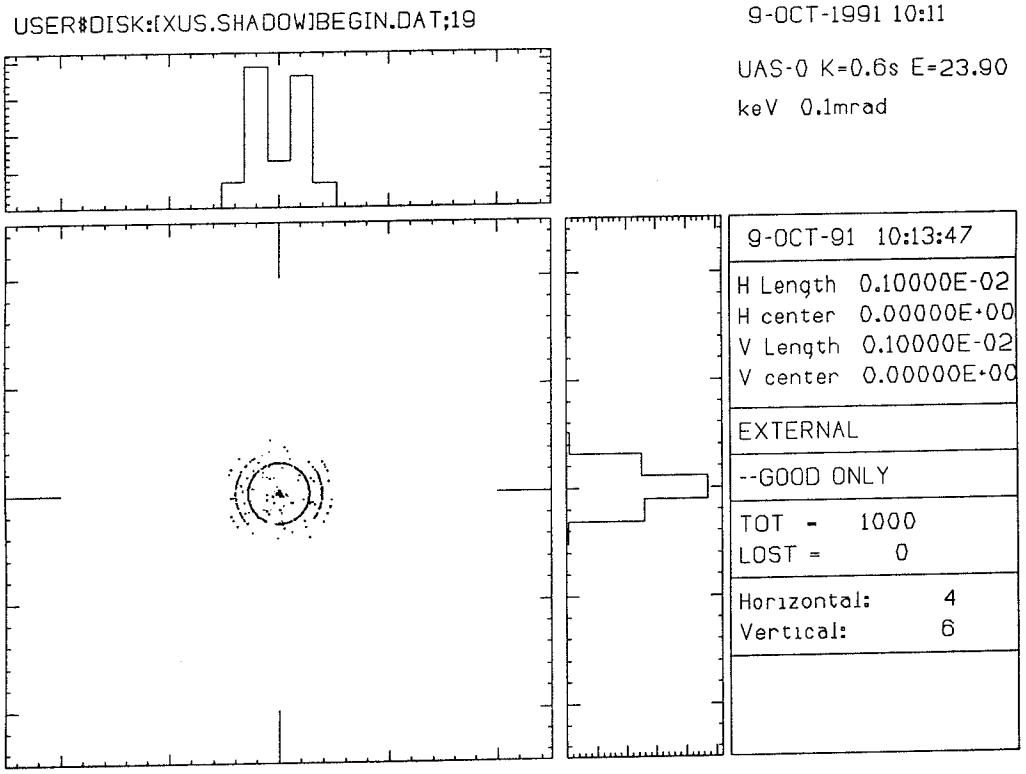


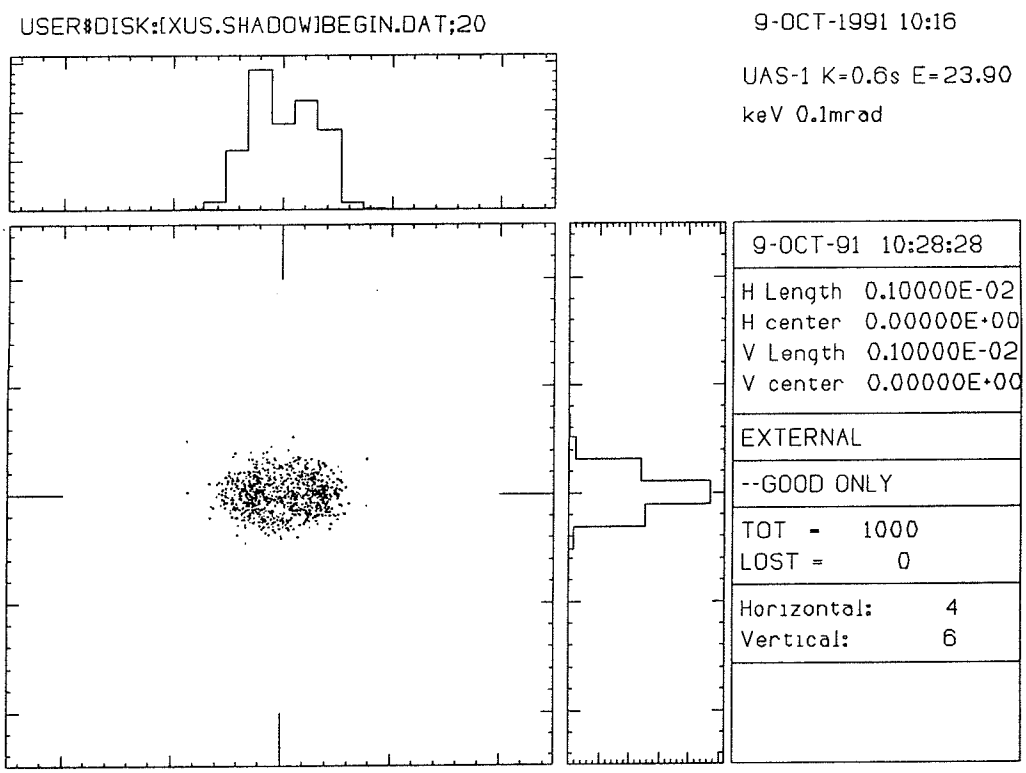


Fig. UA-47. K = 0.6, second harmonic.

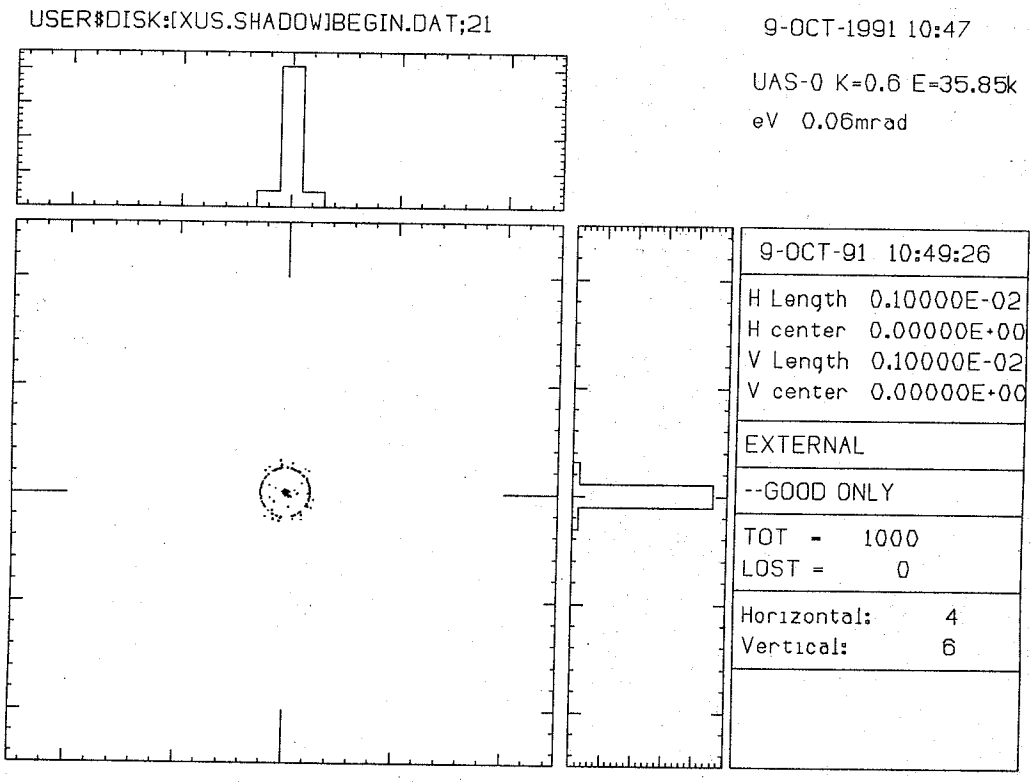


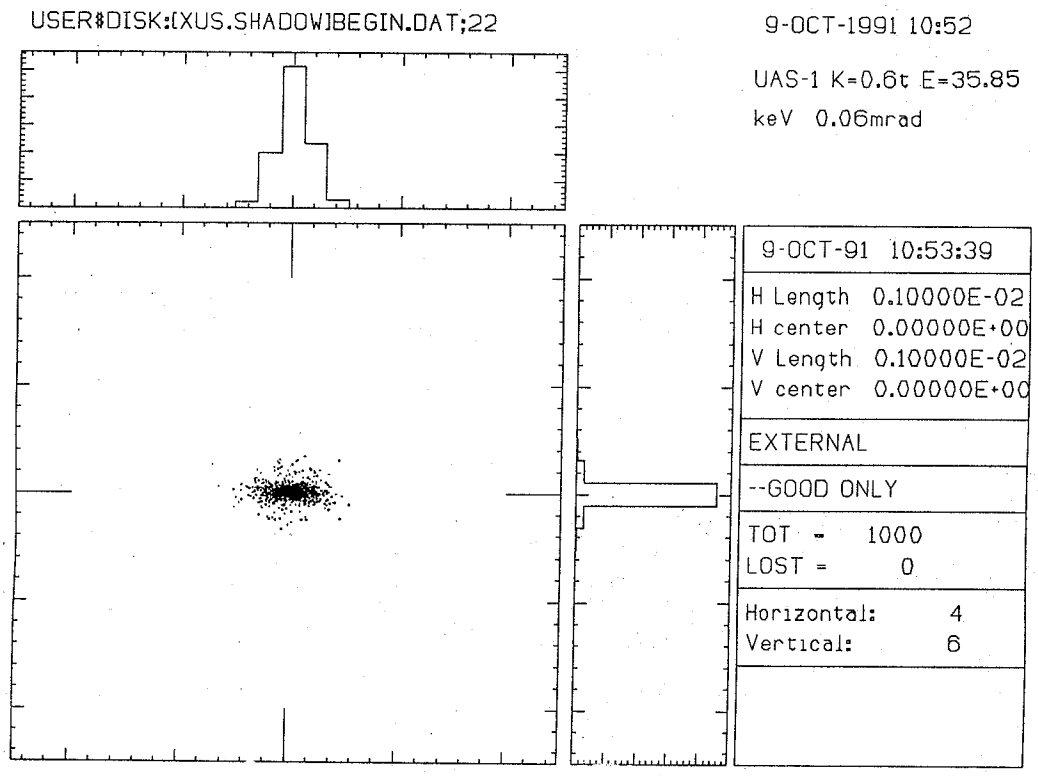


Fig. UA-48. K = 0.6, third harmonic.

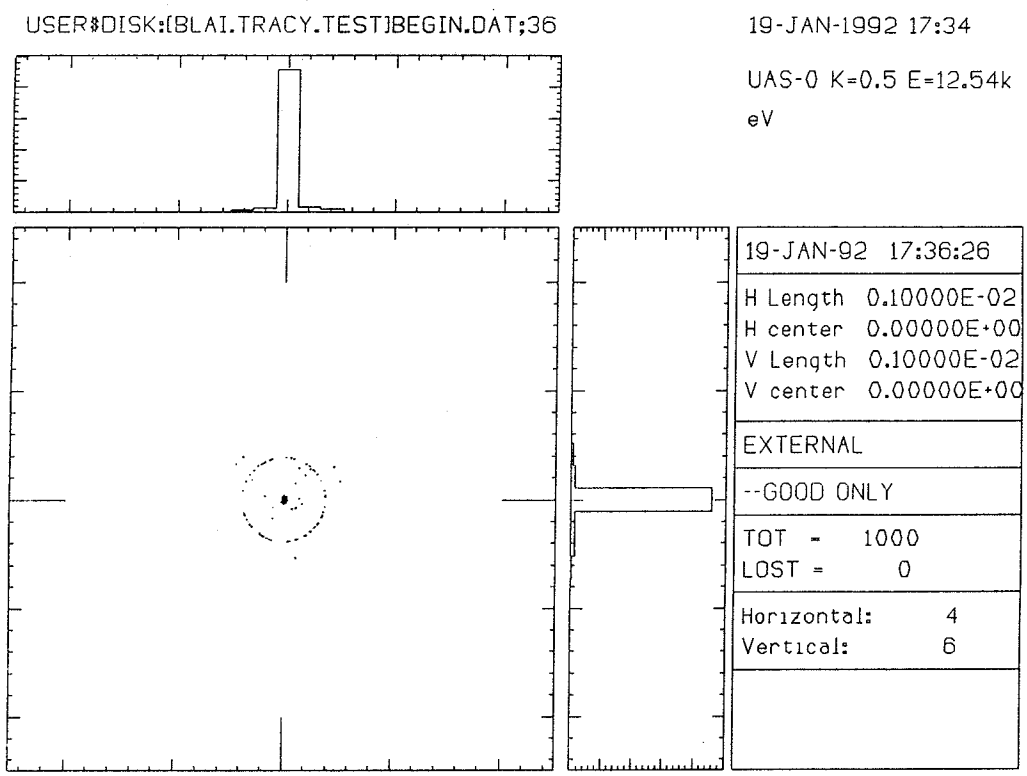


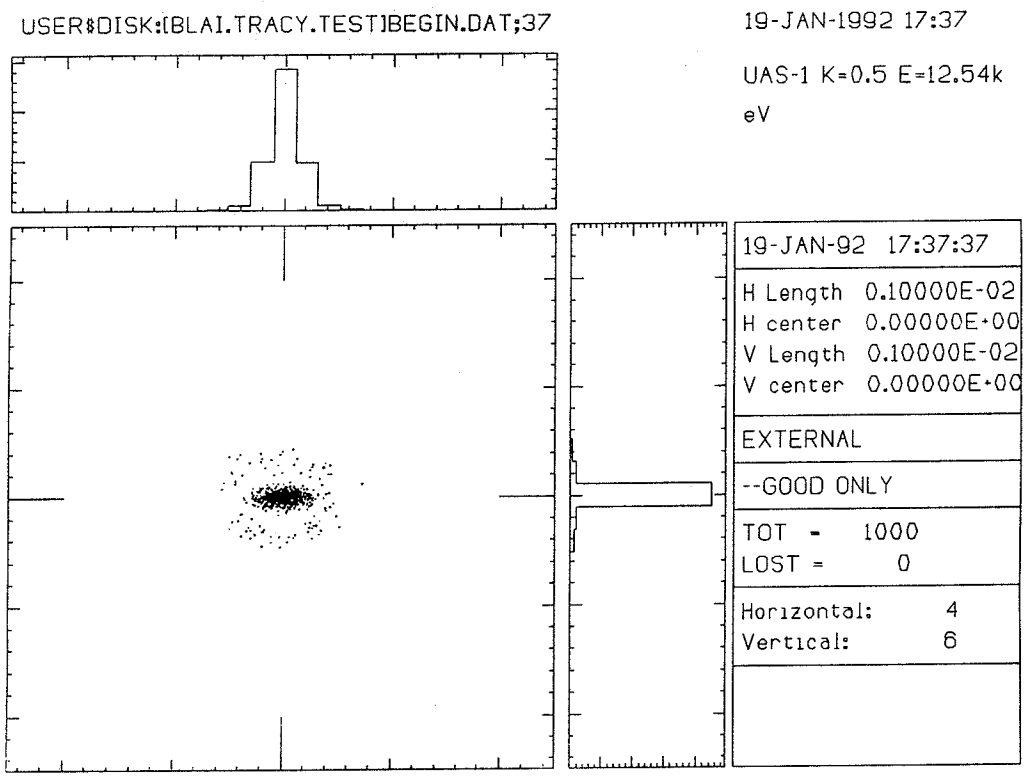


**Fig. UA-49. K = 0.5, first harmonic.**

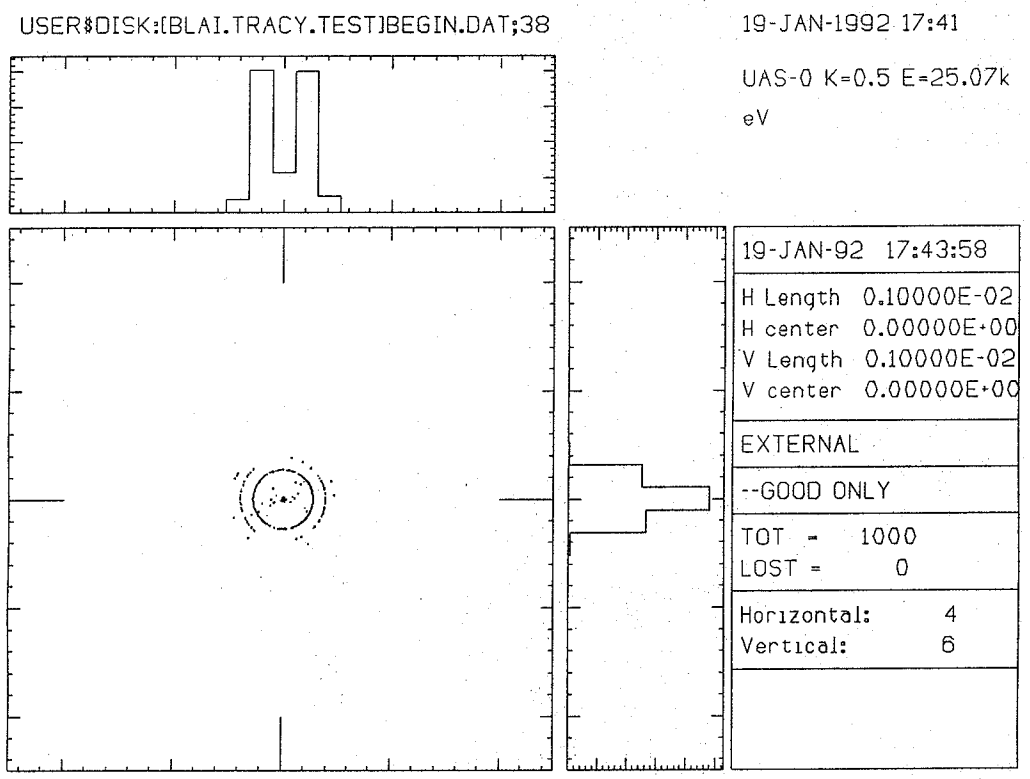


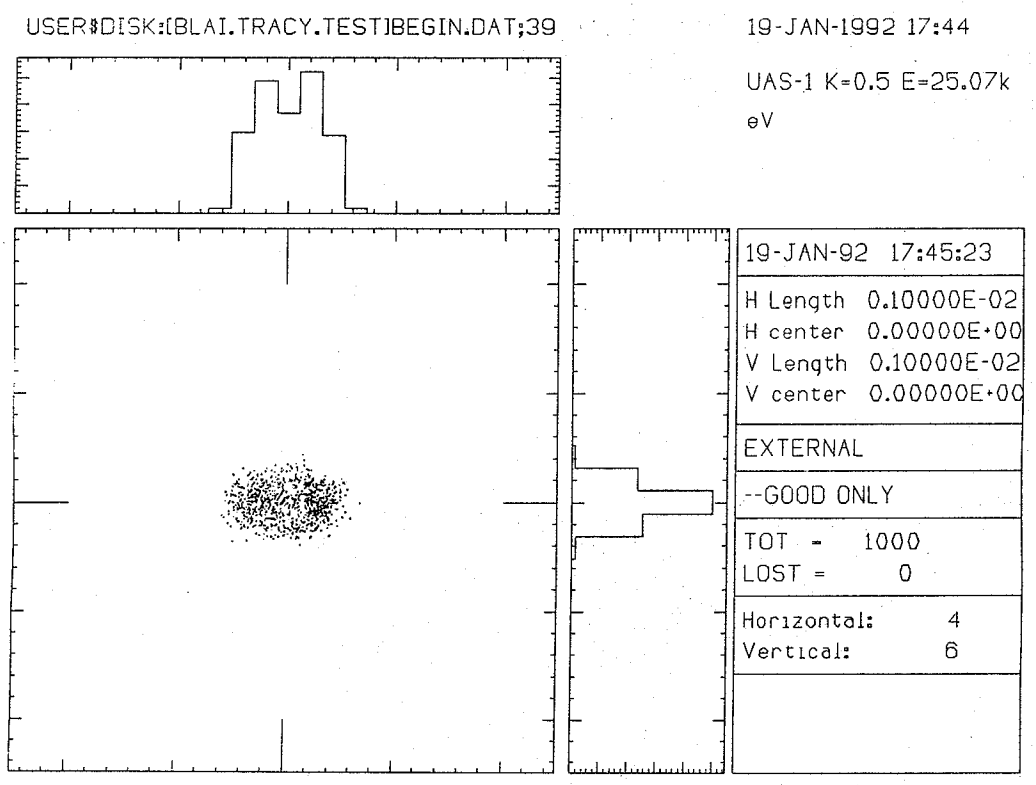


Fig. UA-50. K = 0.5, second harmonic.

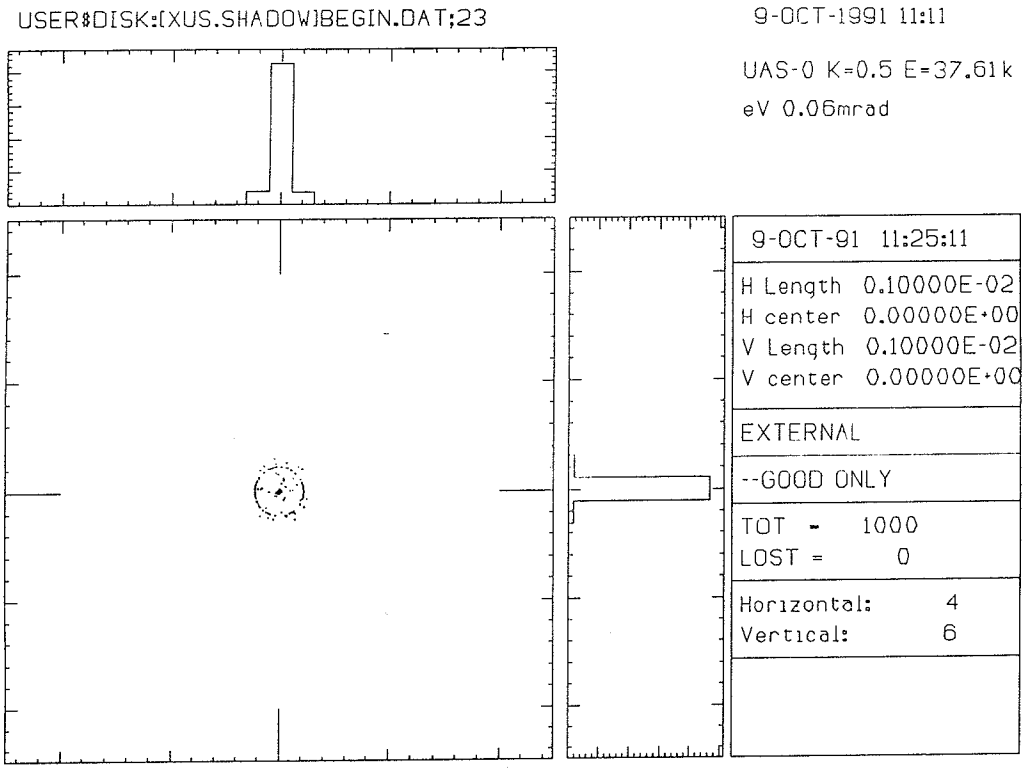


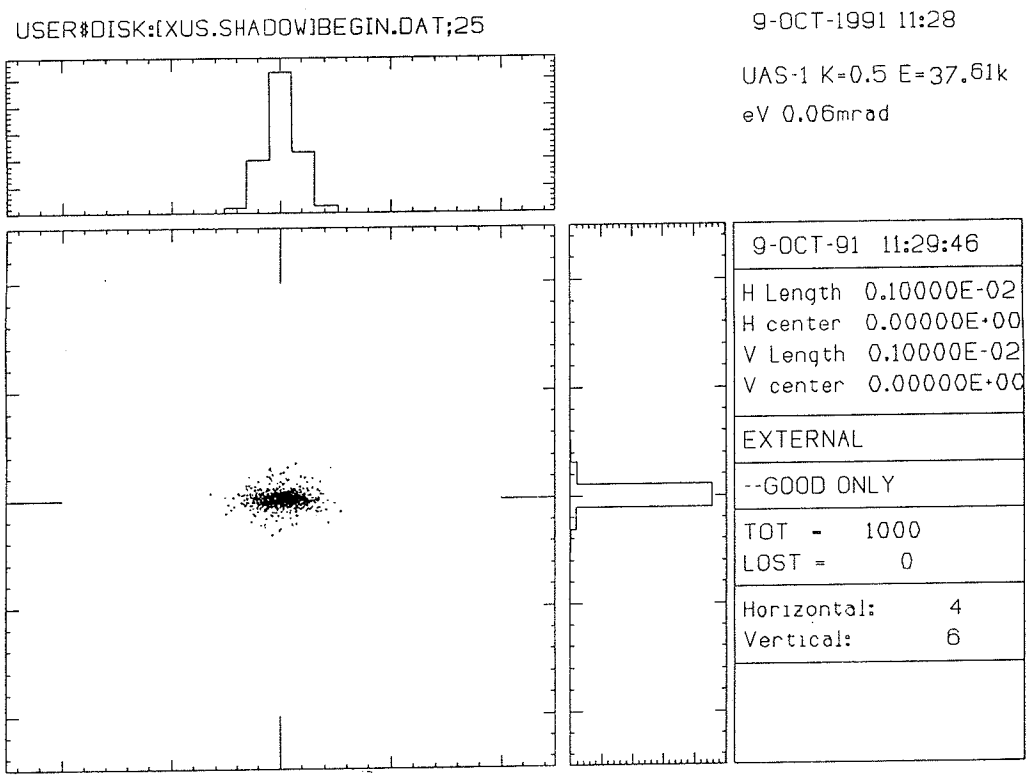


Fig. UA-51. K = 0.5, third harmonic.

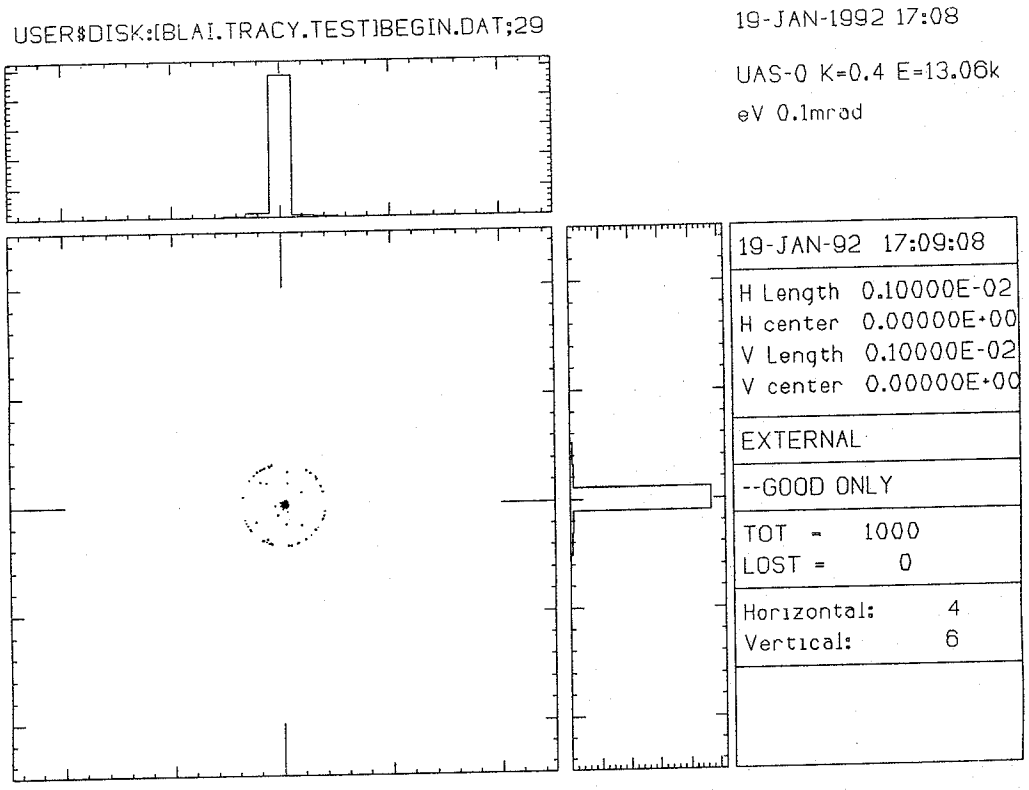


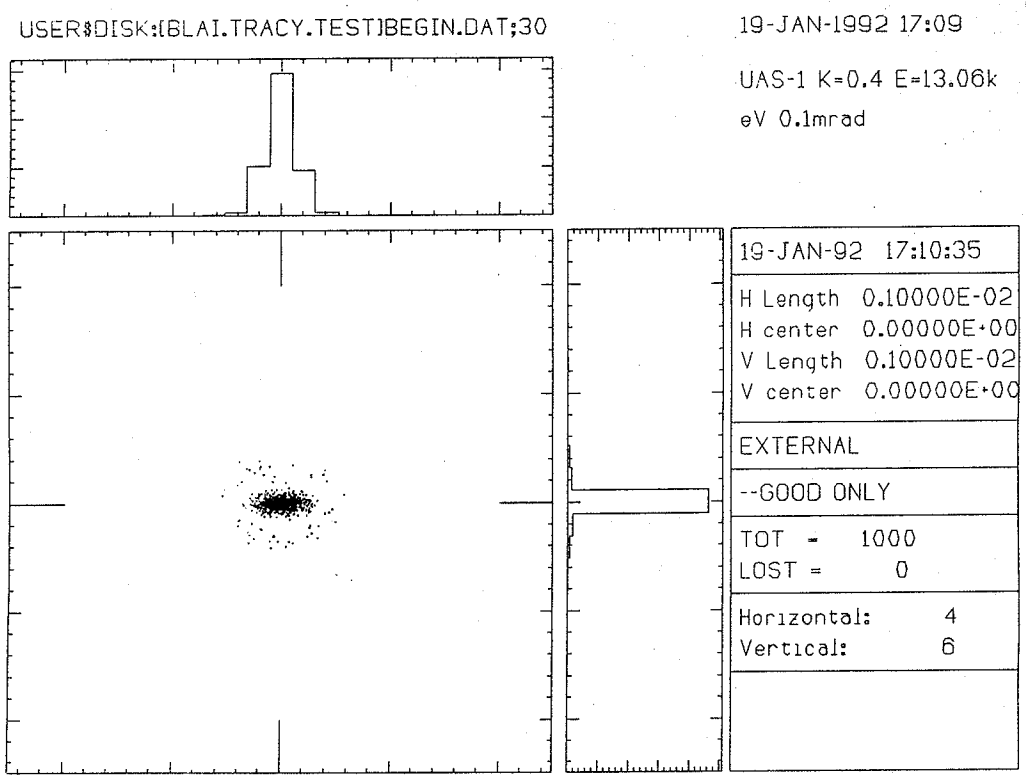


Fig. UA-52. K = 0.4, first harmonic.

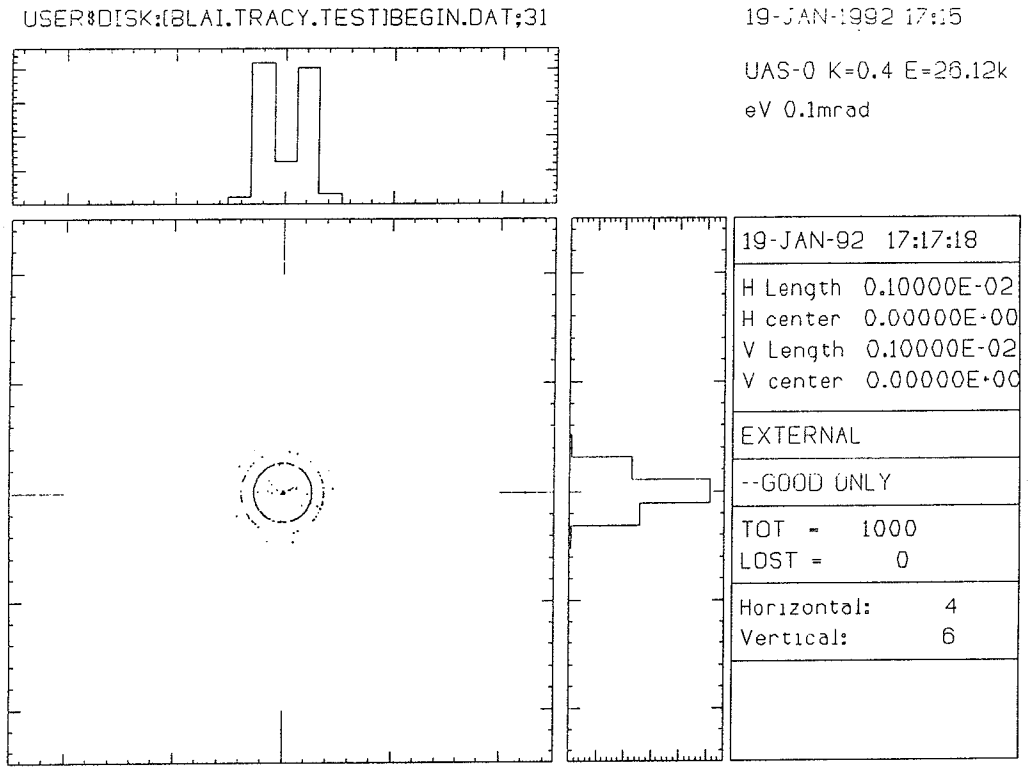


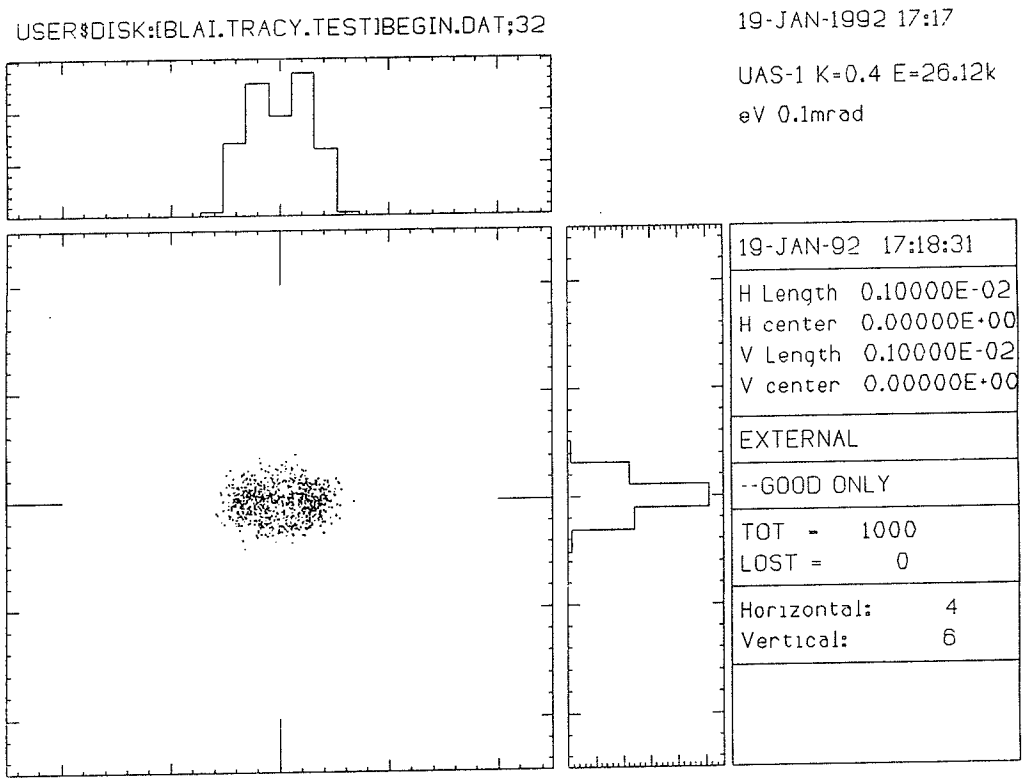


Fig. UA-53. K = 0.4, second harmonic.

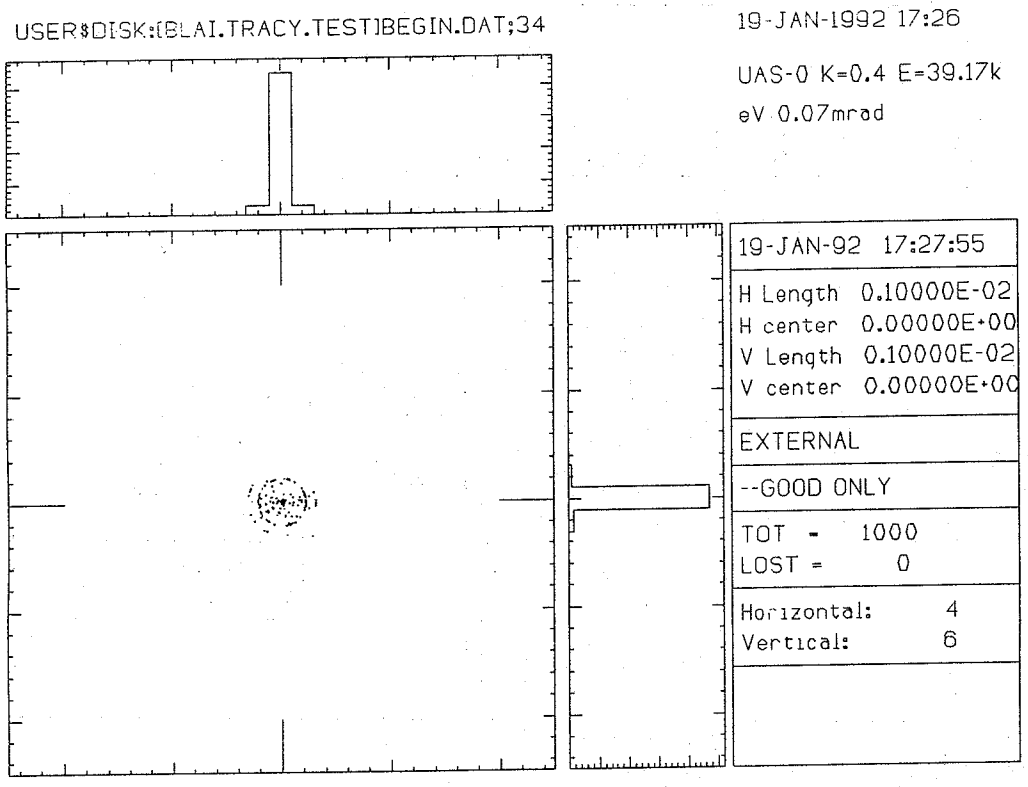


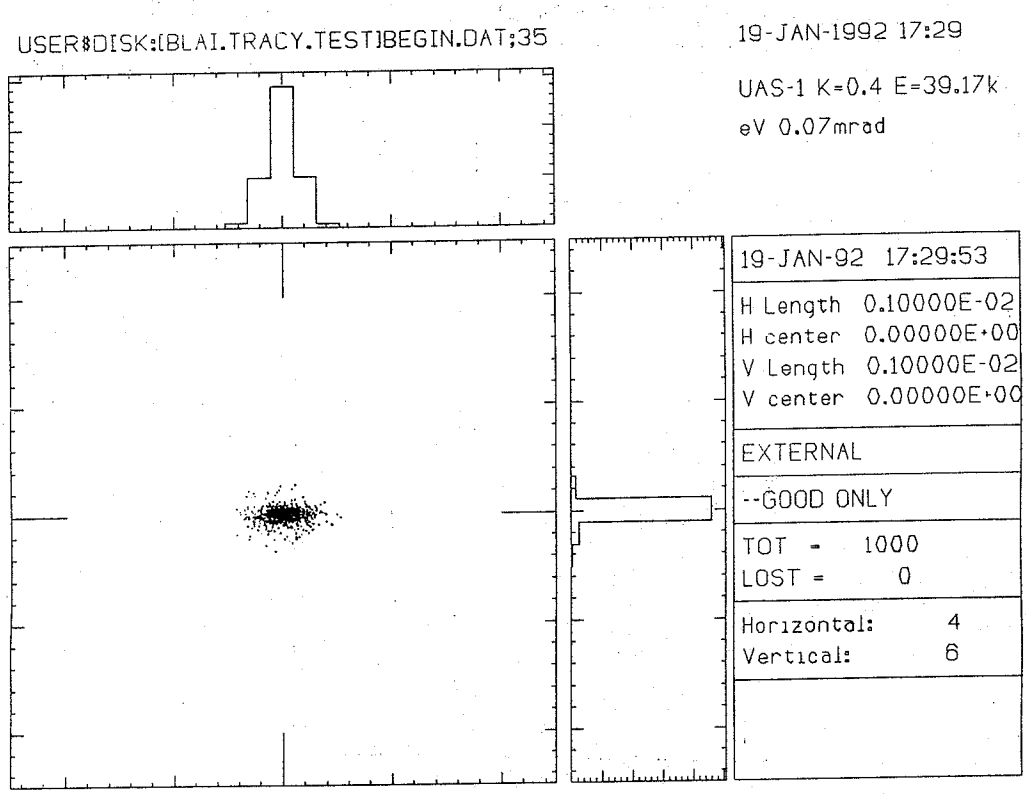


Fig. UA-54. K = 0.4, third harmonic.

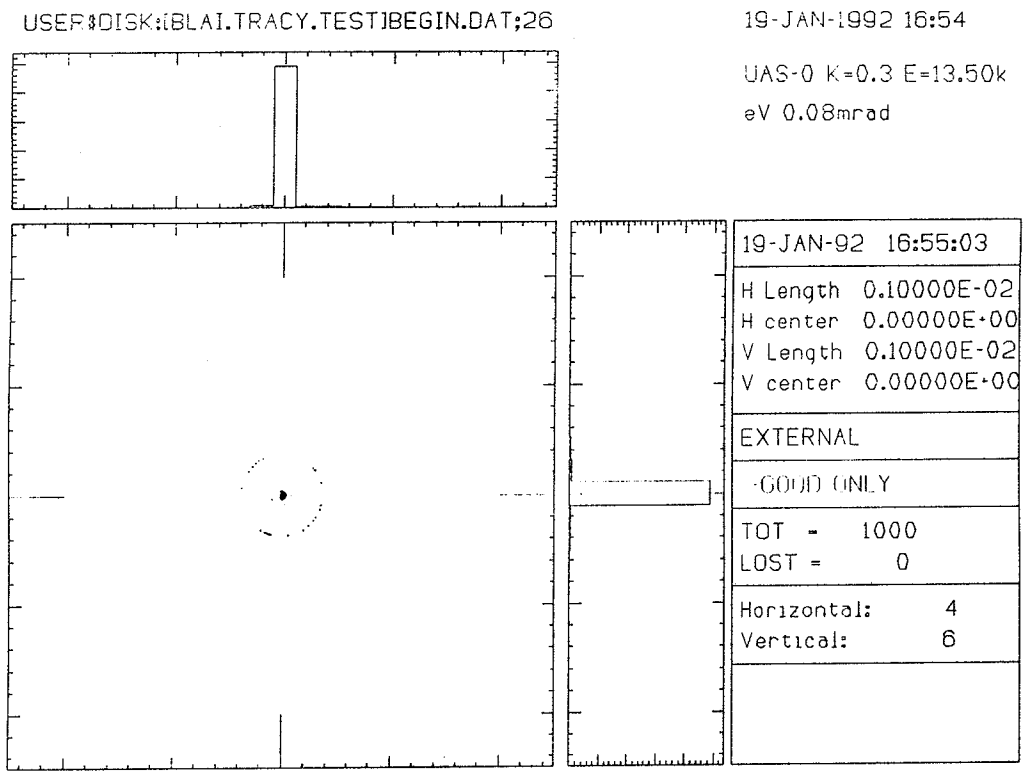


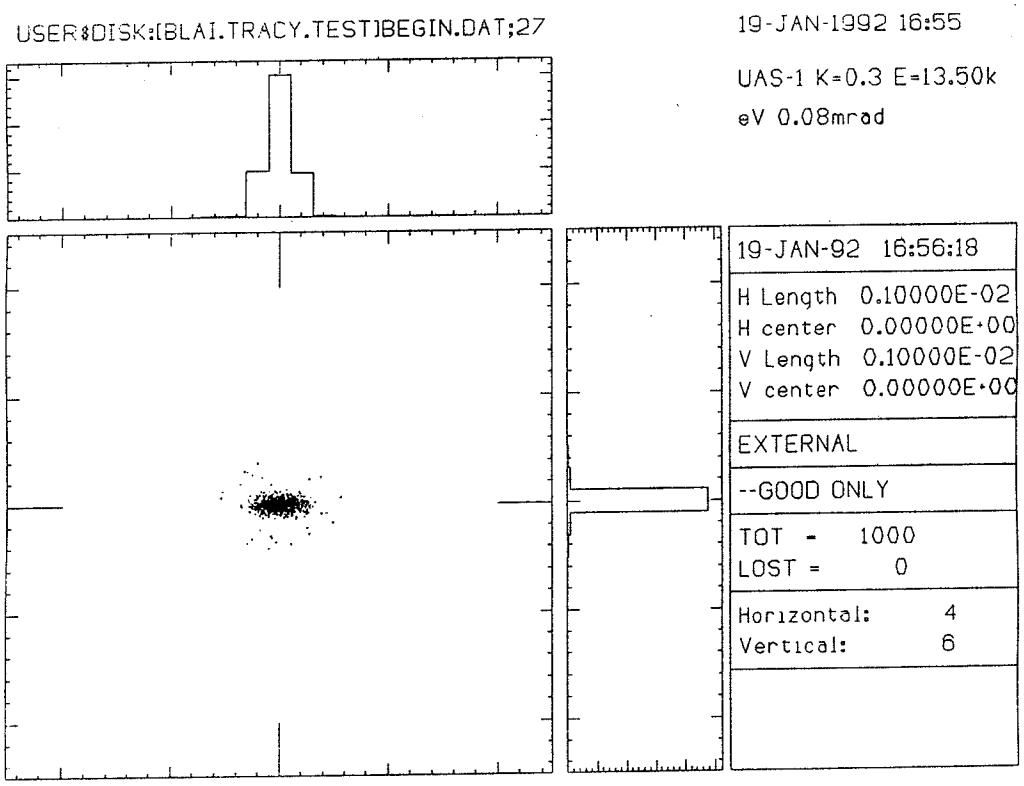


Fig. UA-55. K = 0.3, first harmonic.

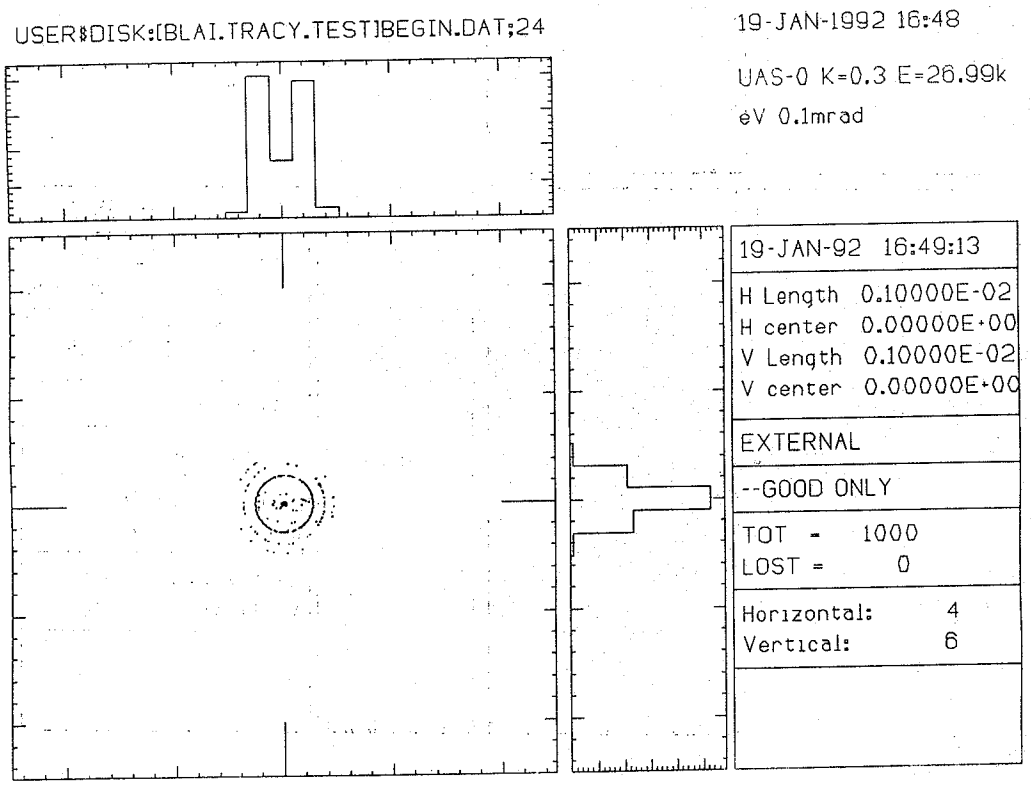


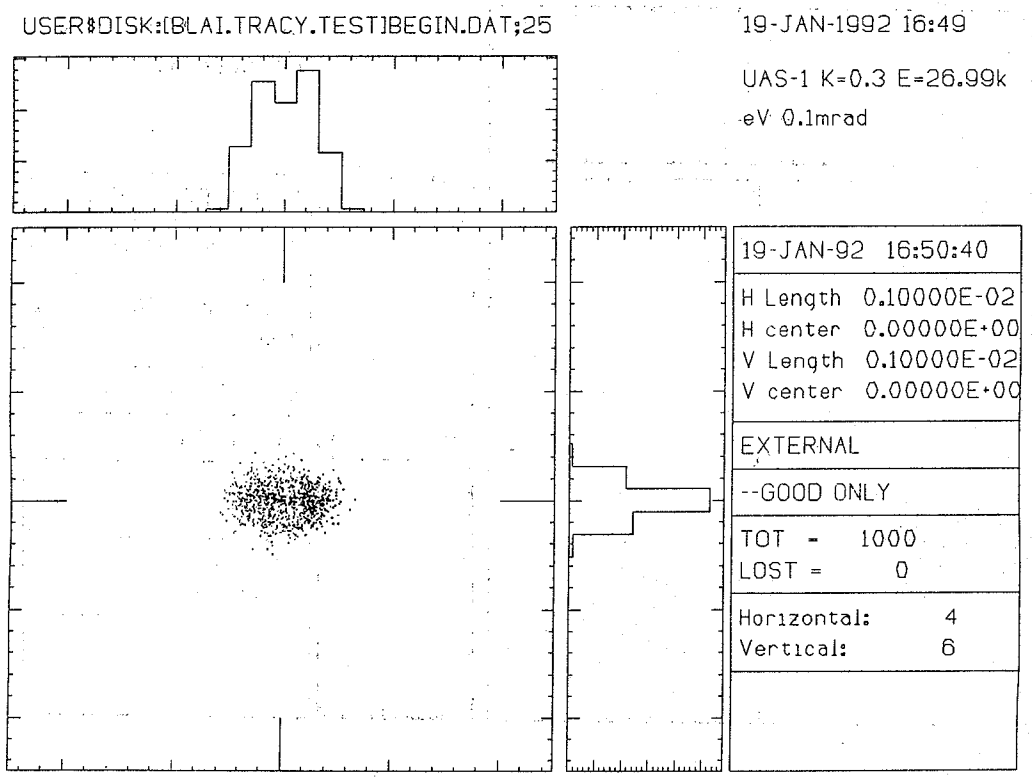


Fig. UA-56. K = 0.3, second harmonic.

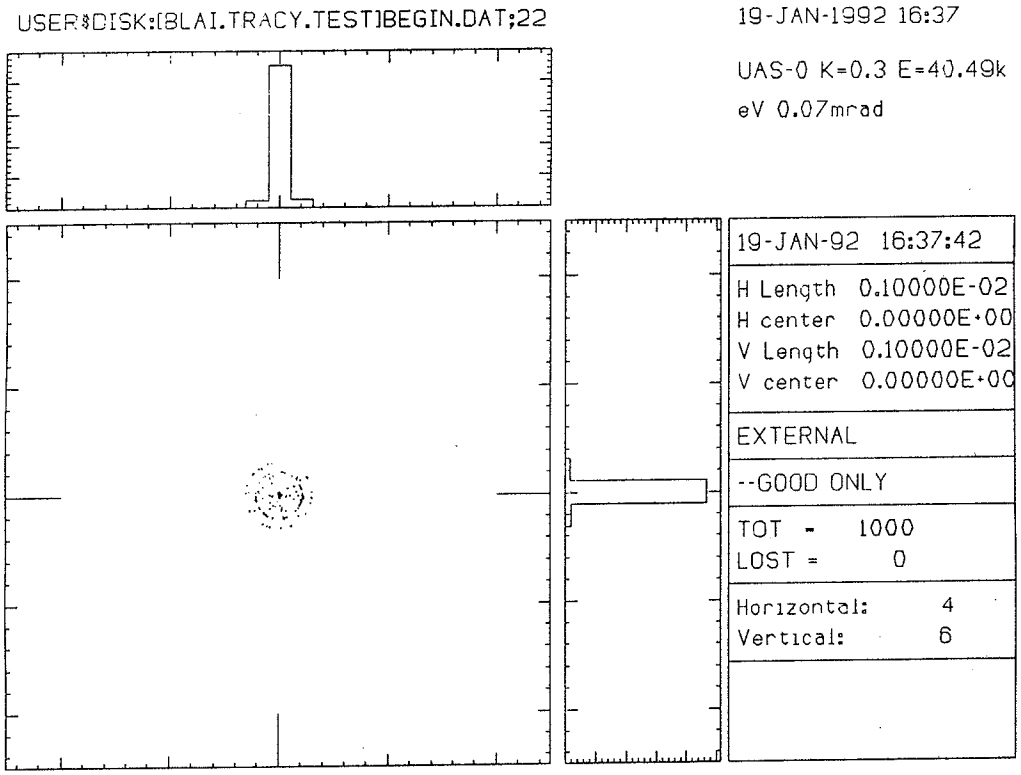


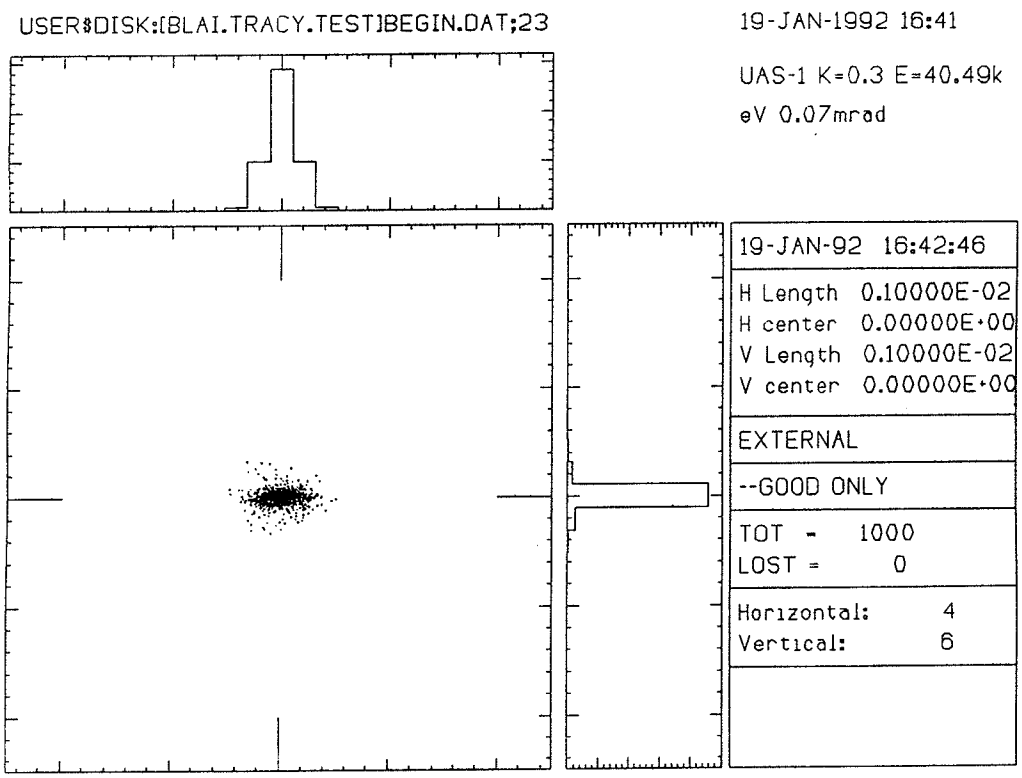


Fig. UA-57. K = 0.3, third harmonic.

# APS WIGGLER A

# RAY-TRACING RESULTS

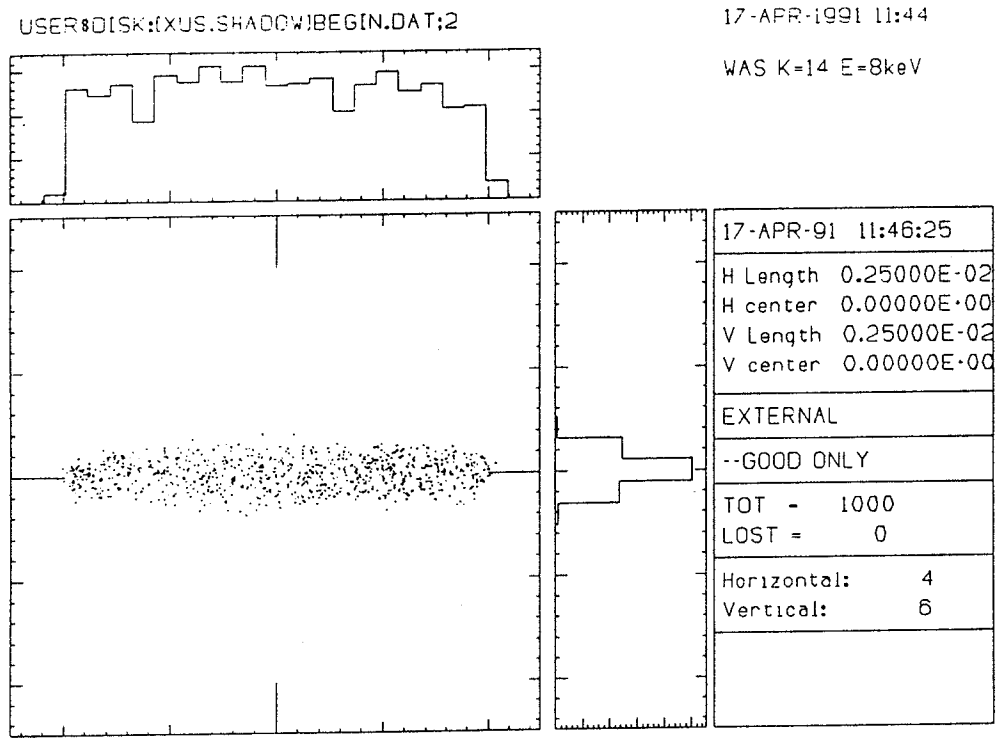


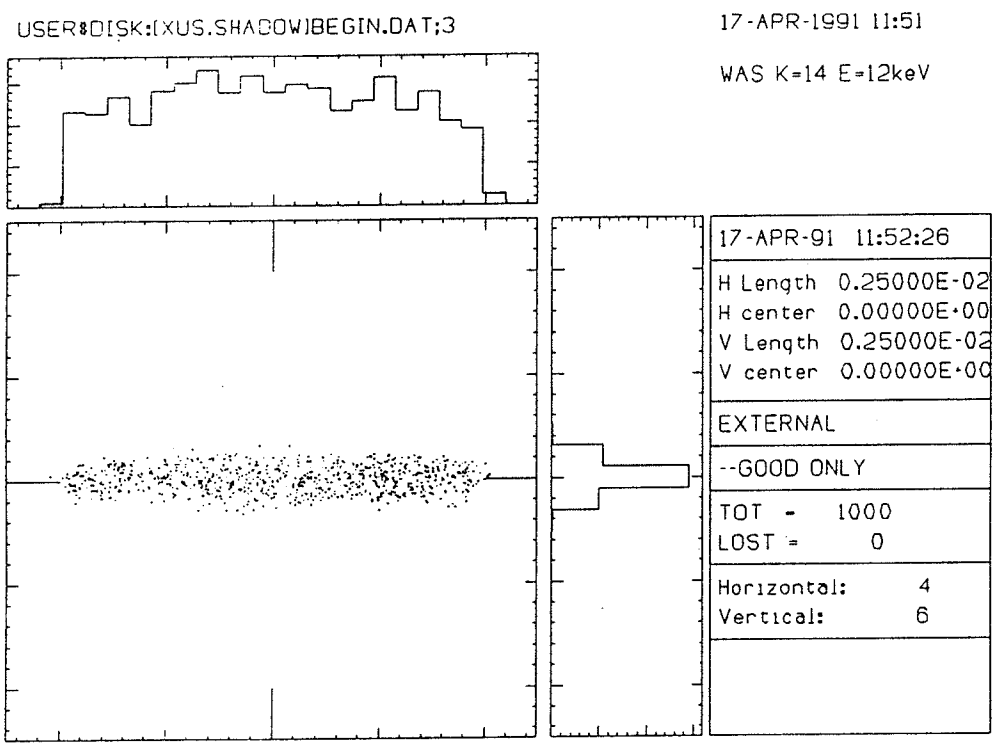


Fig. WA-1. Wiggler A. Top: hν = 8 keV, bottom: hν = 12 keV. The limits for each plot are 2.5 mrad x 2.5 mrad.

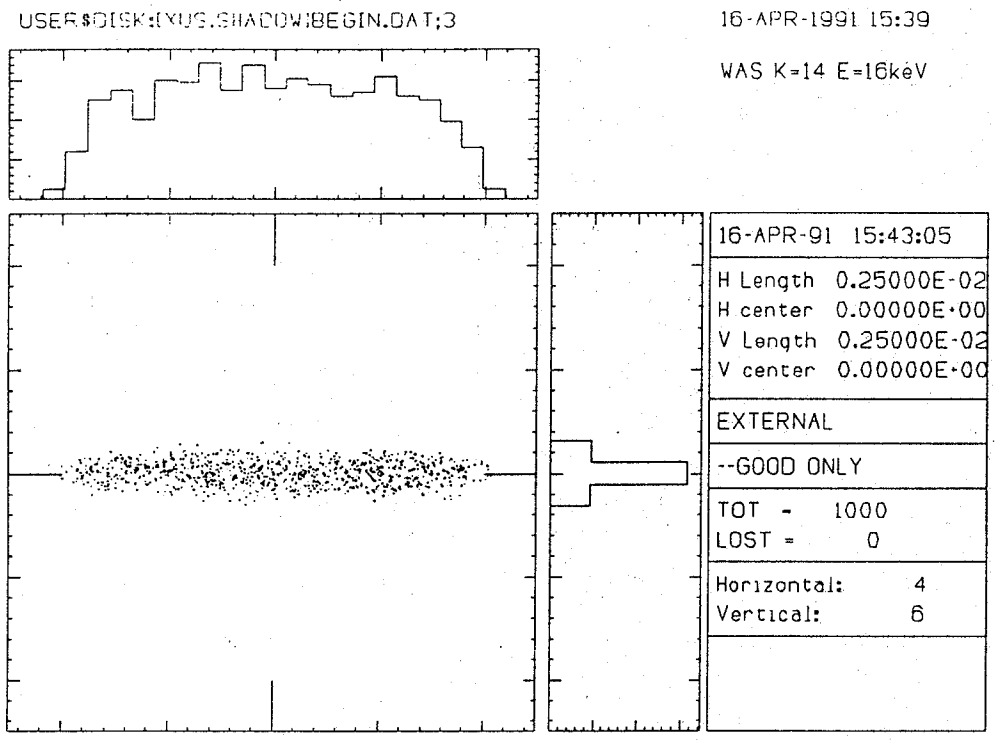


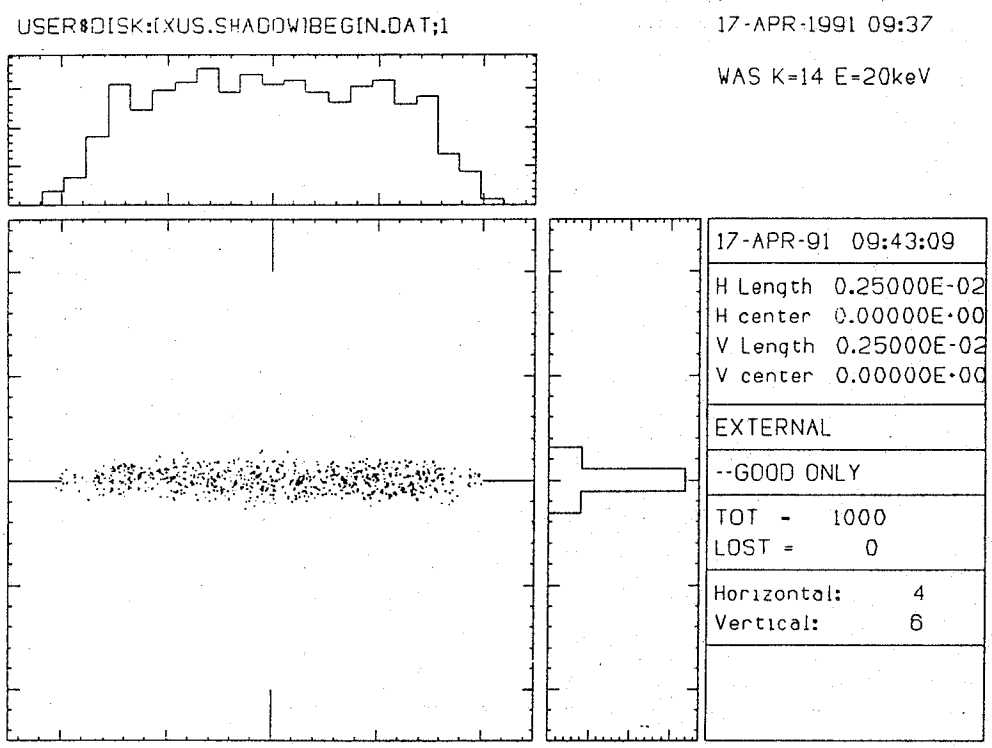


Fig. WA-2. Wiggler A. Top: hν = 16 keV, bottom: hν = 20 keV.

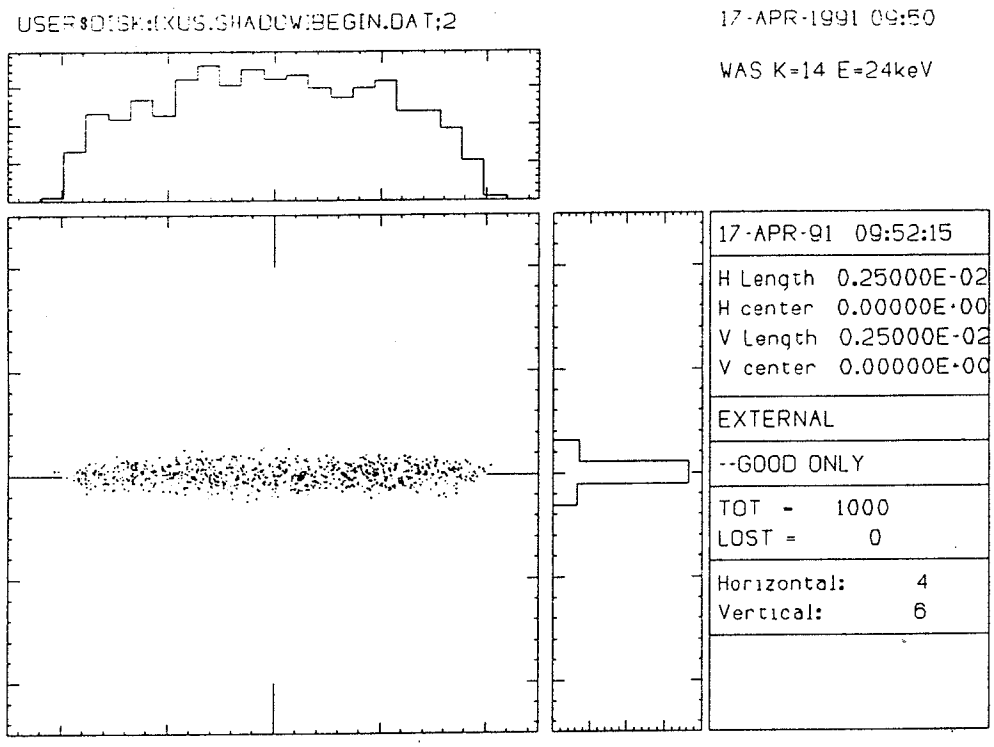


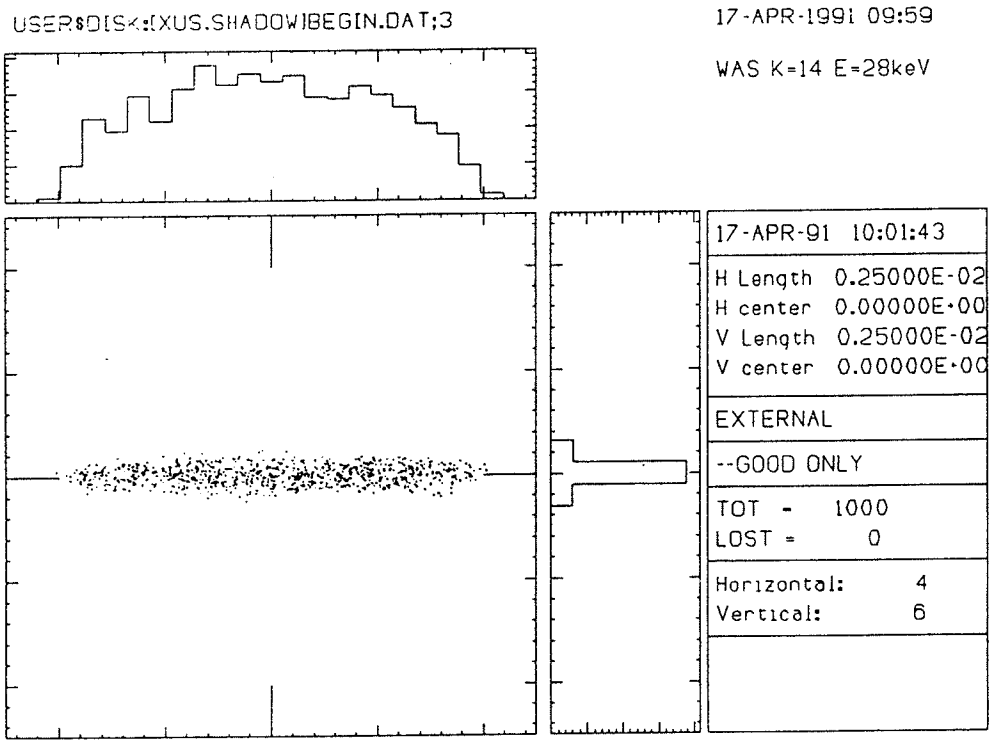


Fig. WA-3. Wiggler A. Top: hν = 24 keV, bottom: hν = 28 keV.

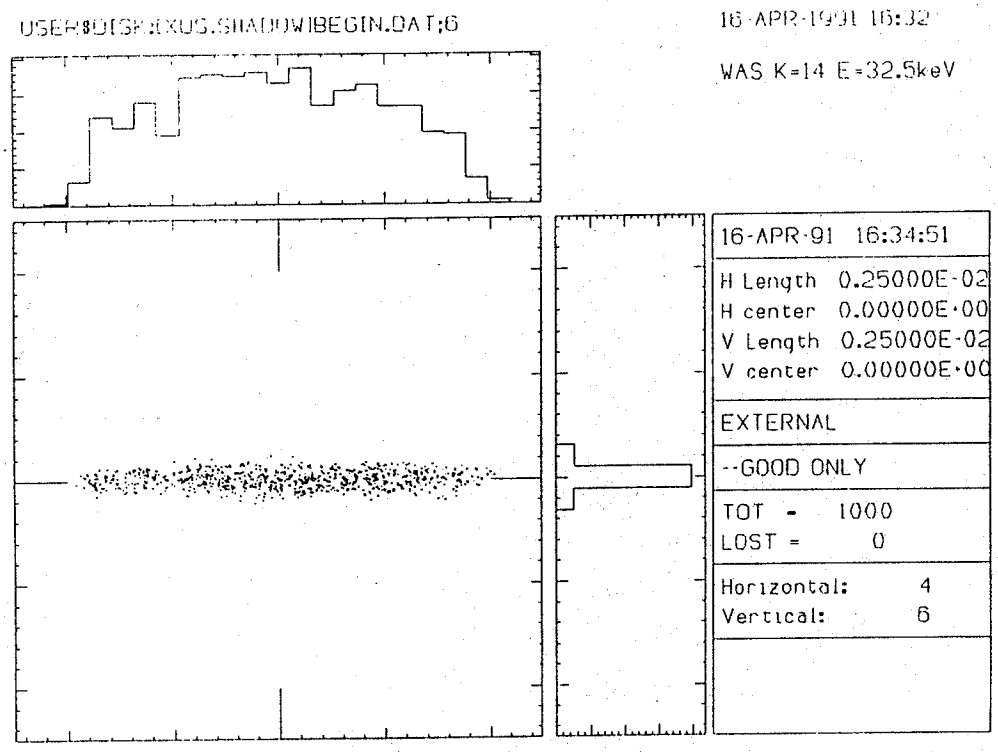


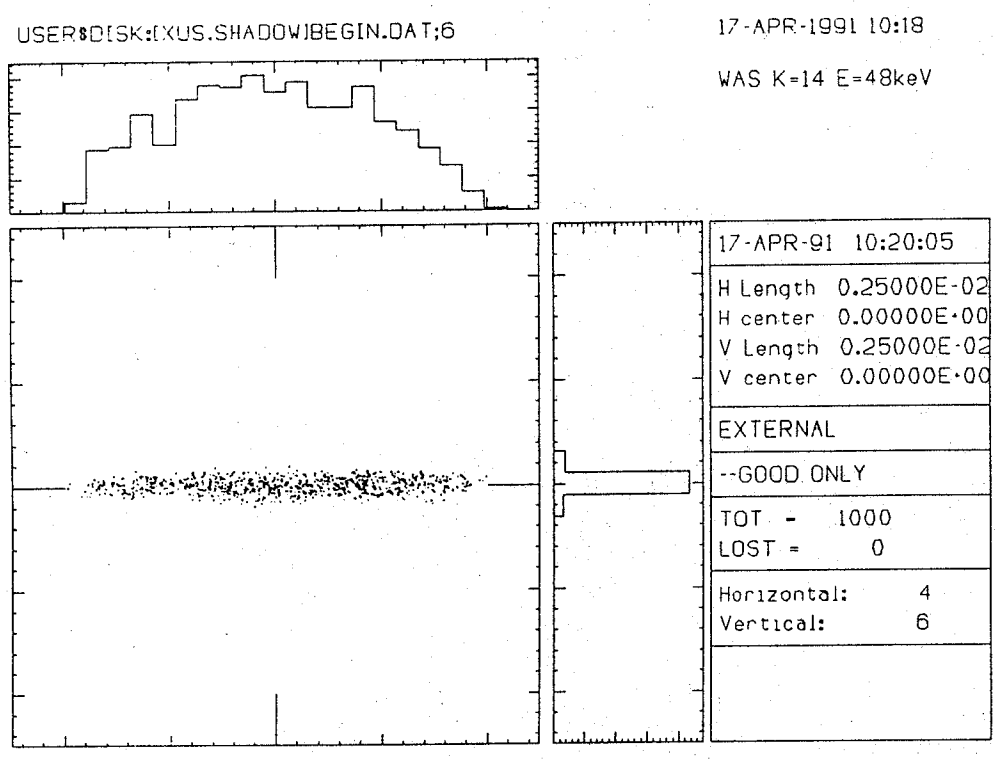


Fig. WA-4. Wiggler A. Top: $h\nu$ = 32.5 keV (=$E_c$), bottom: $h\nu$ = 48 keV.

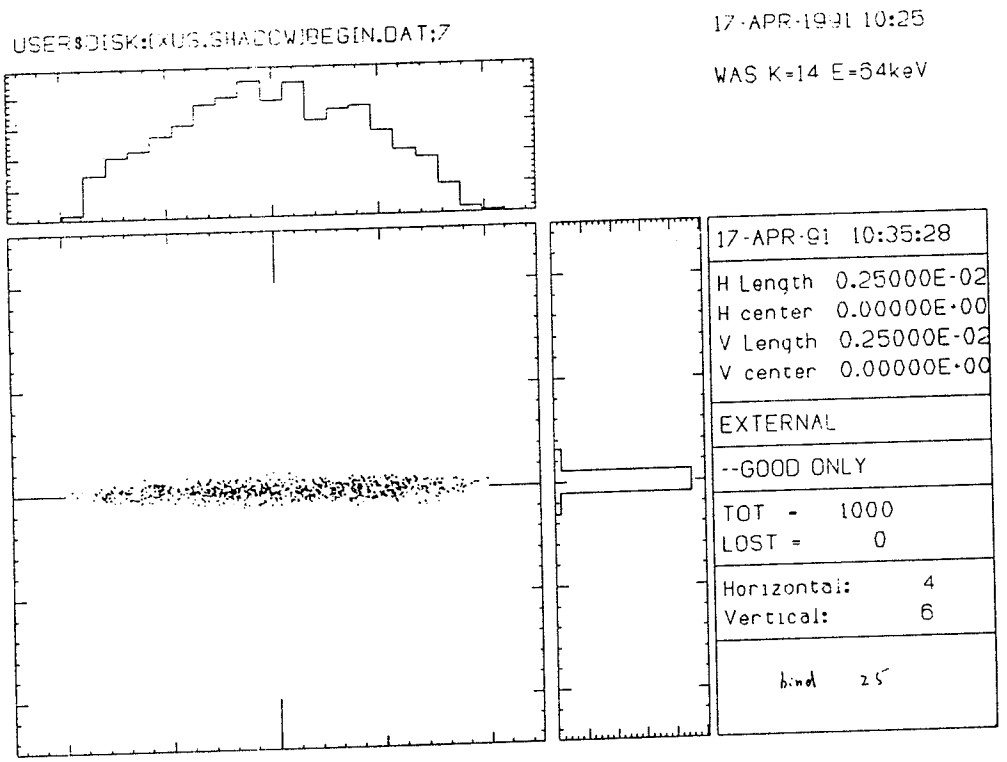


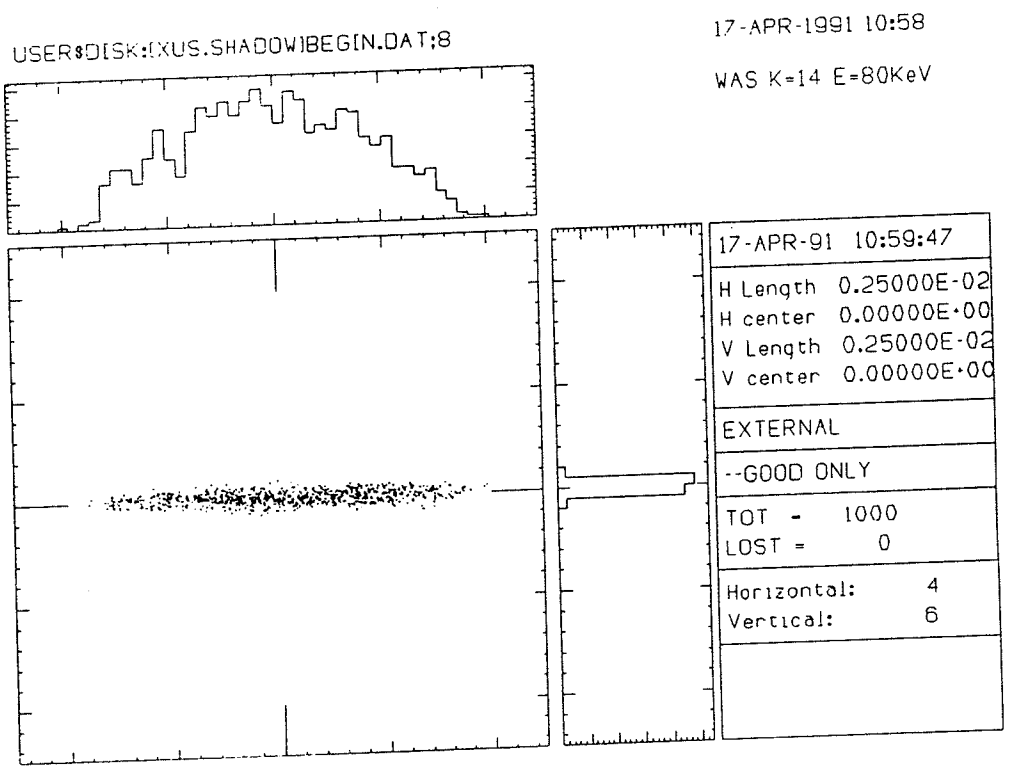


Fig. WA-5. Wiggler A. Top: hν = 64 keV, bottom: hν = 80 keV.

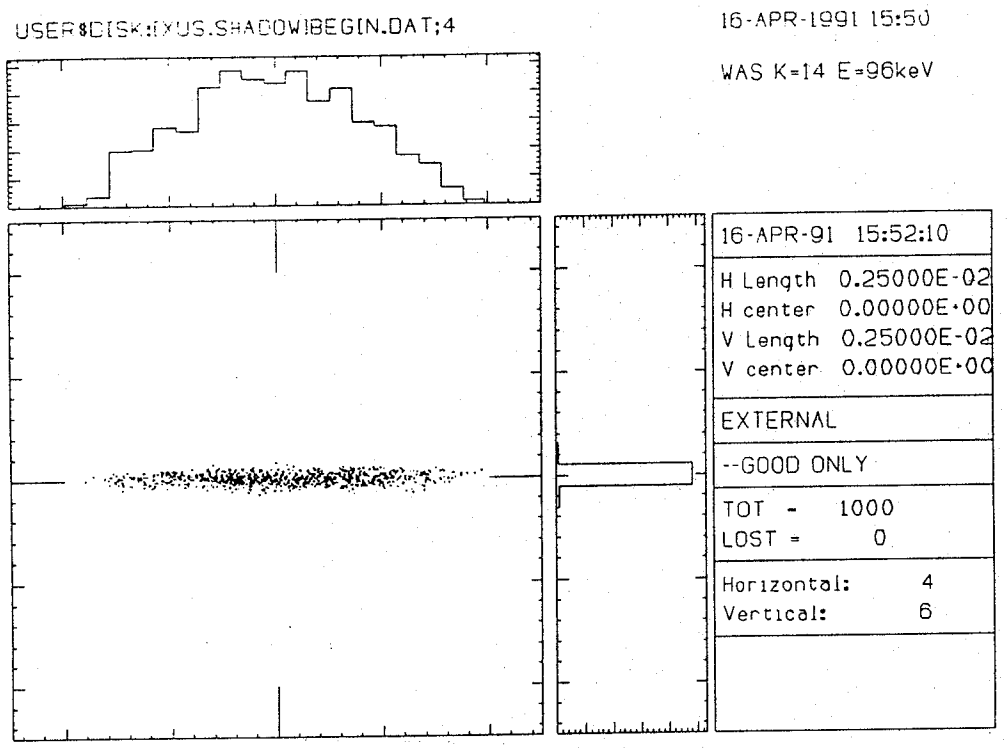


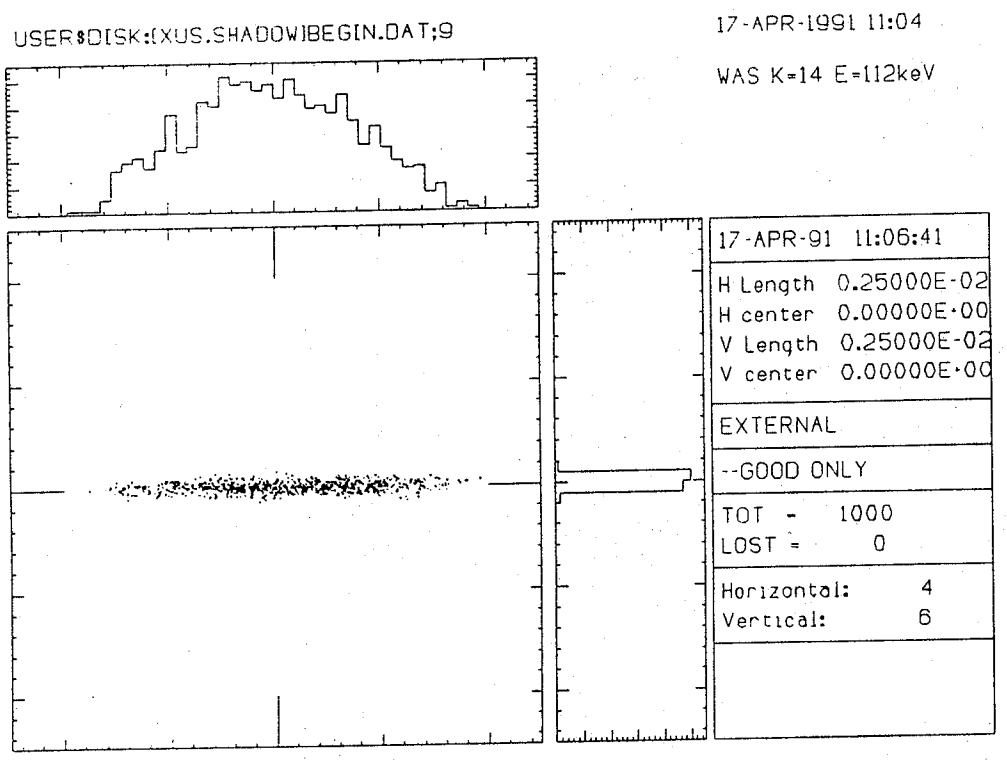


Fig. WA-6. Wiggler A. Top: hν = 96 keV, bottom: hν = 112 keV.

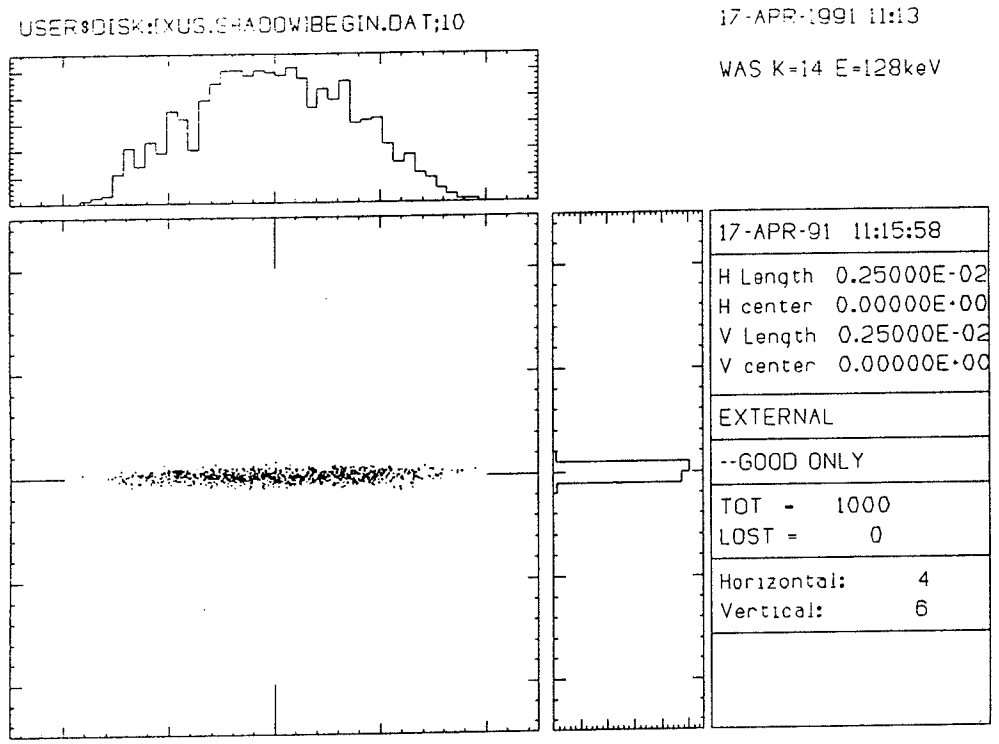


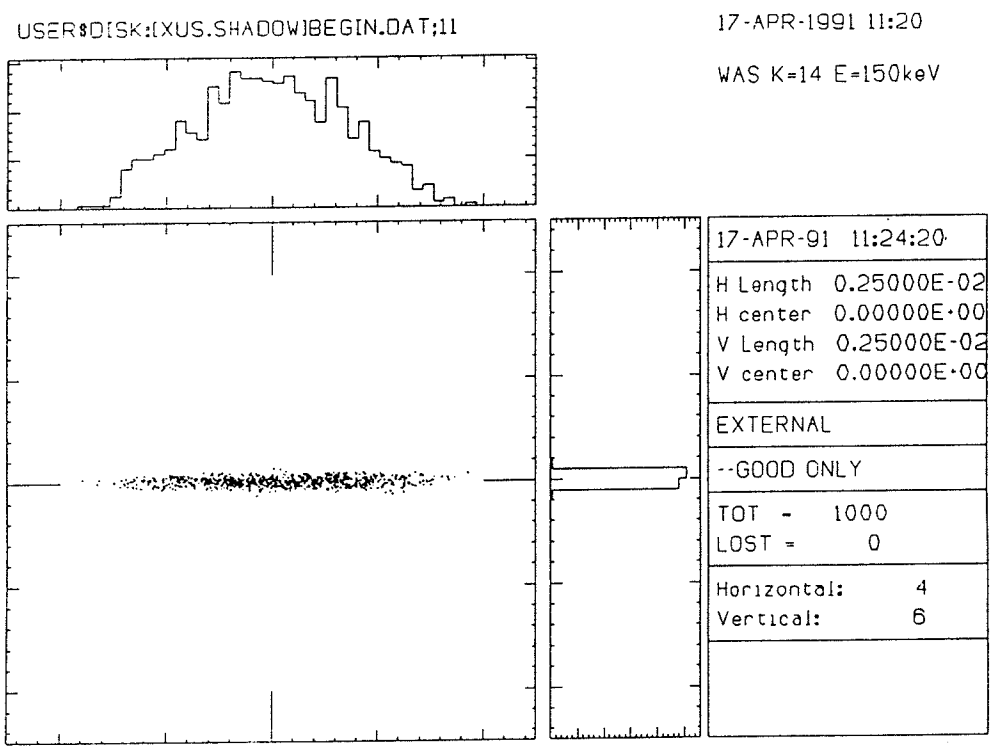


Fig. WA-7. Wiggler A. Top: hν = 128 keV, bottom: hν = 150 keV.

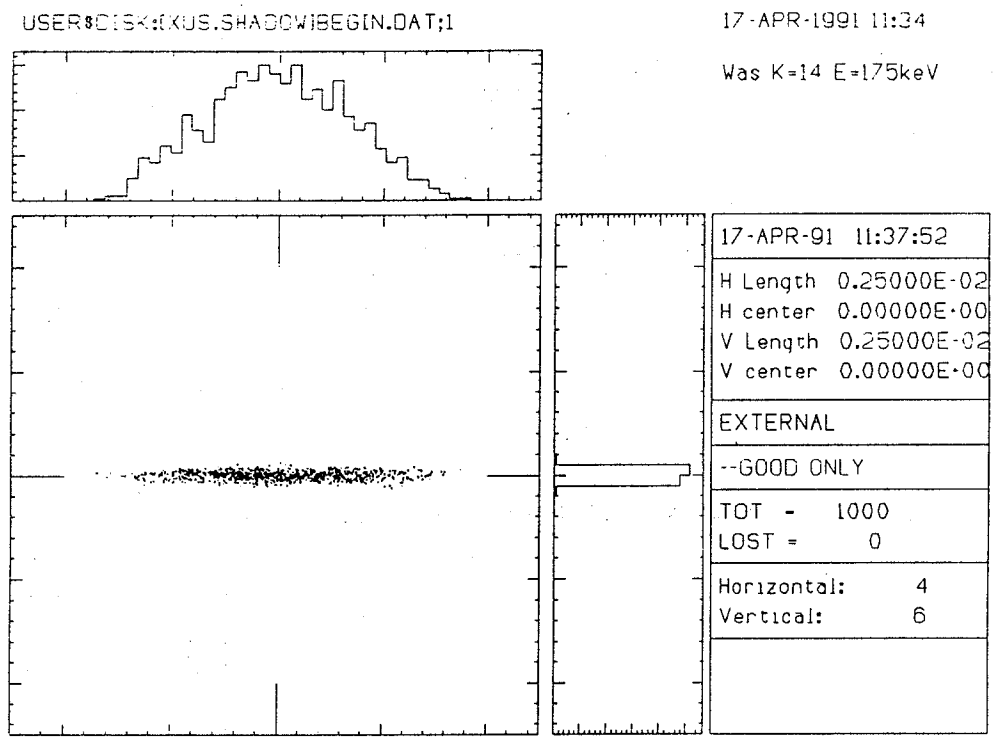


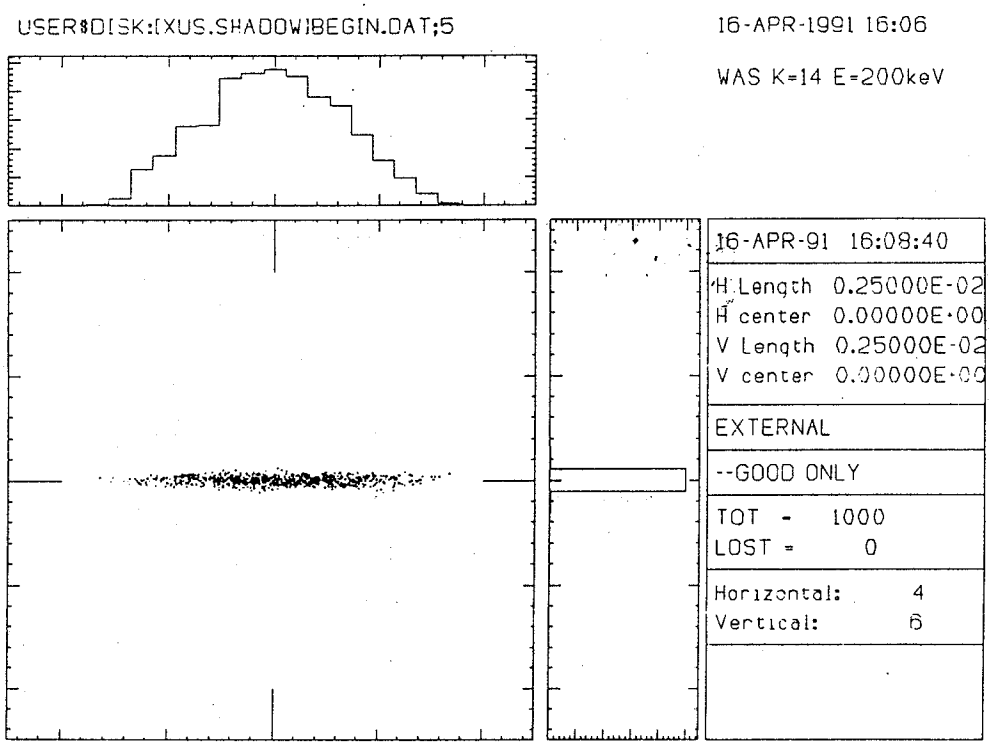


Fig. WA-8. Wiggler A. Top: hν = 175 keV, bottom: hν = 200 keV.

# APS WIGGLER B

# RAY-TRACING RESULTS

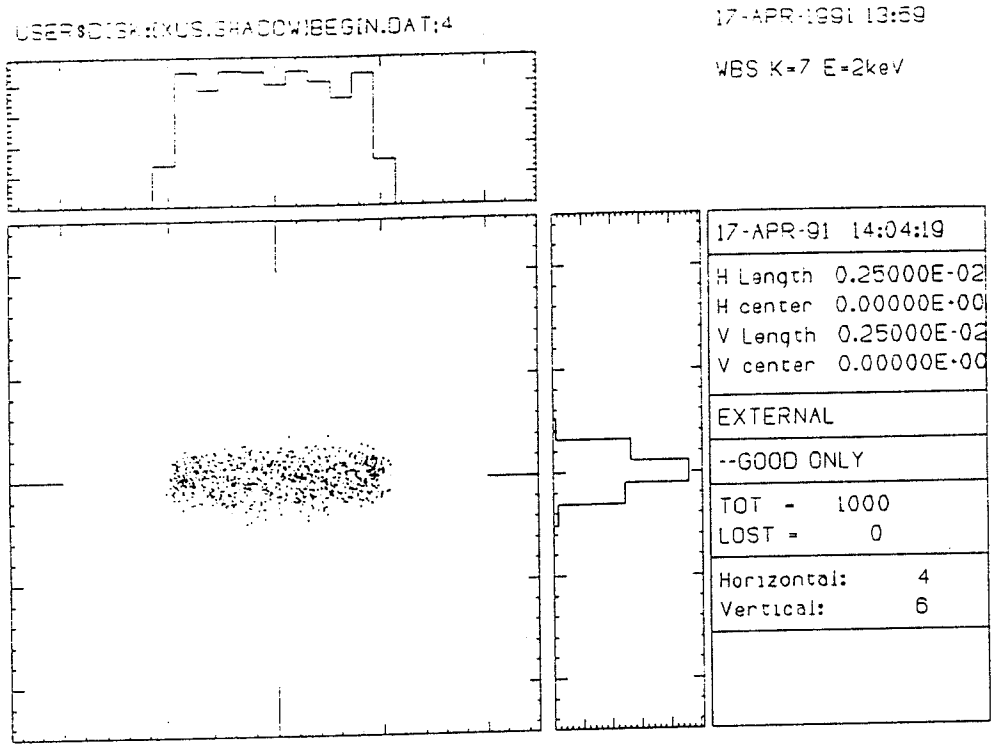


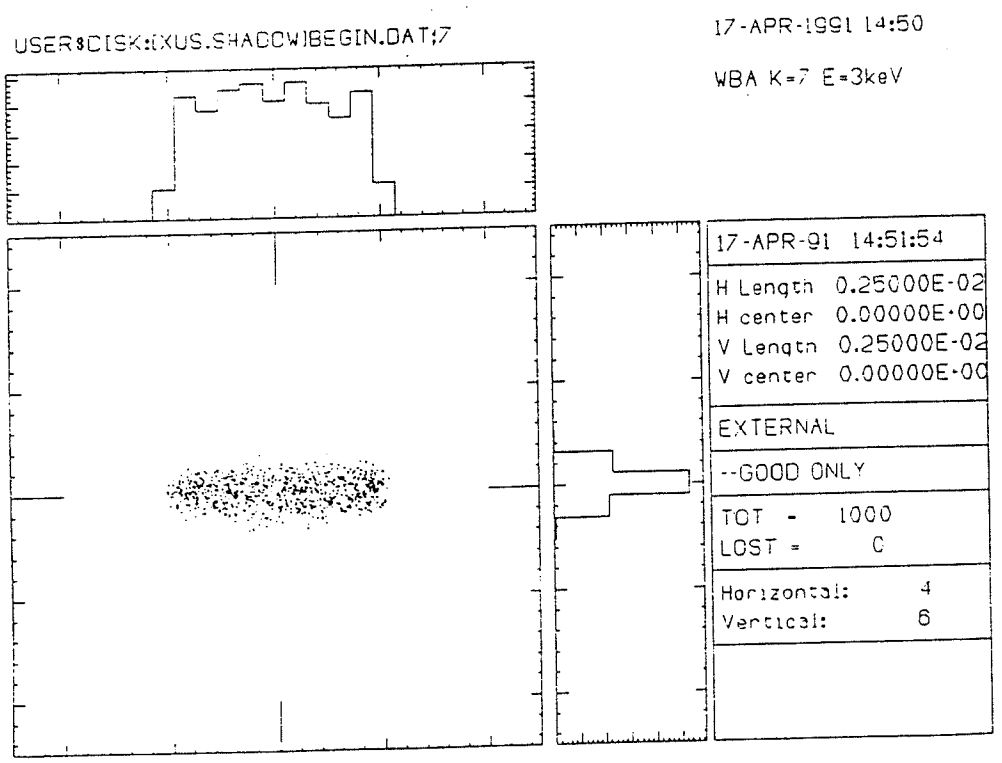


Fig. WB-1. Wiggler B. Top: hν = 2 keV, bottom: hν = 3 keV. The limits for each plot are 2.5 mrad x 2.5 mrad.

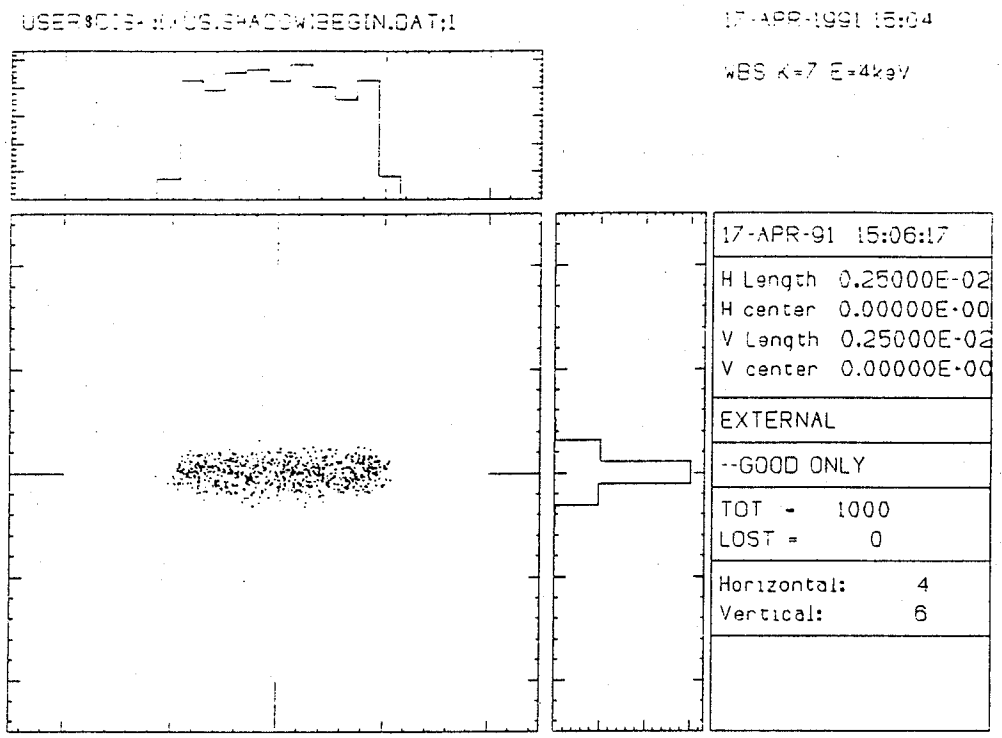


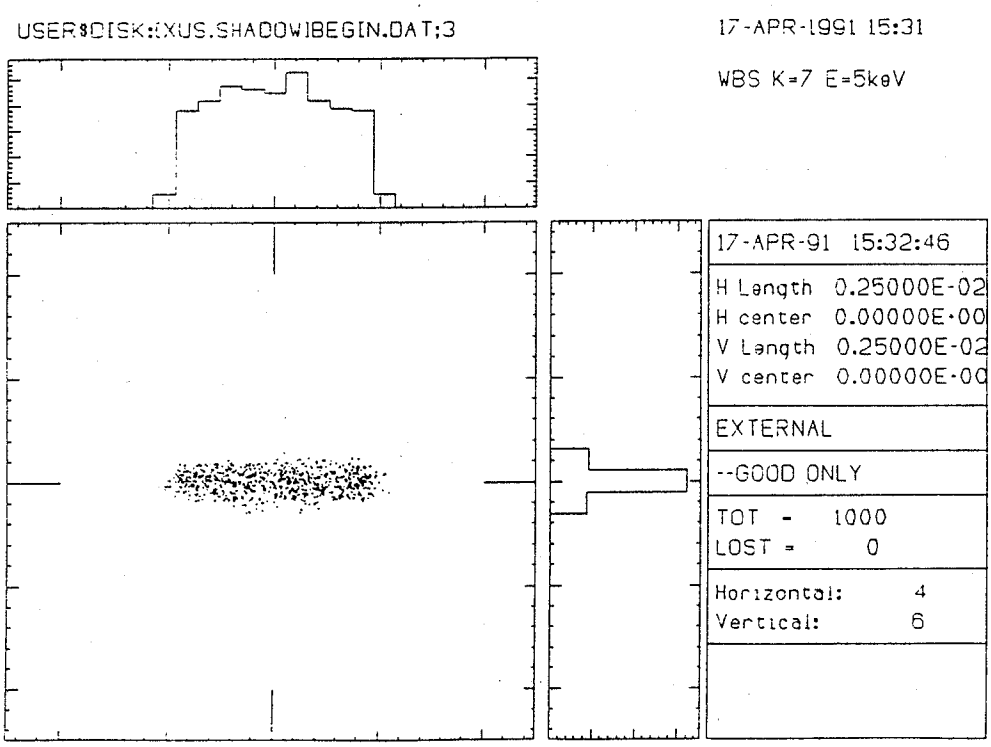


Fig. WB-2. Wiggler B. Top: hν = 4 keV, bottom: hν = 5 keV.

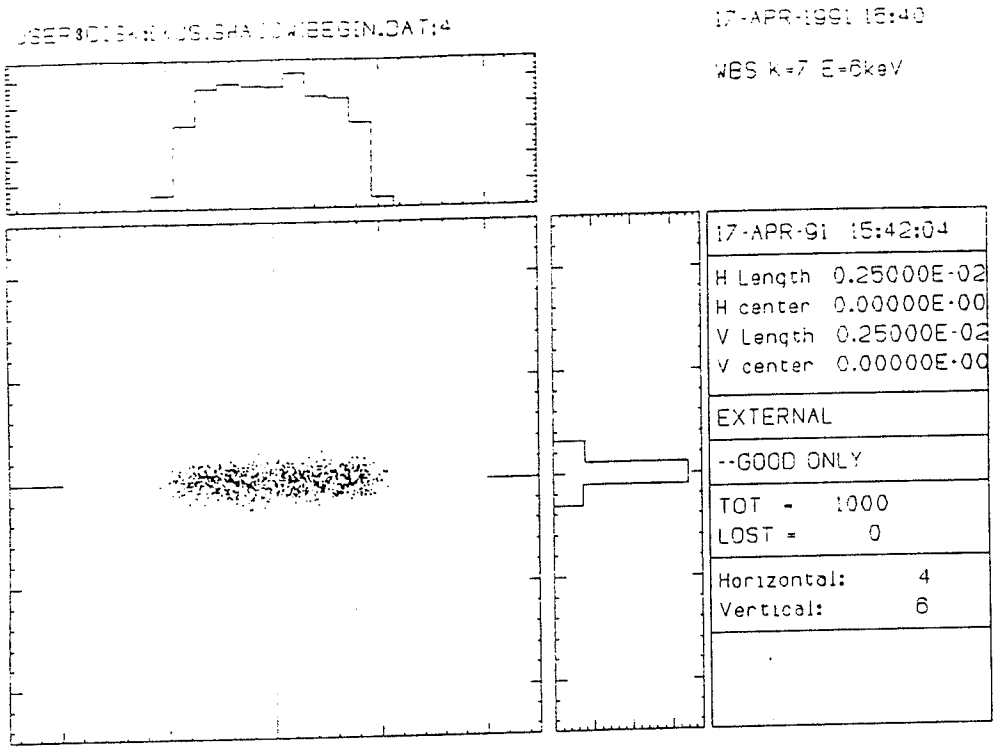


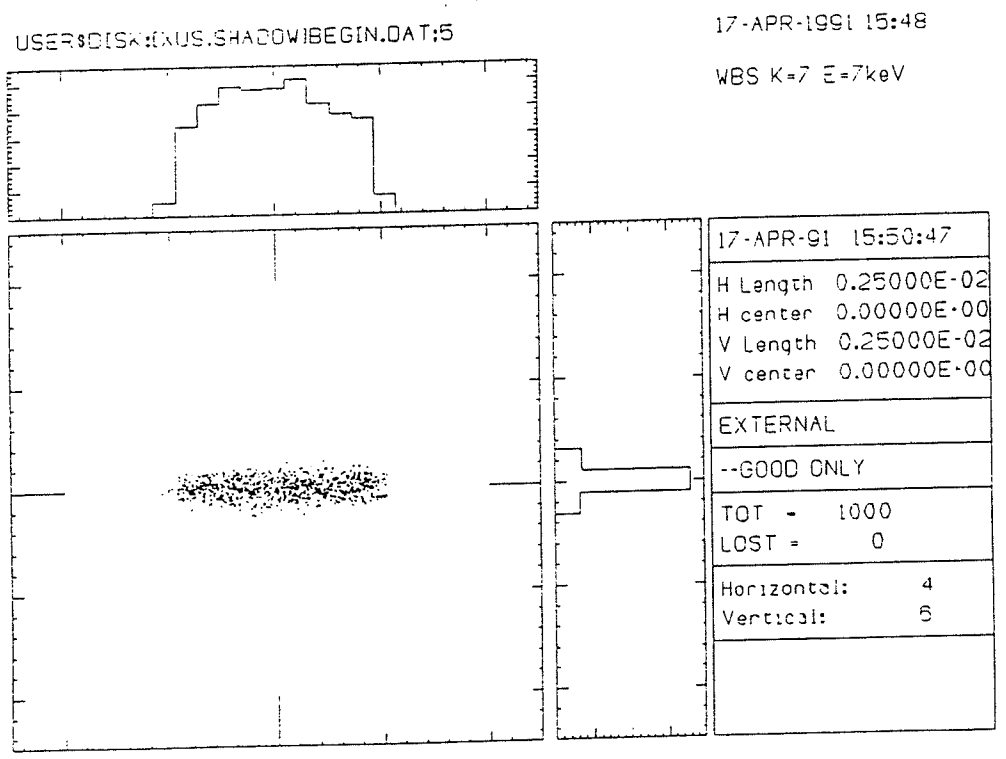


Fig. WB-3. Wiggler B. Top: hν = 6 keV, bottom: hν = 7 keV.

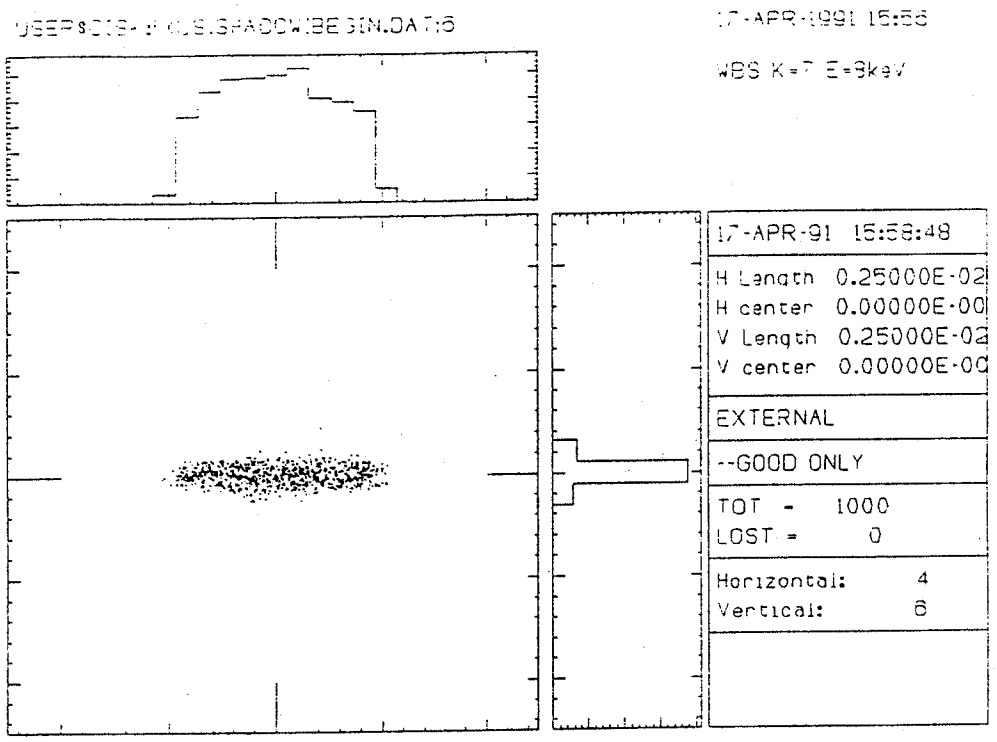


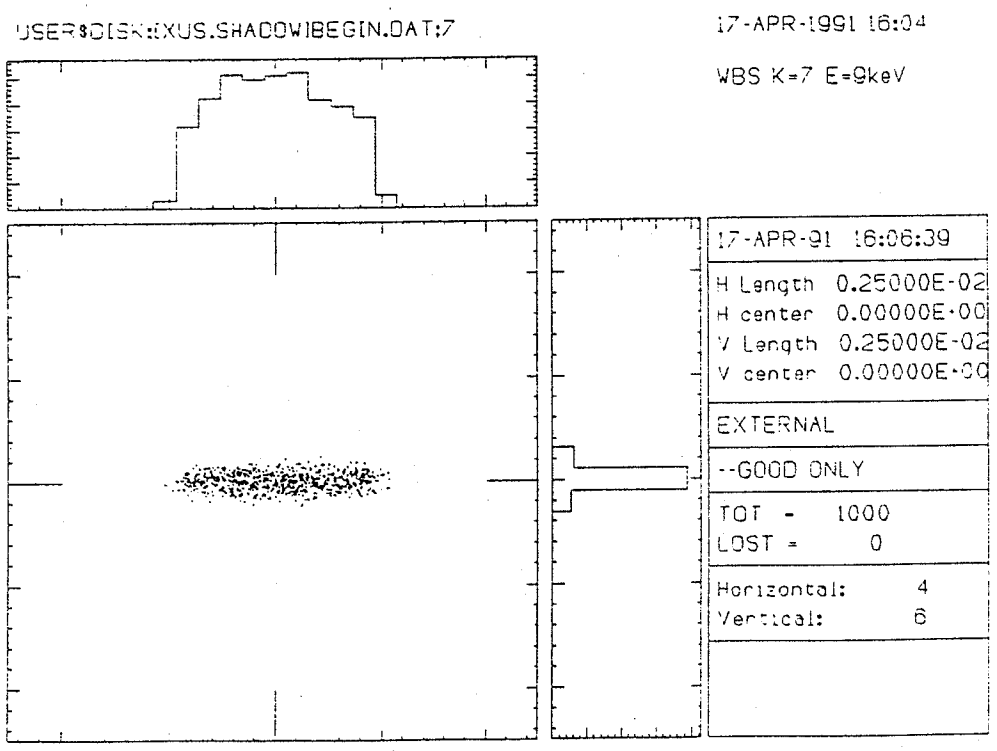


Fig. WB-4. Wiggler B. Top: hν = 8 keV, bottom: hν = 9 keV.

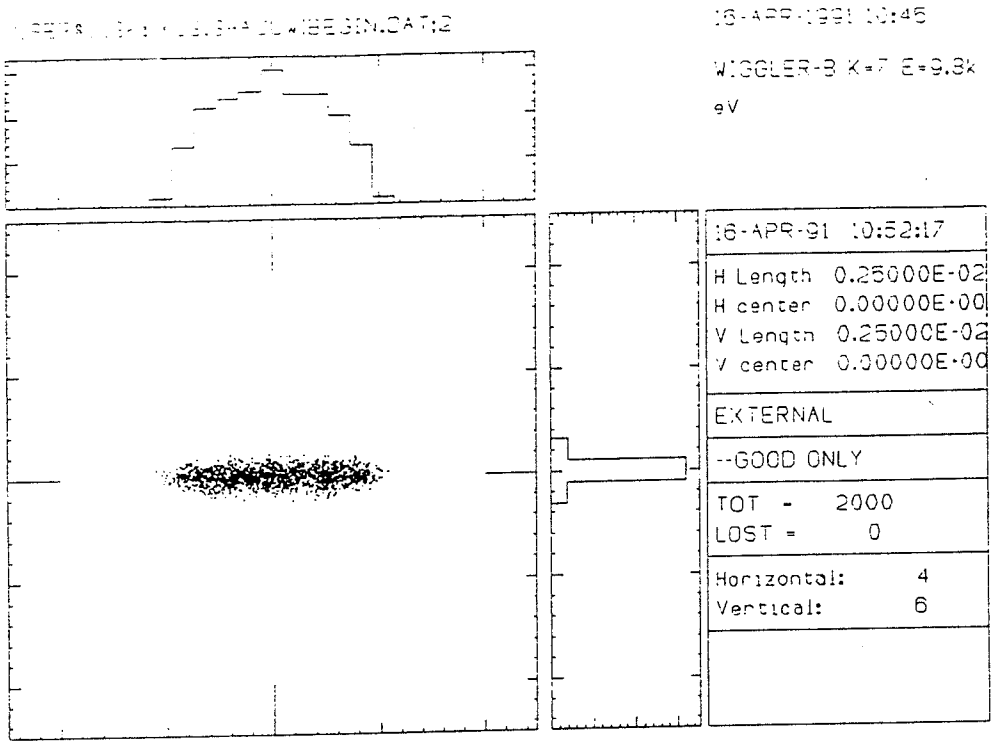


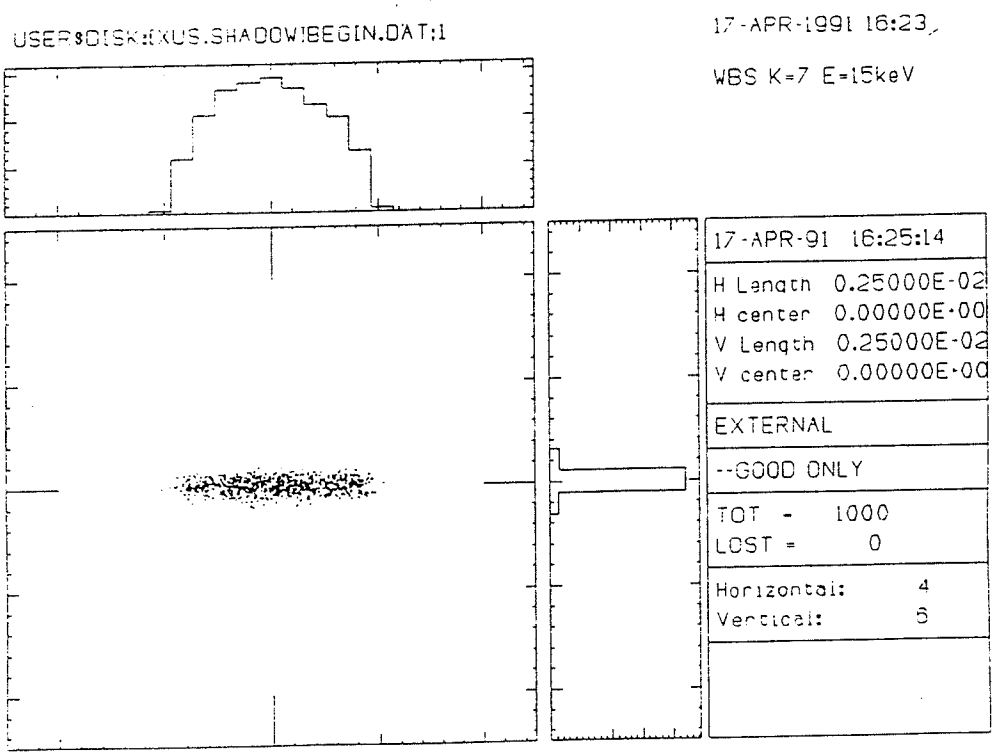


Fig. WB-5. Wiggler B. Top: hν = 9.8 keV (=$E_c$), bottom: hν = 15 keV.

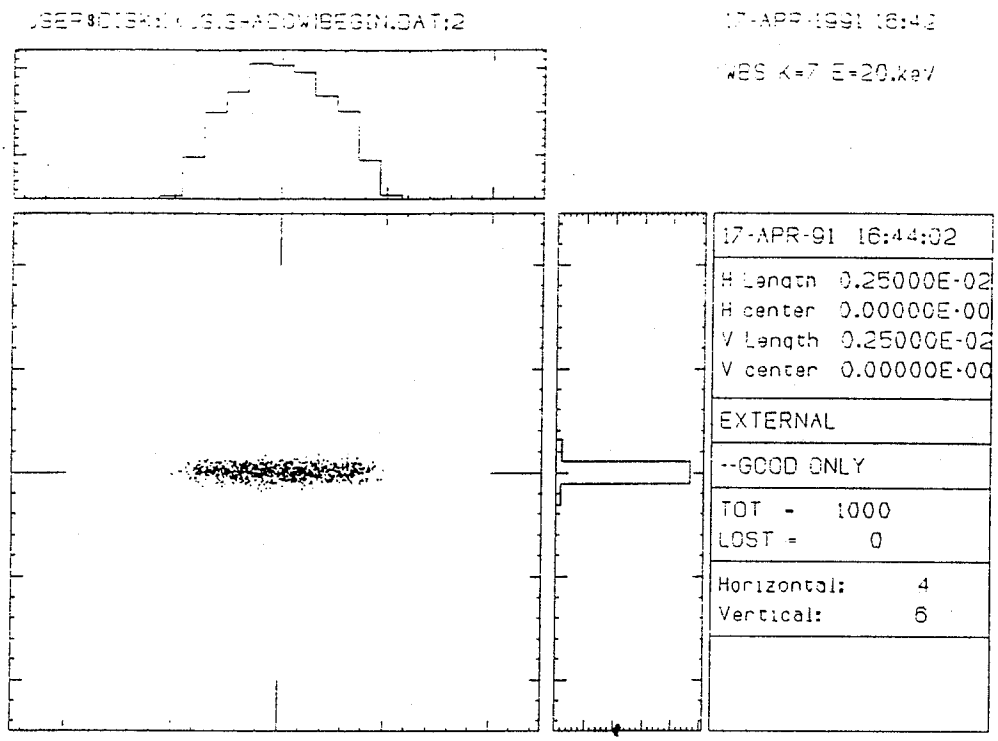


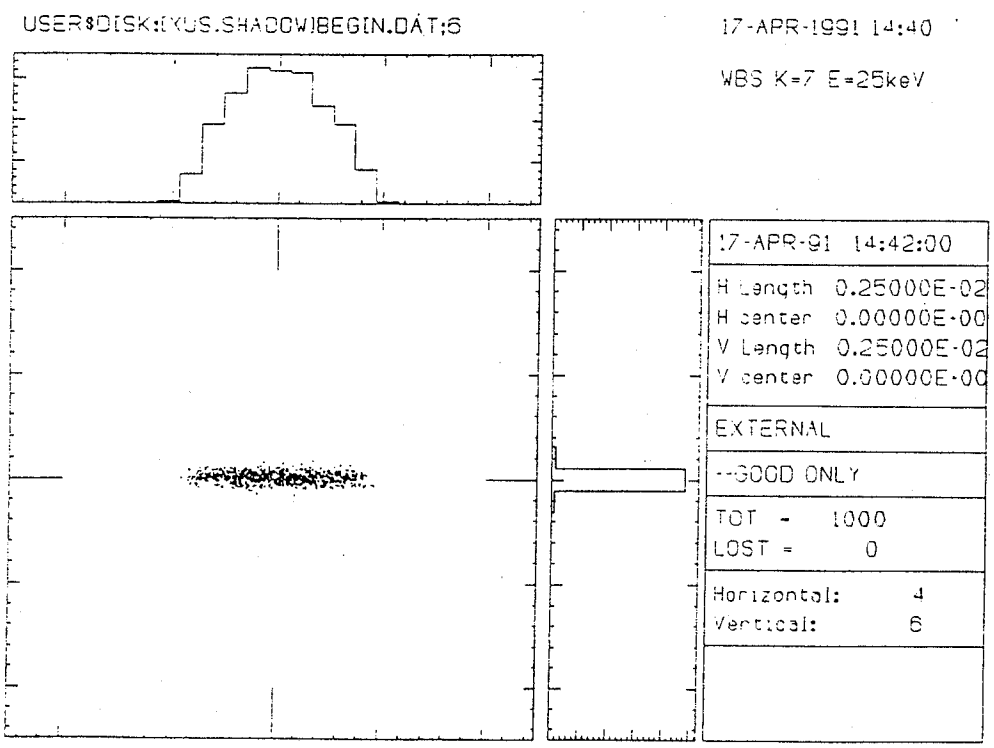


Fig. WB-6. Wiggler B. Top: hν = 20 keV, bottom: hν = 25 keV.

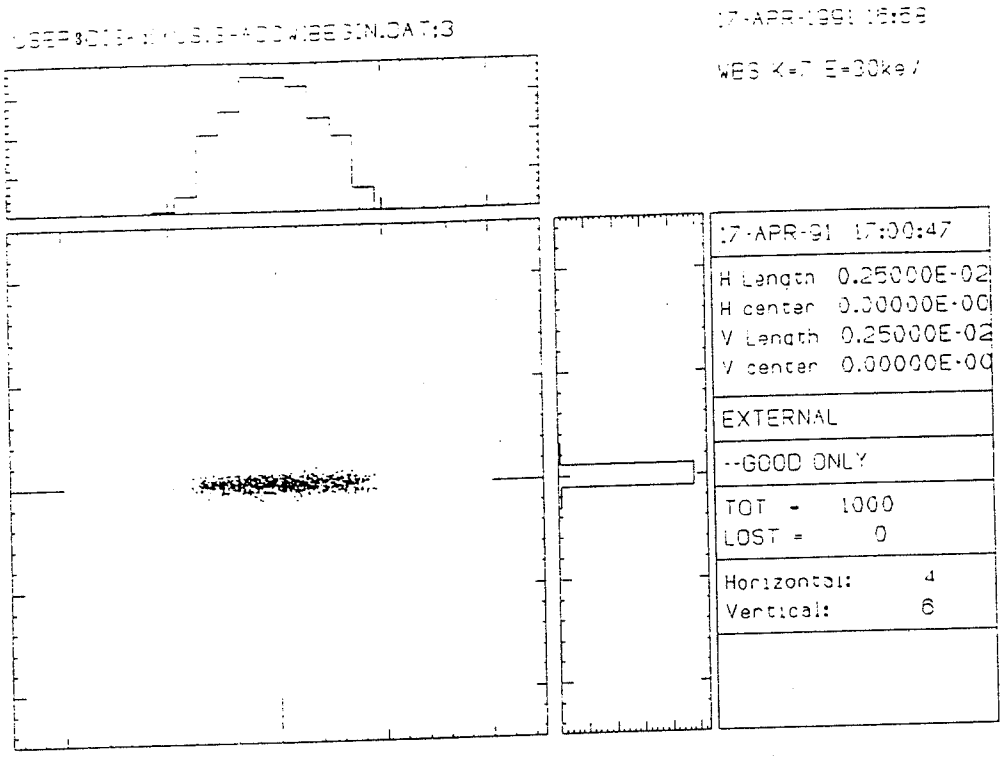


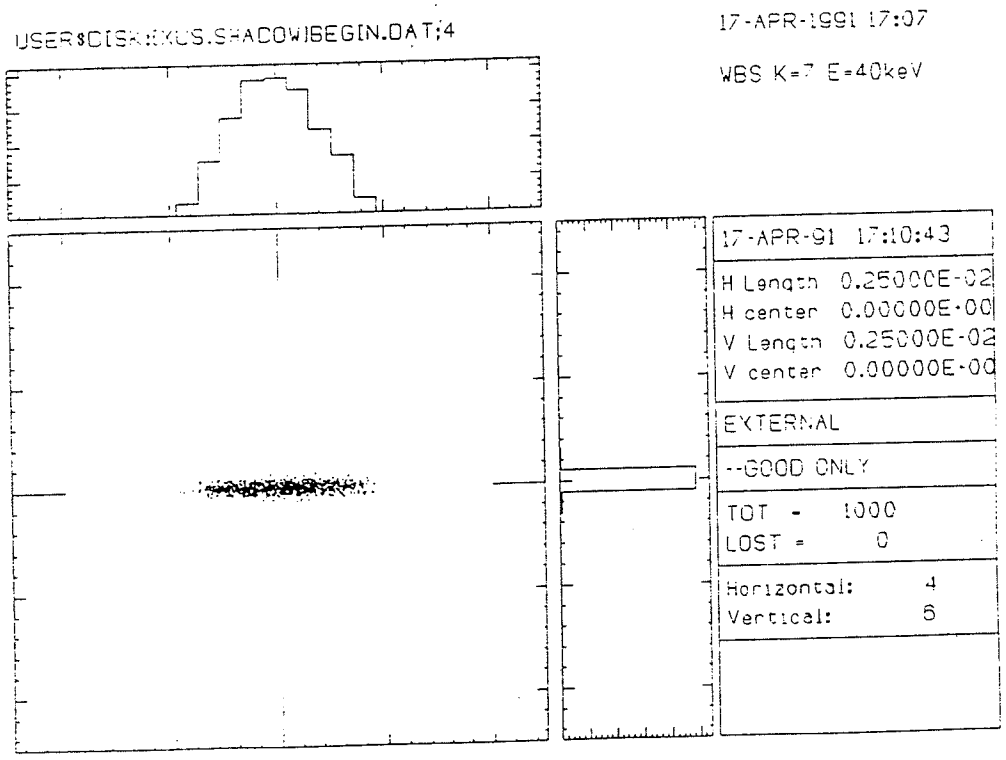


Fig. WB-7. Wiggler B. Top: hν = 30 keV, bottom: hν = 40 keV.

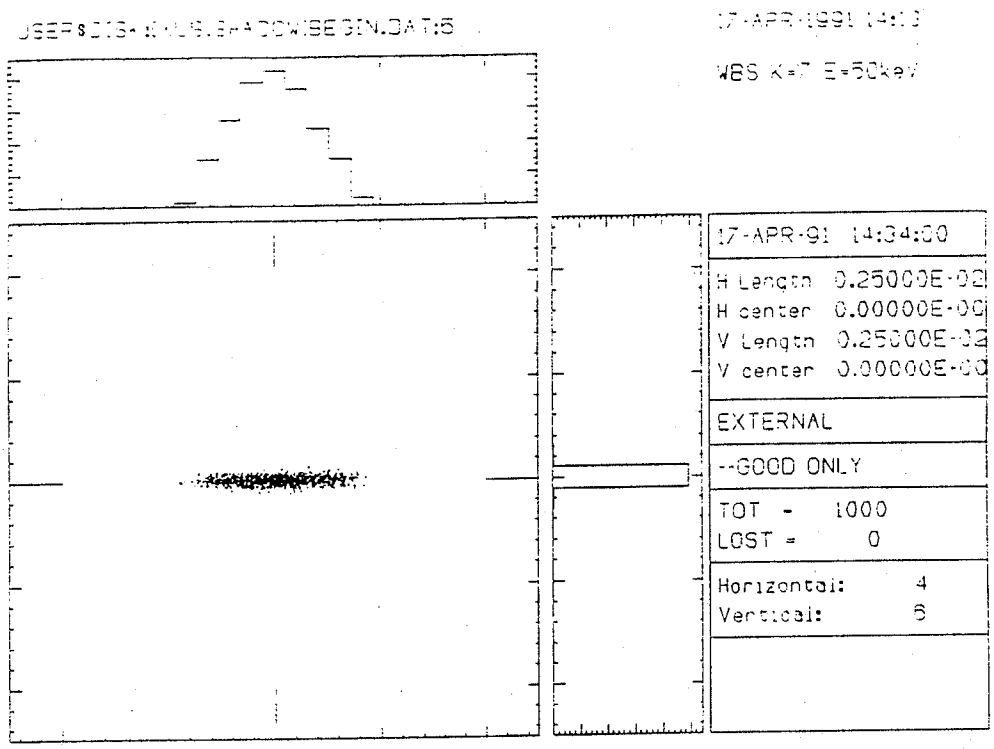


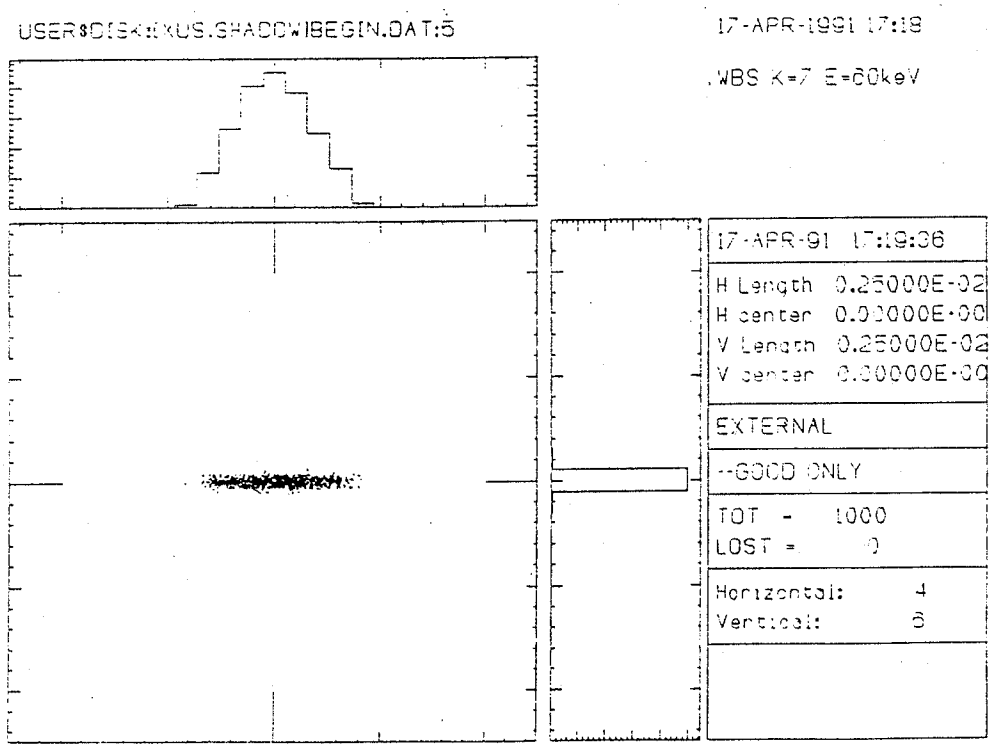


Fig. WB-8. Wiggler B. Top: hν = 50 keV, bottom: hν = 60 keV.